Study on resistance to erosion of irrigation facilities by using cement mixed soils

2019.9

Agricultural and Environmental Engineering
The United Graduate School of Agricultural Science
Tokyo University of Agriculture and Technology

PHENG SOKLINE

Study on resistance to erosion of irrigation facilities by using cement mixed soils

A thesis submitted by

PHENG SOKLINE

Agricultural and Environmental Engineering
The United Graduate School of Agricultural Science
Tokyo University of Agriculture and Technology

In partial fulfillment of the requirements for the degree of Doctor of Philosophy
September 2019

Supervised by

Professor YUJI KOHGO

Environmental Geotechnical Laboratory
Tokyo University of Agriculture and Technology

Acknowledgement

I could not complete this thesis without the support of some people who have been encouraging me from the beginning of my master to doctoral studies. My heartfelt gratitude goes to my main supervisor, Professor KOHGO Yuji. He has always encouraged me, provided opportunities, and made my studies challenging. I am so fortunate to have Professor KOHGO as my supervisor. I am also sincerely grateful to Professor SAITO Hirotaka, Professor OSAWA Kazutoshi, Professor KATO Tasuku and Professor MOHRI Yoshiyuki for his guidance and insightful comments.

I would especially like to thank to Dr. HORI Toshikazu and his colleagues for providing me some administrative and technical support to carry out my experimental study at the National Research Institute for Rural Engineering (NIRE) in Tsukuba. I thank to Mr. Okabe and Mr. Yamada for their helps and guidance for rain erosion resistance tests. Also, my thanks go to Dr. Anusron Chueasamat for providing comments and some academic trainings to enhance my research study. My thanks go to Mr. Magatt Thiam for his kind support in helping me overcome my troubles. He provides me a lot of emotional support during the 1st and 2nd year of my PhD. Also, I thank my friend Mr. Sato Tomotaka for his great help in academic, experiment and my daily life. He always provides a constant help to deal with some difficulties, in particular breaking down the language barrier for me. Ms. Seki Naoko and Ms. Hibi Kinuko deserve my thanks for helping experiment on physical, mechanical properties test and rain erosion resistance tests. My thanks go to Ms. Mai Masutani for helping with some work during thesis writing.

I would express my great gratitude to my beloved parents, sisters for their personal support and patience. My expression of thanks does not suffice for their kindness and support. My deep gratitude goes to Mr. Chan Thanin, my husband, for always gives me a very big support in academic and family life. I am thankful to Mr. Maruyama Kazuhiko for his kind support and consultation for my study and living in Japan. I thank to my Cambodian friends who always cheer me up. They always help me to settle down the difficult tasks and take a good care of me. I would dedicate this work to my beloved belated grandmother who always inspired me to better my academic life. Last, I would like to thank to MEXT scholarship provides the financial support for my study and stay in Japan for 3 years.

Abstract

In most developing countries, earth irrigation facilities are commonly found due to the low construction cost. However, most earth irrigation structures are so sensitive to heavy rainfalls and soil erosion. Surface erosion, one type of erosion involving the detachment of surface soil particles and water flowing on the surface, is one of the main causes of embankment failures. Using the high erodible soil materials to construct earth embankments, the occurrence of erosion has increased. The eroded soils from embankments and deposition of sediment in irrigation systems frequently reduce the capacity of irrigation, block irrigation channels and shorten the lifespan of irrigation systems resulted in most irrigation schemes damage. In Cambodia, most irrigation structures are earthworks. The surface erosion occurred on earth embankments usually caused big concerns for irrigation rehabilitation work. Silt is usually found in irrigation systems, and it is the most sensitive soil to erosion. Therefore, the aims of this study were: (1) to investigate the field situation and eroded earth irrigation facilities in Cambodia, (2) to determine the physical, mechanical and hydraulic properties of soil treated with cement and (3) to assess the resistance of soil treated with cement to surface erosion under rain erosion resistance test. The results of field investigations in Cambodia showed that surface erosion was commonly found on earth embankment and the compaction degree of embankment D values existed within 81-88% indicated as a loose condition. One attempt of the use of cemented soils has been conducted to prevent surface erosion. DL clay, a non-plastic silt, was used to mix with normal Portland cement for experimental study in the laboratory. The consolidated drained triaxial compression test (CD test) was used to clarify the mechanical properties of soil cement. Thirty specimens with 3 confining pressures: 50, 100 and 200 kPa, 4 cement contents: 0, 3, 5 and 7% by dry weight of the soil, and 3 curing times: 7, 14 and 28 days were investigated in triaxial compression tests. The dry density of soil specimens in triaxial compression tests were 1.3g/cm^3; water content was 17%.

From the triaxial compression tests, it was found that the shear strength of the soil cement increased with an increase in cement contents and curing times. The strain softening and dilation behaviour of cemented specimens was found when confining pressure σ_3 = 50 kPa was applied. However, the softening behaviour started to disappear with an increase in confining pressure. The cohesion values could be reasonably evaluated by using the test

results. It was found that the cemented soils with 3 and 5% of cement content have sufficient shear strength values and they may be suitable for erosion protection.

The rain erosion resistance tests were carried out to assess the effectiveness of soil slope covered with soil cement response to rainfall and surface flow by using the slope adjustable equipment. The angle 20-degree (about 36% slope) of this equipment was assigned to this experimental test. Two rainfall intensities, 50 and 100 mm h^{-1}, were applied on six soil slopes, two of soil slopes are untreated soil and other four soil slopes were cemented soils with 3% and 5% of cement content on 10-cm thick top layer. The curing time for soil slopes in the rain erosion resistance test was 7 days. The pore water pressure transducers were inserted into the soil slopes. The results of the rain erosion resistance tests showed the slope model of 0% have a tremendous soil erosion on the surface soil slope. It was 8 times and 60 times larger than soil cement 3% and 5% under rainfall intensity 50 mm h^{-1}. The deepest erosion was found 10 cm and 30 cm in case of 50 mm h^{-1} and 100 mm h^{-1}. However, the surface soil cement remaining in a good condition from 1 to 3 cm of surface crusts was observed. Adding low cement contents to improve soil shear strength, it possibly reduces the soil detachment and soil erosion from the surface soil slopes. Due to the hardened surface of the soil cement, a strong soil detachment was reduced. The soil slope of 0% cement content showed a very large amount of surface runoff compared with soil cement 3% and 5%. The hydraulic conductivity of the soil cement was increased and enhanced the infiltration capacity of the soil cement. The pore water pressure distribution showed that the rain water infiltrated into soil cement slopes faster than 0%, which reduced the surface runoff on the soil surface as well as soil losses. The flow vectors of three soil slopes showed the unsteady and non-uniformity under 100 mm h^{-1}. The direction of flow vectors moved upward indicating the swelling occur in case of soil cement 3% and 5%. From the element and slope model test results, it indicated that the surface soil detachment and erosion could be prevented at the low cement contents, 3 and 5%. The 3% of cement content performed a better resistance in soil detachment and less eroded soils.

Contents

List of Figures

List of Tables

Chapter 1 Introduction

1. 1 Introduction

Soil erosion has been a global environmental concern that threatens sustainable agriculture. Accelerated soil erosion caused by the water flow and seepage that occurs through earth irrigation structures gives the big impact on the sustainability of irrigation systems. The eroded soils from embankments and deposition of sediment in irrigation systems frequently reduce the capacity of irrigation, block irrigation canals and shorten the lifespan of irrigation systems resulted in most irrigation projects have been damaged. Earth irrigation structures are mostly constructed in developing countries (i.e., Cambodia). Earth canals are simply dug in the ground, and the bank is made up from the removed earth (Brouwer et al., 1985). The high risks of earth canals are surface and seepage erosion. For instance, in Cambodia, where irrigation as a major component of poverty reduction and economic development, erosion along the earth embankments has caused many million dollars to rehab and is threatening the function of irrigation structures in the country. Even the earth irrigation structures were serious deteriorated; there is no available information related to erosion of irrigation facilities in Cambodia.

In geotechnical engineering work, the poor properties of soils are the most important issues affecting the quality of earth irrigation construction. Erosion due to rainfall and water-flow occurs when the erosion resistant forces of soil materials are less than the erosion forces, in such a way that the soil particles are removed and carried with water flow. Lack of surface protection, earth embankments are highly susceptible to surface erosion. When surface erosion continually develops, the embankment will finally be dysfunctional and failed (Powledge et al., 1989). Thus, understanding the process of surface erosion remains vital to evaluate possible protection methods and to reduce the risk of erosion for the earth irrigation structures.

The process of surface soil erosion by water starts from falling raindrops creating compression and shear stress to detach soil particles (Al-Durrah and Bradford, 1982). While some water infiltrates into the soil, the excess of water contributes to surface runoff (i.e., overland flow). The detached soil particles are then transported by surface overland flow (Fig 1.1). Smith

and Wischmeier (1962) grouped the influential soil properties on soil erodibility by water into two categories: (1) properties that effect the infiltration rate and permeability; and (2) properties that can resist particle dispersion, splashing, abrasion and transporting forces of rainfall and runoff. The detached soil particles by raindrop strikes may clog soil pores that reduces the amount of water entry into the soil, thus increasing surface runoff and the amount of surface soil losses (Návar and Synnott, 2000). On the other hand, when soils can absorb falling raindrops energy, rainwater can flows gently on the soil surface where it gradually infiltrates into the soil; in this way, the clogging of soil pores can be prevented (Derpsch, 2008). The detachment of soil particles by raindrop strikes depends on several factors such as the intergranular shear, the viscosity of pore fluid, the kinematic energy of raindrops, and the mechanical bonds (Cruse and Larson, 1977). Ellison (1948) pointed out that each soil may vary in its detachable and transportable characteristics depending mainly on its texture and cohesion. Wishmerier and Mannering (1969) mentioned in their studies that soils with high silt contents are the most erodible materials. Because of low resistance to raindrop strikes and shear stresses, silts can cause serious erosion.

Regarding to surface erosion, surface runoff is one of the main erosive agents caused serious soil erosion; but surface runoff can be successfully controlled by protecting soil with a surface cover (Smets et al., 2008). Various soil surface covers were used to reduce the direct impact of raindrops and runoff on surface bare soils, including mulches and vegetation (Hueso et al., 2015). However, these types of the soil surface covers can affect soil structure due to the presence of decaying plant residues, which can block soil pores resulting in a slower water entry rate (Angers and Caron, 1998). Aside from the obstructing soil pores, vegetation cover can lead to embankment deterioration because of roots penetrating through the embankment body associated with soil fragmentation (Zanetti et al., 2011). In practice, it is important for earth irrigation structures maintain its integrity and stability, thus, a better surface cover, which has less effect on the structural stability, should be considered.

Many studies have shown that adding a small percentage of cement to the soil can dramatically increase soil strength (e.g., Kawamura and Diamon, 1975; Lade and Overton, 1989; Abdulla and Kiousis, 1997; Sasanian and Newson, 2014). Soil cement, known for its low cost, has been successfully used to increase stability for various earth structures such as road,

foundation of irrigation structure and brick or block materials for houses (Ola and Mbata, 1990; Mubee, 2005; Sariosseiri et al., 2011; Agrela et al., 2012; Mehenni et al., 2016). However, using soil cement as a control against surface erosion for earth irrigation structures has not been fully studied. In most studies investigating soil particle detachment and surface erosion, untreated soils were used (Young and Wiersma, 1973; Poesen, 1981; Nearing and Bradford, 1985; Khaledi et al., 2014). The mechanism of soil particle detachment, and roughness of soil surface were frequently focused on rain erosion resistance tests; rather than study on the precaution of surface bare soil protection (Romkens et al., 2002; Gomez and Nearing, 2005; Zhao et al., 2018). Therefore, purposes of this study were to get detail information on soil cement mechanical properties and the effectiveness of soil cement application used for surface erosion protection for earth embankments.

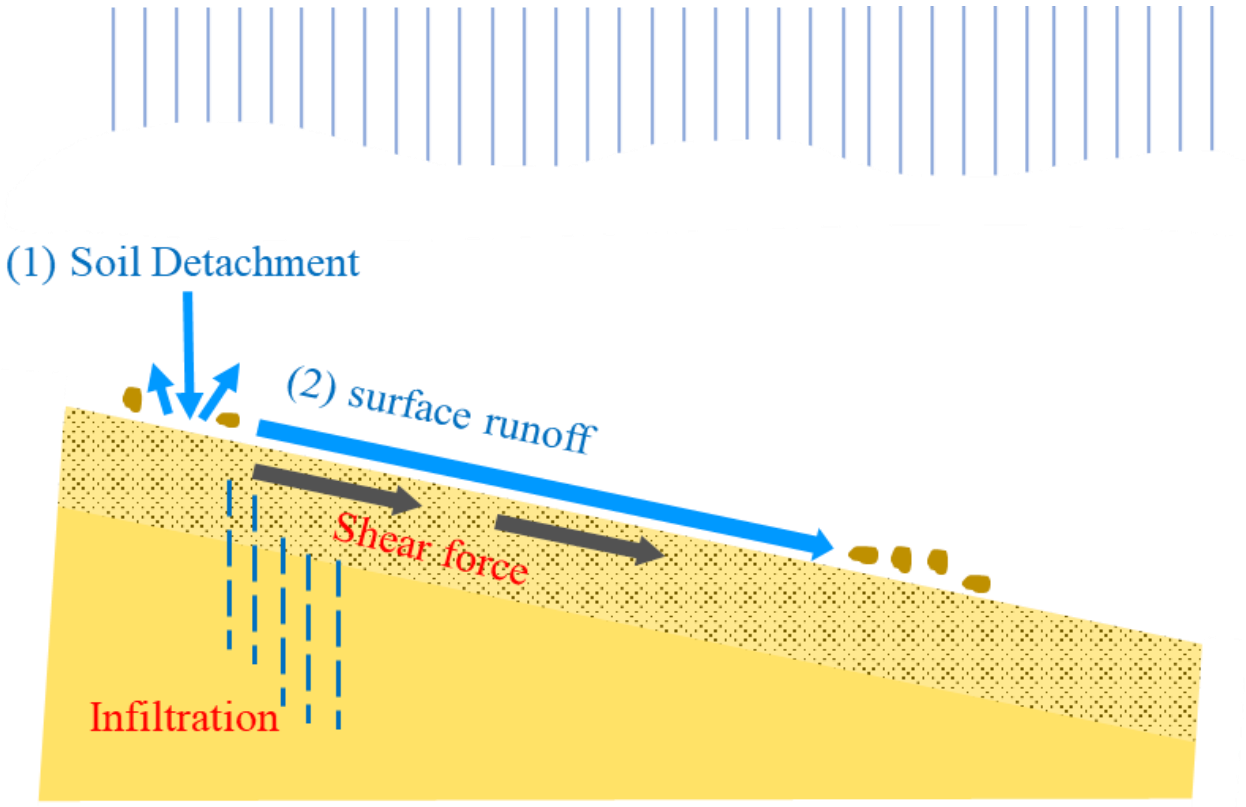

Fig 1. 1 General layout of soil surface detachment and transportation on earth embankment

1.2 Objectives

The overall objectives of the research presented in this thesis are:

1) To investigate the field situation and eroded earth irrigation facilities in Cambodia,
2) To determine the physical, mechanical and hydraulic properties of soil treated with cement,
3) To assess the resistance of soil treated with cement to surface erosion under rain erosion resistance test.

The first objective was responded by measuring the erosion trenches on earth embankment and obtain a fundamental soil physical properties from investigation sites. The second objective was addressed by experimentally testing the physical, mechanical and hydraulic properties of soils, particularly in regard to shear strength of silt treated with cement using the triaxial test with different cement contents, curing times and confining pressures. The soil resistance to erosion was then evaluated experimentally using rainfall simulator with soil slope covered with the cement mixed with silt on the surface slopes.

1.3 Conceptual framework and scope

The general conceptual framework of experimental study in this research is shown in Fig 1.2. To assess the effectiveness of soil cement application against surface erosion, the mechanical and physical soil properties tests are conducted, which include grain size distribution, soil density, compaction, and soil shear strength. Besides conducting physical and mechanical test, hydraulic property test, which focused on hydraulic conductivity and soil water retention, is also investigated. Rain erosion tests of soil cement are carried out under two different rainfall intensities: 50 and 100 mm h^{-1}. This study is targeted on surface erosion.

1.4 Thesis outline

This thesis consists of 7 chapters. Chapter 1 describes a general background of soil erosion on earth irrigation structures, study objectives, conceptual framework and scope of research study. Following the introduction chapter, in Chapter 2, previous experimental works and gaps of those

studies are reviewed. The field investigation on erosion occurred on earth irrigation structures in Cambodia is presented in Chapter 3. In Chapter 4, the experimental designs, experimental procedures and data analysis are described. The results of element testing, in which the changes in soil properties after stabilization and detail on shear strength parameter achieved in different cement contents, curing times and confining pressures are discussed, are presented in Chapter 5. The resistance of soil cement to surface erosion under rain erosion tests are presented in Chapter 6. The conclusion and suggestions for further research are presented in Chapter 7.

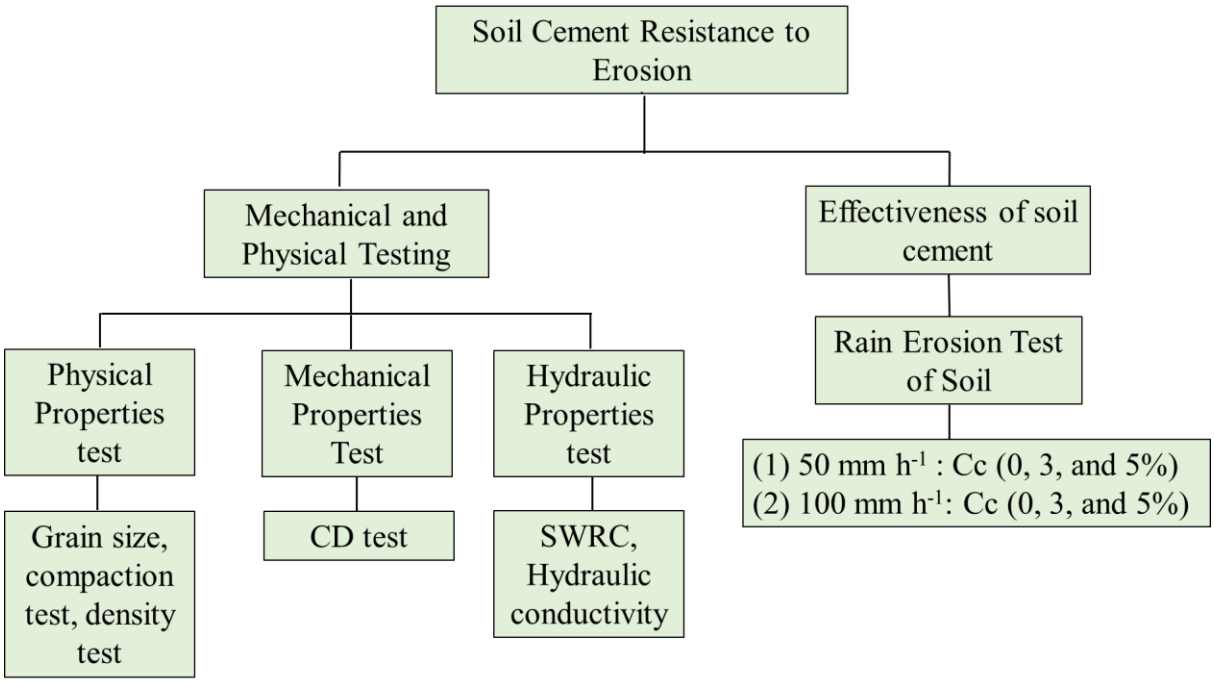

Fig 1. 2 Diagram of conceptual framework of research study

Chapter 2 Literature Review

Erosion on earth irrigation structures occurs when the erosion resistant forces of soil materials are less than erosive forces. Most studies were devoted to erosion mechanism; soil erodibility and soil surface structure degradation caused by rainfall and surface runoff. In this chapter, some of the theoretical erosion; soil detachment and the previous studies related to rain erosion experiments are reviewed. Some of the measures against erosion applied in earth irrigation structure are also included in this chapter.

2.1 Erosion zone on embankment

The earth irrigation structures are frequently encountered with water erosion. Surface and seepage erosion is commonly found in earth embankments. However, the surface erosion is the main cause of earth embankment failure. The poor construction soil material, strong rainfall, and runoff can cause serious surface erosion on earth embankments. As mentioned by Powledge et al. (1989), earth embankments will be quickly deteriorated due to continuing surface erosion.

Fujisawa et al. (2008) pointed out that embankment erosion due to runoff is the most frequency cause of embankment failures. Earth irrigation structures are usually in danger of soil erosion due to low resistance forces of soil materials (Indraratna et al., 2012). Thus, it is important to know the erosion zones on earth embankment. Powledge et al. (1989) described that flow regimes and erosion zones of an embankment can be possibly divided into three zones (1) on the dam crest, (2) dam crest to downstream slope, and (3) on the steep downstream slope. On the erosion zone (3) described above, surface flow is rapidly accelerated due to the steep slope, and increases the velocities that lead to increase the tractive stress creating high erosion potential (Fig 2.1). Thus, structural protection systems need to consider this effect in the design stability analyses. However, the stability of the embankment and erosion rate is directly related to many factors such as rainfall, slope gradient, in particular the strength of soil used for construction.

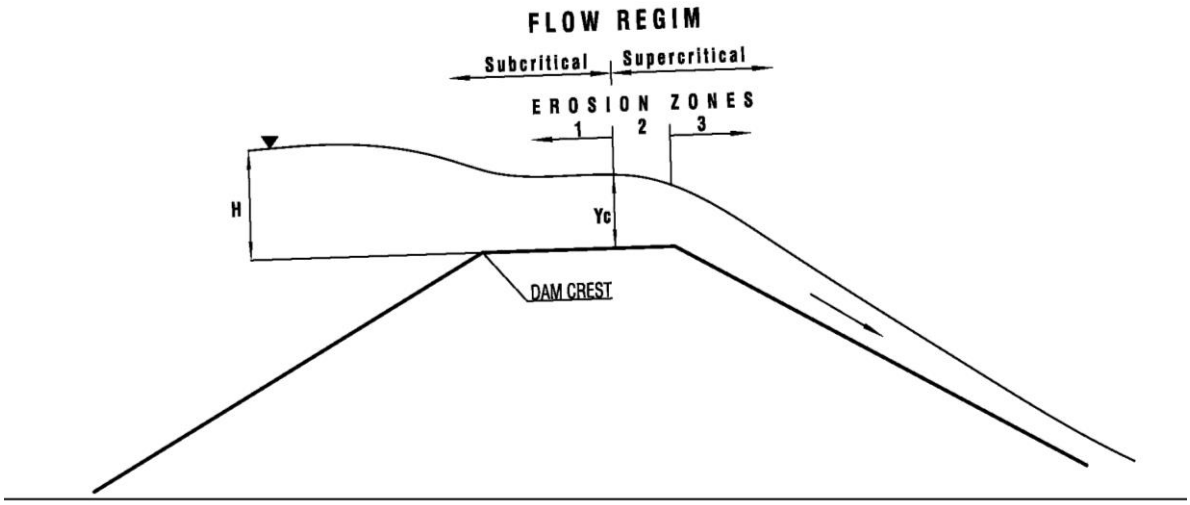

Fig 2. 1 Flow regime and erosion zones on embankment (Powledge et al., 1989)

2.1.1 Embankment protection systems

To prevent the erosion on earth embankment from rainfall and overflow, numerous protection systems have been proposed. Powledge et al. (1989) made a summary on the most common protection systems from rainfall detachment and overflow in Table 2.1. Only limited use of the system in Table 2.1 have been devoted specifically to embankment overtopping protection. This most common application of surface soil protection against surface erosion is vegetation covers. From a hydrological point of view, plants reduce soil erosion rates by intercepting raindrops, enhancing infiltration, transpiring soil water, providing additional surface roughness, and adding organic substance to the soil (Morgan, 2005). Vegetation for reducing soil erosion was considered as an important method which was commonly used in soil conservation practices on agricultural fields or construction sites. However, combination of different external factors such as biological (old wormholes), chemical (pH, nutrients), hydrological (water content), microclimatic (soil temperature) and physical (soil texture, soil mechanical impedance, soil structure) was affected on efficiency of resistance of plants to erosion (Gyssels et al., 2005). Some researchers also found the negative impacts of vegetation covers on soil structures; the roots had a significantly stabilizing effect on aggregate stability, but dead root mass did not significantly influence splash for a silt loam soil in their rainfall simulation experiment. Thus, roots may have stabilized the soil aggregates, but these

stabilizations are not strong enough to sustain the impact of raindrops (Angers and Caron, 1998; Ghidey and Alberts, 1997).

Table 2. 1 Embankment protection systems (Powledge et al., 1989)

Protective System	Description
Vegetation/Geotextile	Grass established on embankment surface Wide range of manufactured fabric, mats, or larger-scale cells that can be incorporated within embankment surface before grass is established.
Cements	Used to form either a soil-cement or roller compacted concrete surfacing of selected embankment section
Concrete blocks	Specially shaped precast concrete blocks that are designed to interlock mechanically or that tied together by cables that are run through the interior of the blocks
Riprap	Well-graded stone of a specified mean diameter placed on embankment surface to a specified thickness.
Gabion	Uniformly graded stone contained in wire mesh cells covering embankment surface

2.2 Mechanism of erosion processes

Erosion is a process continually transforming the soil surface. The mechanism of surface erosion on the embankment is initiated by the rainwater fallen on the soil surface that create soil detachment through compression and shear stress. Some water infiltrates into soil. When the soil is saturated or water falling on the ground is greater than the infiltration rate of surface, surface runoff appears. Then, this surface runoff transports the detached soil particles, this process is called transportation which detached particles are transported. In general, soil erosion is considered as two phases process consisting of detachment of soil particles and their transport by erosive agents such as surface runoff (Morgan, 2005).

2.2.1 The mechanism of raindrop detach soil surface

To discover the mechanism of soil detachment caused by a single raindrop, Mihara (1951) used a high speed camera to capture the splash on the sand. The results showed that a raindrop initially detached and simultaneously penetrated the soil surface and outspread.

However, the depth of detachment depended on the soil surface conditions; in particular the water content. The low water content of the surface soil, the raindrop could quickly percolate down through the soils. In contrast, the high water content of surface soil, the rain water was very slowly penetrated. Due to the limitation of Mihara study, Al-Durrah and Bradford (1982) extended the study by increasing the number of soil specimens by adding more variables such as water potential, bulk density and soil surface conditions.

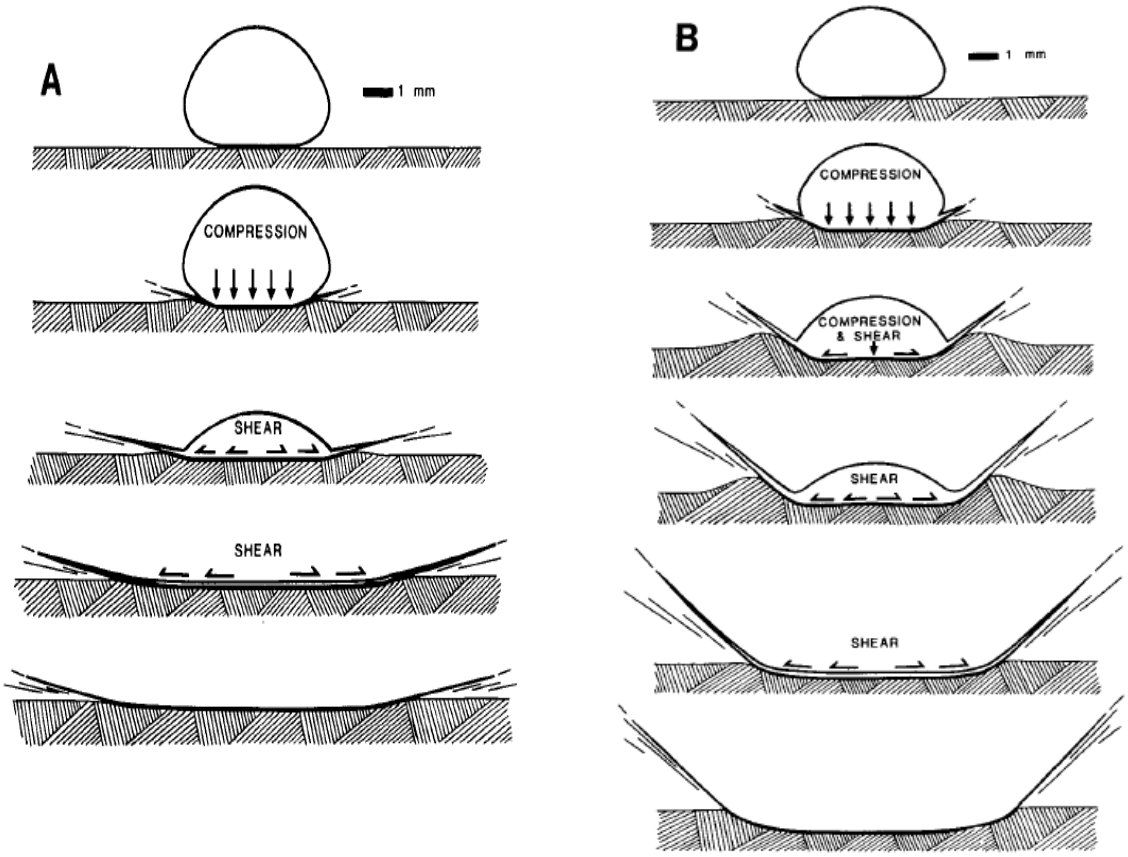

Fig 2. 2 Splash mechanism at high strength (A) and low strength soil (B) (Al-Durrah and Bradford, 1982)

Al-Durrah and Bradford (1982) used a high-speed camera to capture the impact of raindrops on soil specimens. For high strength soils or a dense density specimen, the cavities were larger in diameter but much shallower in depth, resulting in smaller volume cavities than those with low strength soils (Fig 2.2). Ellison (1945) mentioned that when raindrops strike the surface soil, they break down the clods and aggregates; this separation of soil particles develops a single grain structure in the soil. From this point, the erosion is initiated by great force of raindrops as they strike the surface soil. The earth embankments are prone to erosion, a thin layer of topsoil on the embankment is easily removed; this is called sheet erosion.

When the sheet erosion continues to develop, rill erosion subsequently occurs due to runoff water and forms small channels as it concentrates down to a slope. If the rills become deeper, gully erosion occurs afterward.

2.2.1 Relation of erosion with soil texture, detachment and transportation

Ellison (1948) demonstrated a relationship between soil texture and erosion was that each soil would vary in its detachable and erodibility characteristics, as well as in its transportable characteristics. Soil texture was believed to influence erodibility and transportation. Several studies suggested that large soil particles were more resistant to transport due to the greater force required to entrain them. Meanwhile no fine particles were resistant to detachment because of low cohesiveness (Ellison, 1948; Young, 1980)

For a better understanding of how and to what extent each of various soils affects its erodibility, Wischmeier and Mannering (1969) conducted a long-term experiment to assess the soil properties that resist detachment and transportation. They found out that soils with high content of silt, low one of clay, and low one organic matter were the most erodible. Richter and Negendank (1977) also reported that the least resistant particles were silts and fine sands. Thus soils consist of 40% of silt were highly erodible. The amount of clay content also effected on soil erodibility; 9% and 30% of the clay content was the most susceptible soil to erosion (Evans, 1980). The erodibility decreases as the clay fraction becomes larger; this effect is probably attributable to increase cohesiveness. As Trout and Neibling (1993) addressed that the erodibility of the soil depended upon the strength of bonds between particles, namely cohesion of soil.

2.2.2 Shear stress and soil shear strength related to erosion

In geotechnical engineering, shear strength is one of the most concerns because in most problems related to foundation and earthwork engineering; failure of earthwork frequently results from excessive applied shear stresses. To investigate shear strength of soil specimens, there are many different experiments such as direct shear test; tensile shear test; vane shear test and triaxial compression test. In an early study of soil mechanic, direct shear test was the most popular testing method often used to investigate the shear strength of soil because it was very simple and directly measure shear and normal stresses. Adams and Lewis (1997) stated that a tensile shear test was also commonly used for primary non-technical reasons to

determine shear properties of soil. Unfortunately, the tensile shear test was not reliable quantitative test because the stress state in the specimen was complex. Another shear test is vane shear test; it is used to determine the undrained shear strength of soils especially soft clays. The vane shear test can be conducted in laboratory or in the field directly. To improve the accuracy of shear testing methods, another new shearing test was developed called cylindrical compression test or triaxial test. The triaxial test is much more complicated, but also much more flexible. The triaxial test is a better design compared to the previous shearing test methods due to the controlling of drainage and stress path. The complete state of stress is assumed to be known at all stage during the triaxial test whereas only the stresses at failure are known in the direct shear test.

According to Brunori et al. (1989), shear stress and soil strength is an important parameter governing soil erodibility. Léonard and Richard (2004) described that soil shear strength is often presented as the best soil property to predict critical shear stress; it is usually used as a basis for understanding the detachability of soil particles by raindrop. The shear strength of the soil refers to a measure of its cohesiveness and resistance to shearing forces exerted by gravity, moving fluids and mechanical loads. Morgan (2005) explained that soil strength is derived from frictional resistance met by its constituent particles when they are forced to slide over once another or to move out of interlocking positions. Soil shear strength is a measure of resistance to failure under applied force. Shear strength is generally expressed by an empirical equation:

$$\tau = c + \sigma \tan \phi \qquad (2.\ 1)$$

Where τ is the shear stress required for failure to take place; c is cohesion or apparent cohesion, σ is the total normal stress and ϕ is the angle of internal friction. The c and ϕ are strength parameters of soils rather than physical properties of the soil.

Bryan (2000) proposed that cohesion appeared the most important control on the resistance of coherent soils, but it was difficult to obtain useful measurements for the portion of the soil directly affected by erosive forces. Because of the difficulty in estimating the critical shear stress between soil particles, critical shear stress is often considered as a calibration parameter in soil erosion models (Léonard and Richard, 2004). Gilley et al. (1993) stated that critical shear stress values estimated from flow experiments on various soils were

statistically related to different soil properties, such as soil texture, soil organic matter, and soil bulk density.

2.3 Investigation and measurement of soil erosion

2.3.1 Rainfall simulator background

To obtain the information on soil detachment and soil resistance to water induced erosion, rainfall experiments are usually conducted. Rainfall simulation experiment is a useful technique, which can obtain the relationship of soil and hydrology response to rainfall characteristic. Rainfall simulation test is commonly used by many researchers in erosion studies (Young and Wiersma, 1973; Ola and Mbata, 1990; Römkens et al., 2002). Smith and Wischmeier (1962) reviewed that rainfall simulation equipment was developed in 1930 to measure the erodibility and infiltration of soil. The main purpose of designing rainfall simulator is to generate the actual rainfall intensity which can provide precise information on soil erosion and hydrological processes. More important of rainfall simulator is to imitate natural rainfall and release the rainwater to fall uniformly on the surface soil in order to measure the runoff and determine soil losses (Van Dijk et al., 2002). Two types of rainfall simulators, nozzles and drop formers, are commonly used in rainfall experiment. Wilcox et al. (1988) mentioned that the nozzle simulator could classified into two types (1) gravity fed; (2) pressurized; which could potentially produce heavy rainfall depending on the number of nozzles were equipped. The more nozzles used, the greater the water pressure needed, and the more water intensive the simulator became. Nozzle simulators can produce a range of drop sizes closer to, but still not exactly that of, natural rainfall, due both to the design of the nozzle and the operator's ability to manipulate the water pressure. Drop size distribution is one of the most important variables of rainfall simulation, a key indicator of the kinetic energy released by the drops, and therefore their potential for eroding soil. Other key variables are the height of the drop-formers above the plot surface in meters, which affects impact velocity and, therefore, kinetic energy, the duration of the simulated rainfall, the intensity of the rainfall, and the spatial distribution of the rainfall over the plot surface.

2.3.2 Laboratory studies on rain erosion test

Young and Wiersma (1973) investigated on raindrop impact and flowing water to soil erosion. To determine the impacts, an experimental laboratory was conducted with three different types of soils: loam, silt loam and sandy loam, were subjected to rainfall simulator. A 1.52 x 4.52 m soil plot was used and set up to 9% of gentle slope for testing. On the surface soils, two furrows were formed. The rainfall intensity 4.6 $cm.h^{-1}$ was applied to the soil plot. The schematic of plot setup is shown in Fig 2.3. The results showed that 80-85% of the soil loss was transported to a rill before leaving the plot. Although rainfall impact energy was primarily responsible for soil detachment, transport of detached particles from the plot was carried by the rill flow on the soil surface.

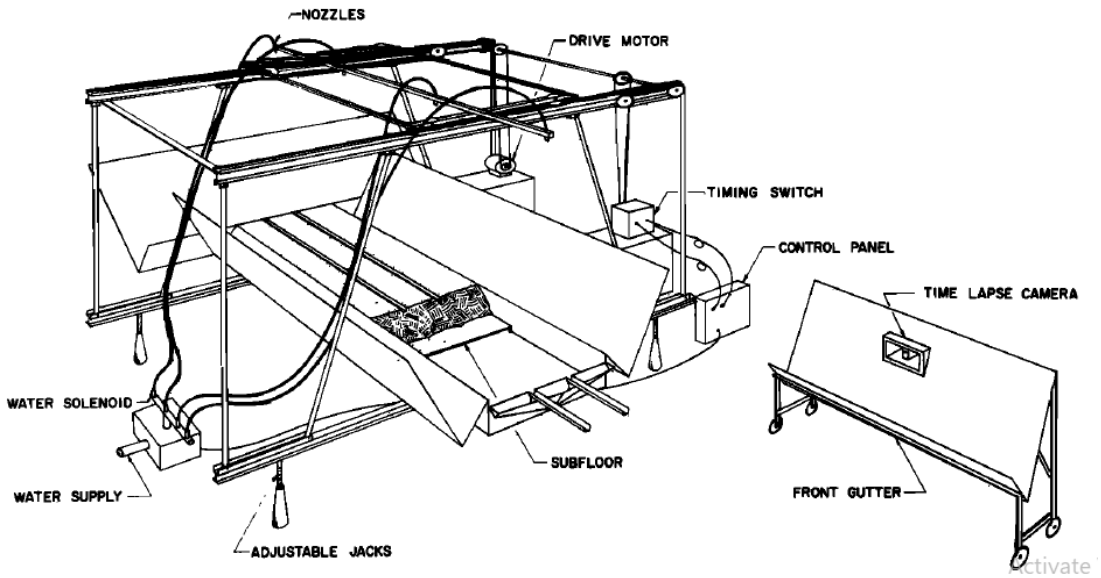

Fig 2. 3 Schematic of plot setup for experiment (Young and Wiersma, 1973).

Römkens et al (2002) conducted an experimental study on soil erosion under different rainfall intensities, using slope adjustable flume equipped with rainfall simulator, to assess the surface roughness and soil water regimes response to erosion (Fig 2.4). The scale of the equipment 3.7 x 0.61 x 0.23 m which could adjust 0-17% slope. This equipment was attached to an inlet tank at the upper head of the flume that could produce overland flow. In this experiment, a series of four rainstorms were applied and reversed a sequence, having the same amount of rain, but with different rainfall intensities, 60, 45, and 15 mm h^{-1}. The experimental soil consisted of 18% clay, 80% silt, and 2% sand. The soil surface conditions were smooth

with surface elevation variations of about 1 mm or less, a surface roughness by placing air-dried clods and aggregated soil material on the surface soil bed. The slope steepnesses were 2%, 8% and 17%, which were really gentle compared to the embankment slope of irrigation structures. The surface topography was determined by using a laser mircroreliefmeter, grid spacing was 3 mm. Surface and subflow were collected separately. In addition, the tensiometer was inserted into the soil bed to monitor the soil water pressure. The results showed that smoother surfaces had less soil loss than rough surfaces.

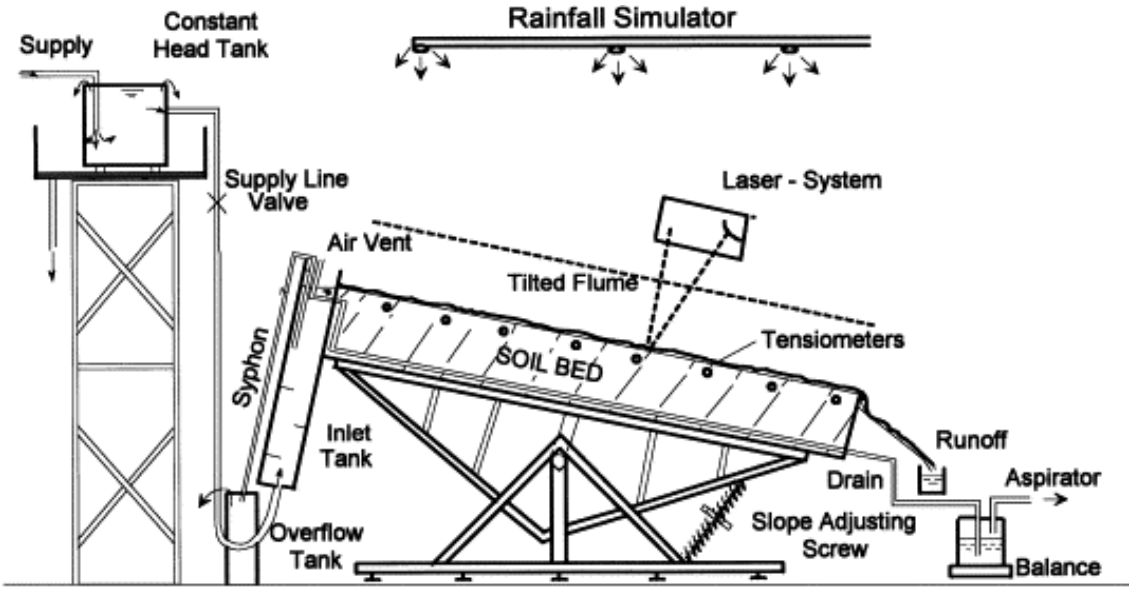

Fig 2. 4 A slope adjustable flume and experimental set-up (Römkens et al., 2002)

Surface roughness conditions determine drainage network development, sediment yield rates are related to the local topographic gradient distribution, and rainfall intensity sequences affect soil loss. Subsurface soil water pressure substantially affects the sediment concentration regime.

2.3.3 Studies of stabilization of soils against erosion

There are many different techniques for erosion control such as mulching, vegetation cover, Geomat and soil stabilization with chemical addictive. Soil treatment with different types of treatment products is extensively used in geotechnical engineering to improve soil characteristic. Soil cement is one of the soil stabilization techniques widely used for erosion control. The natural soils usually do not meet the required engineering properties to serve as a

good construction material. Therefore, to improve the engineering properties of less desirable soils; stabilized agents are added. There are many studies related to soil stabilization against erosion, thus some reviews of those studies are discussed in this section.

Akky and Shen (1973) studied on erodibility of a compacted cement stabilized sand by using the rotating cylinder apparatus. Sandy soil was used to stabilize with cement content at 1, 1.5, 2 and 3 percent of cement by dry weight. The curing time of the soil sample was 7 days in a constant temperature moisture room. To investigate the erodibility of cemented sand, wet-dry or freeze-thaw cycles were applied to various samples to determine the effect of environmental changes on the mechanical and hydraulic stability of the soil. The results showed that the erodibility of a cement stabilized sandy soil decreased as the unconfined compressive strength increased. Note that the unconfined compressive strength of soil increased with cement content. Akky and Shen (1973) concluded that a simple relationship between the unconfined compressive strength and the critical shear stress could be established in the range of cement content addition. However, a realistic of soil erodibility is not possible unless the influence of the environmental factors on soil properties is considered.

The erodibility of the soil is quite complex due to the fact that the amount of cement content or unconfined compressive strength is not the only variable to assess the resistance to erosion, but the hydraulic parameters and the field conditions also important factors distribute to soil erodibility.

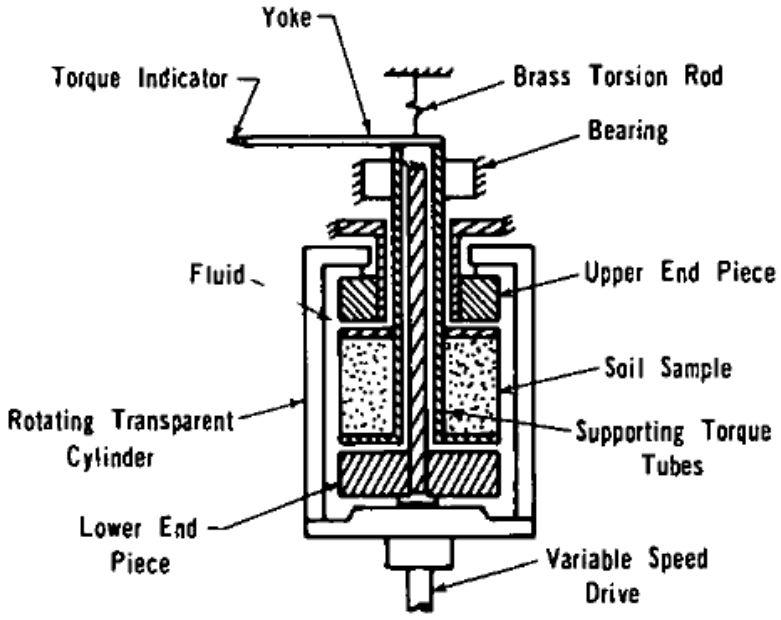

Fig 2. 5 The rotating cylinder apparatus (Akky and Shen, 1973)

Kawamura and Diamond (1975) conducted a laboratory study on stabilization of clay soil against rainstorm erosion to prevent soil detachment. The simulated rainfall equipment was used to deliver a rainstorm at rainfall intensity, 82 mm h^{-1} to three different soil groups. Lime and cement were used to stabilize clay soil with the low content 1, 2.5 and 5% by dry weight. The soil specimens were compacted into a 4 inch diameter mould and maintained at an angle of 5 degrees to horizontal to permit free runoff. The runoff from each specimen was collected. The sediment was removed from runoff, dried and weighted to obtain the direct assessment of erosion loss. The results showed that soil stabilization with cement effectively reduced or eliminated raindrop impact associated with soil losses. The soil stabilized with a minimal amount of cement and lime in this study was not rendered impermeable or developed a high strength. However, it could reduce the impact and amount of soil loss at a certain extend. A major problem with applying hydrated lime and cement in inadequate amounts to highly acid soils would increase erosion loss due to the fact that pH level increase, raising pH sufficiently to destabilize previously existing acid flocculation bound aggregates.

With a small amount of cement can improve the resistance of soil specimens to rainfall, but soil properties should be well identified before adding the stabilized agents. This study provided the general view of soil stabilization used for erosion control, but the specimen used for the experiments was small which could not cover the big aspect of the erosion process. It covered the detachment process under severe rainstorm, rather than focused on soil loss related to surface flow with the longer length plot.

Ola and Mbata (1990) carried out rain erosion resistance test on brick made from soil mixed with cement. However, the purpose of this experiment was to assess the strength of soil cement brick for building construction. Soil cement bricks were tested under simulated rainfall equipment. The schematic of the rain simulating apparatus is shown in Fig 2.6. The results showed that the resistance of the soil cement bricks to erosion was enhanced by an increase in compaction pressure and cement content. The bricks stabilized with 5% of cement were found more durable to rain erosion. The higher cement content added, the lower weight losses were observed. However, higher water velocities of rainfall resulted in corresponding higher losses in weight of the soil cement bricks during rain erosion test.

Another soil stabilization by using waste rock powder and lime was investigated by Mubeen (2005). The purpose of the research was to improve the strength and the workability of soft clay soil in irrigation project to avoid the problems of soft clay on irrigation structures.

A high plasticity and low shear strength soil, namely Dutch soft clay, were used in this study. The laboratory experiment condition is shown in Fig 2.7. The results showed that the unconfined compressive strength showed an excellent increase in strength and workability. The strength improvement caused by waste rock powder is more significant improved for those soils which have a low clay content. It has also been found the stabilization cost of structures on soft clay can be significantly reduced compared to other methods.

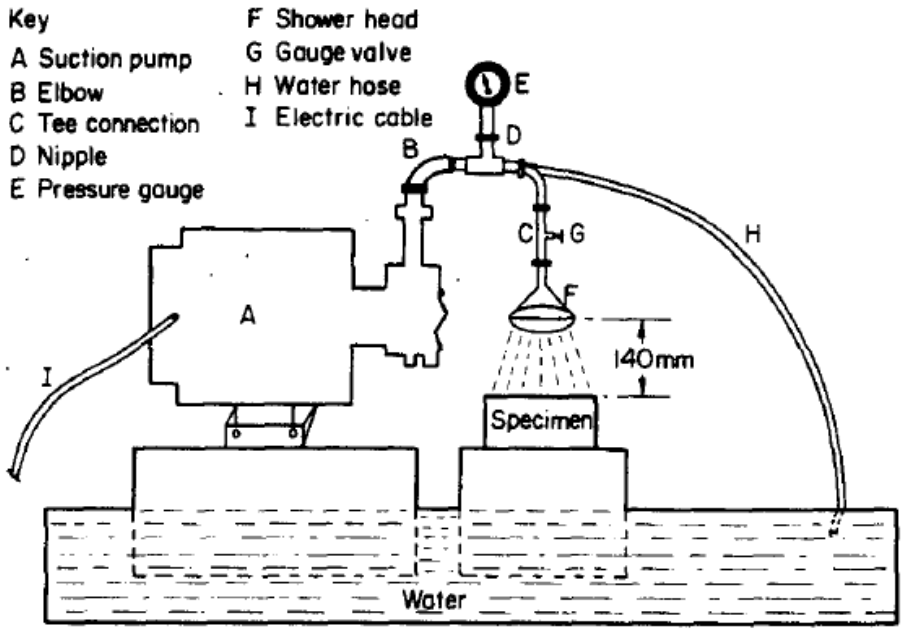

Fig 2. 6 Schematic representation of rain simulating apparatus (Ola and Mabata, 1990)

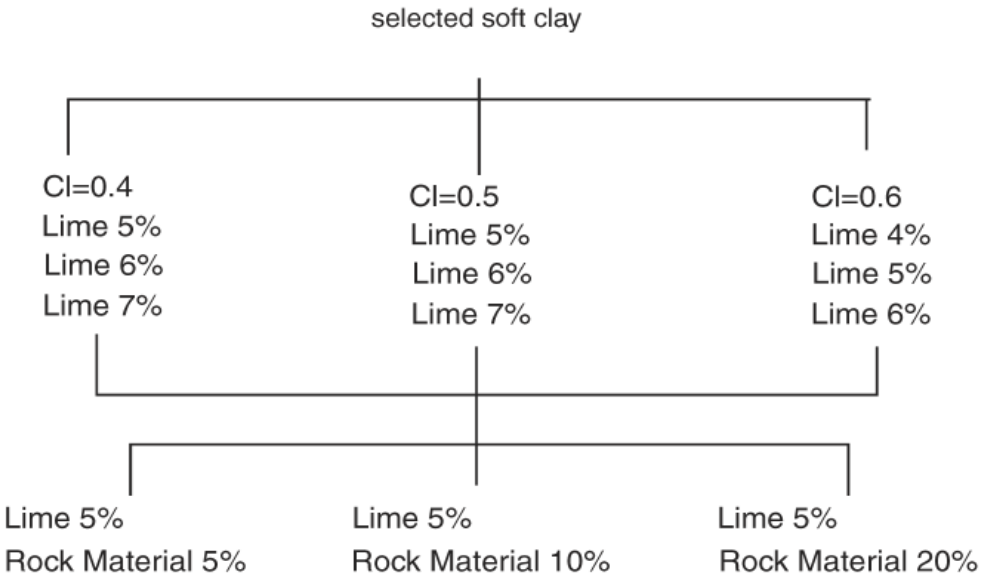

Fig 2. 7 The scheme of research investigation (Mubeen, 2005)

Sariosseiri et al. (2011) researched on the erosion control of slopes by using cement kiln dust (CKD) to stabilize soil. A natural slope under severe erosion in the field was selected to examine the effectiveness of soil stabilization against erosion, while another element test was conducted in a laboratory by collecting six soil samples to investigate its physical and mechanical properties. The slope with a surface area of 80 m^2 was divided into four sections. No additive was added to the first section of slope while the top 30 cm soil of the second, third and fourth section was treated with 5, 10 and 15% cement kiln dust by dry weight, respectively. The slope angle of this study was about 23^o. For field investigation, the slope was surveyed monthly in order to measure the soil losses. The results of the in-situ and laboratory experiment showed that soil treated with CKD increased compressive soil strength and reduced soil erosion significantly in slope field.

In a field of erosion study, it is necessary to know the relationship between rainfall intensity and soil loss. However, there is no information on erosive agents in particular the variation of rainfall intensity in this area. In this study, the measurement of soil loss from slope was surveyed monthly without mentioned the variety of rainfall, or wind condition. Thus, setting up the condition of the study is very important to obtain the precise data on the soil cement application for erosion control.

Mehenni et al. (2016) used soil cement for an internal erosion study. Silt was used to mix with various types of treatment products such as kaolinite, bentonite, quicklime and cement. The percentage of stabilized agents were calculated based on dry soil weight. The hole erosion test (HET) was used to measure the erodibility rate of soil stabilization. This study also described the effects of stabilized agents on soil. A new enhanced HET was developed to apply a high inlet pressure up to 650 kPa which generated a hydraulic shear stress up to 10,000 Pa. The internal erosion resistance was determined by the coefficient of soil erosion and the critical shear stress. The results of this study showed that cement treatment primarily increased the critical shear stress of silt. This increase was higher with cement treatment. Note that the enhancement occurred rapidly for 3% cement, whereas higher percentages required additional curing time to reach greater erosion resistance.

It is necessary to extend the study of soil cement application to surface soil erosion on earth embankments since most embankment erosion due to overland flow is the number one cause of embankment failure (Fujisawa et al, 2008). A rain erosion resistance test on a large scale of soil slope model is necessary to obtain a detail information on how soil cement

application can prevent surface erosion on earth embankments. The interactions between rainfall intensity, soil detachment and soil losses have been studied before, but the quantitative information about the effects of soil cement on soil erosion under rain erosion test is still limited. For soil stabilization, the soil water content is reduced, but increases the cohesiveness of the soil which can reduce detachability by runoff shear force and raindrop impact. However, a low water content of the soil cement application might increase aggregate slaking and breakdown upon a rapid wetting under rainstorm event and raindrop, subsequently soil is easily transported by overland flow. Thus, it should be carefully investigated the relationship of a low soil water content response to soil detachment under high rainfall intensities.

2.4 Mechanism of soil cement stabilization

The ordinary Portland cement consists of various components such as lime (CaO), Silica (SiO_2), Alumina (Al_2O_3), Iron Oxide (Fe_2O_3), Magnesia (MgO) and Sulphur Trioxide (SO_3). These compositions are major strength producing components. When the water with soil comes into contact with the cement, the hydration reaction of the cement occurs rapidly and primarily forms a cementitious product called soil cement. The cement particles bind the adjacent cement grains together during hardening and form a hardened soil bodies. According to Bergado et al. (1996) mentioned that the cement hydration and the pozzolanic reaction can last for months or even years after the mixing, thus the strength of cement treated soil are expected to increase with time.

2.4.1 Factors effect on the hardening characteristics of soil cement

The hardening characteristics of soil cement depend on number of factors. The effects of some predominant factors on the strength of the soil cement are briefed as following:

2.4.1.1 Type and amount of cement content

The type and quantity of various stabilizers have different effects on the strength development of different soils (Porbaha et al., 2000). Porbaha et al. (2000) also mentioned that an increase in the quantity of the stabilizing agent will increase the compressive strength at different rates, depending on the type of soil and properties of the stabilizing agent. For

instance, the study on the effects of cement content on compressive strength of soil cement by Uddin et al. (1997) in Fig 2.8 showed that the higher amount of cement content added, the high compressive strength obtained.

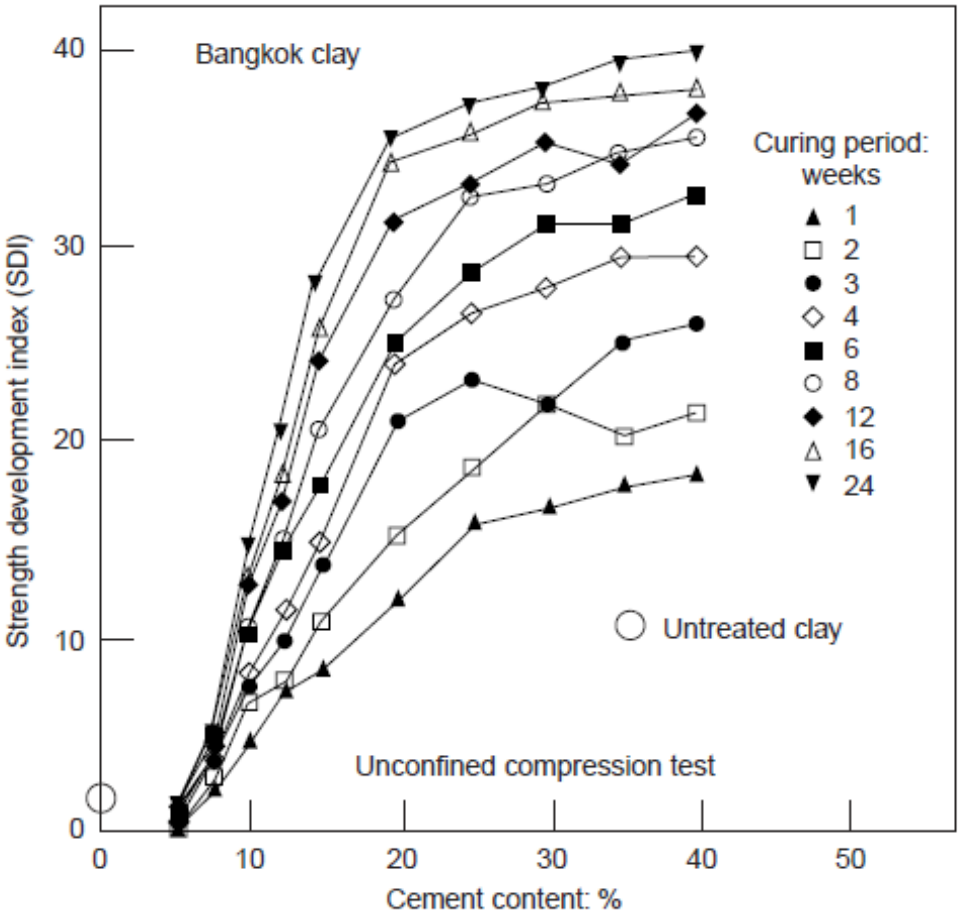

Fig 2. 8 Variation of strength development with cement content (Uddin et al., 1997, verified by Porbaha et al., 2000)

Yoon and Abu-Farsakh (2009) conducted the experiment on cemented sand also found out that the improvement effect mainly depended on the amount of cement content added. In the earlier study by Kawasaki et al. (1981) investigated ordinary Portland cement on the strength characteristics of two different Japanese soils. It was concluded that the improvement effect solely depends on the chemical components of cementing agent and also the properties of the local soil (Fig 2.9). Ahnberg et al. (1995) studied the effect of different stabilizing agents on various soft soils by using cement, lime and cement with lime. The results showed in Fig 2.10 indicated that cement increased soil strength better than other types. Thus, cement is commonly used to improve soil strength in various geotechnical engineering works.

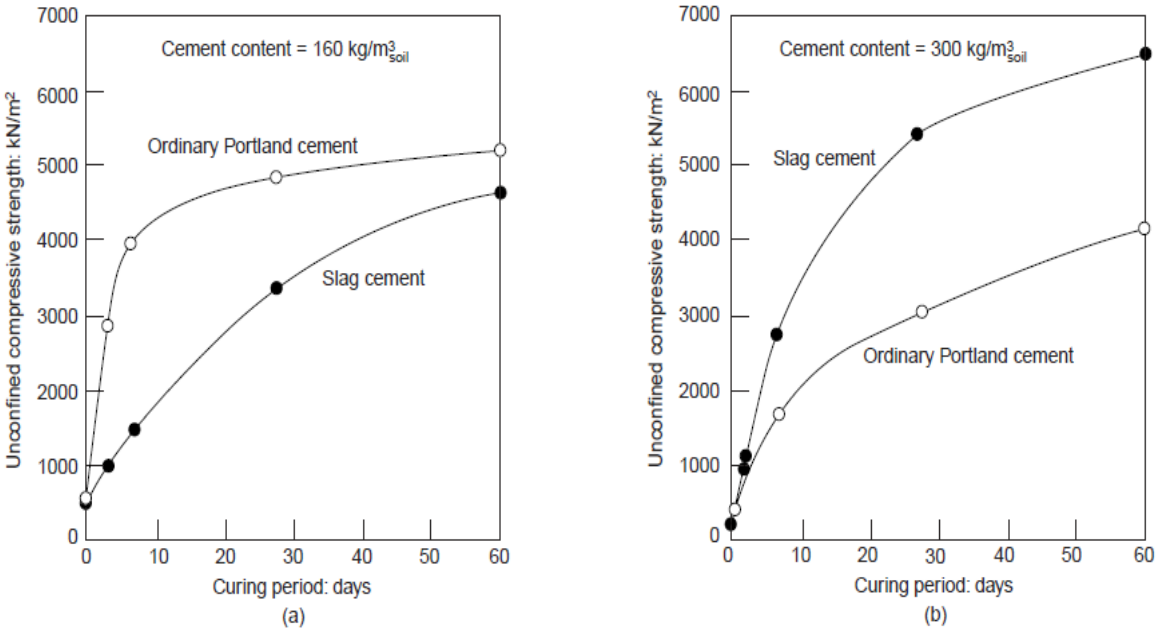

Fig 2. 9 Effect of cement type on soil cement strength: (a) soil from Kanagawa in the Tokyo bay (b) soil from Saga in Kyushu Island (Kawasaki et al., 1981; verified by Porbaha et al., 2000)

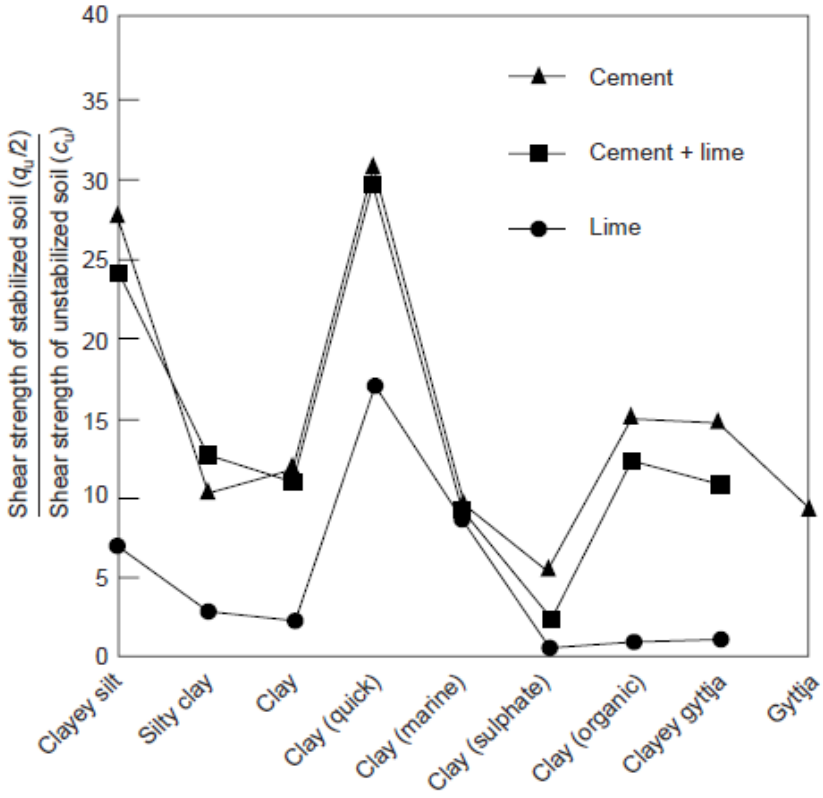

Fig 2. 10 The effect of different stabilizers on compressive strength of soil in Sweden (Ahnberg et al., 1995; verified by Porbaha et al., 2000)

2.4.1.2 Curing time

The strength of the cement treated soil increases with the increase of curing time (Kawasaki et al., 1981; Uddin et al., 1997; Horpibulsuk et al., 2010). Porbaha et al. (2000) reported that soil cement strength generally increases in the early stage of the treatment and thereafter decreases with time. Nevertheless, reduction of strength depends on the amount of cement added. Hayashi et al. (2003) carried out a field observation of long-term strength of cement treated soil in Hokkaido. The results showed that in the central portion of the soil cement columns, the steady strength increase after 17 years was confirmed; however, the leaching of Ca from treated soil was observed. The extent and magnitude of strength reduction at the outer layer of soil cement columns should not be a big concern since this deterioration process was very slow.

2.4.1.3 Soil characteristic

Porbaha et al. (2000) mentioned that the physic-chemical properties of the soil (grain size, water content, pH, organic matter content) affect the properties of the treated soil. In general, the coarse grained soil shows that the largest increase in strength as compared to the fine grained soil for a given cement content. Bergado et al. (1996) reported that the rate of increase in strength of treated soil decreases with the increase of the percentage clay content. The special considerations are also needed in the case of soil with high organic content and soils with an excessive salt content (Porbaha et al., 2000). The rate of increase of strength in cement treated organic soil is commonly reported at a very low strength rate. Not only clay and organic matter, but the silt content is also effected on the strength of cement treated soils. Wischmeier and Mannering (1969) mentioned in their studies that soils with high silt contents are the most erodible materials. Because of low resistance to raindrop strikes and shear stresses, silts can cause serious erosion.

The water content is also effected on the strength of cement treated soils. Miura et al. (2001) studied the behaviour of cement stabilized clay at high water content. The results showed that the clay water/cement ratio is the prime parameter for analysis of strength and deformation behaviour of induced cemented clay at high water content. Miura et al. (2001) concluded that for a given soft clay, the cementation bond strength increases as the clay-water/cement ration decreases due to the final water content of the treated soil is reduced. Yin

and Lai (1998) found that at the higher initial water content of the untreated soil lead to the relatively higher reduction of water content after cementation. A similar result was also found by Uddin et al. (1997); at a certain percentage of cement content the reduction of water content is very high, and thereafter the water content rapidly decreases. Reductions of water content were also found with the increase of curing time. It was suggested that the hydration reaction continues with time leading to the reduction of the final water content of treated soil reduction.

2.4.2 Physical and mechanical properties of cement treated soils

2.4.2.1 Permeability characteristic

Permeability is an important factor in internal and external erosion protection. In internal erosion, where the seepage exist, the cement stabilization was used to construct the cut-off walls to prevent seepage flow (Nussbaum and Colley, 1971). For external erosion, where erosion occurs on the surface soil, soil cement was used to prevent soil detachment and reduce the surface flow. Porbaha et al. (2000) indicated that the pore size, which is formed through hydration process, influences the coefficient of permeability. In general, the permeability of the cement treated soil might reduce with the increase of cement content. As Quang and Chai (2015) mentioned that the cement treated soils, less than 8% cement content by dry weight, the value of k is almost equal to that of untreated soils; however, the k value decreases significantly when the cement content is higher than 8% (Fig 2.11).

Noted that the reduction of permeability due to cement content added might not be able to apply to all types of soils. It has been supposed that when a small amount of cement is added, the cementation products will fill the intra-aggregate pores or bind several small aggregates into a large aggregate, but the entire soil sample is not yet bound together at the low cement content; with the increase in amount of additives, the cementation products will bind the aggregates together and fill the inter-aggregate pores.

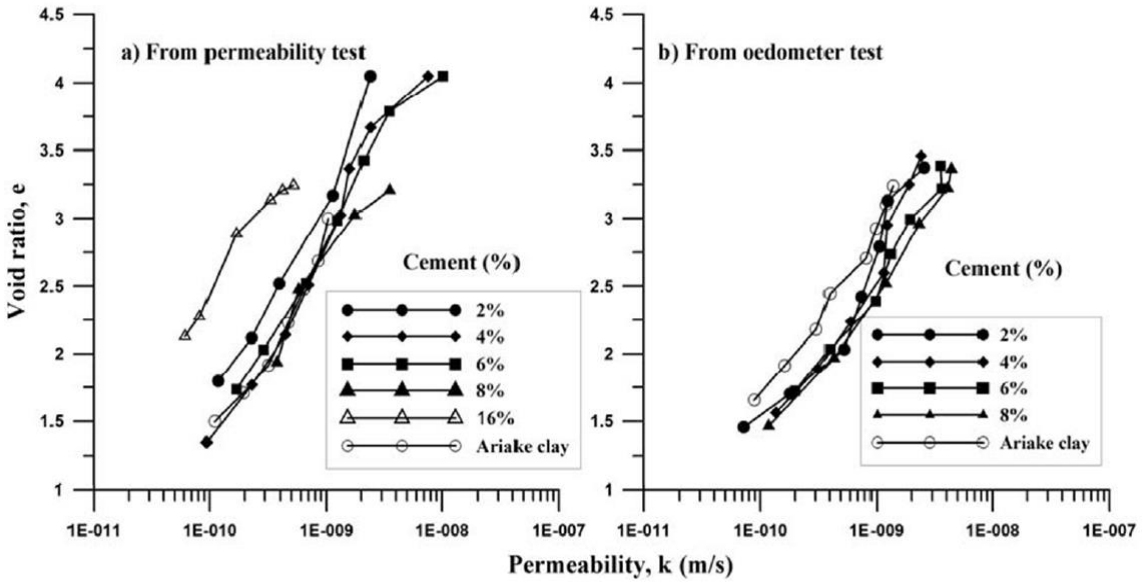

Fig 2. 11 Permeability of cement treated Ariake clay (Quang and Chai, 2015)

2.4.2.2 Strength of soil cement

Unconfined compressive strength of soil cement is normally used to express the effect of cement content on soil strength (Abdulla and Kiousis, 1997; Yoon and Abu-Farsakh, 2009; Horpibulsuk et al., 2010). It is observed that when cement content increases, unconfined compressive strength of fine grained as well as coarse grained soils increases. The strength of soil cement is also increased with curing time (Shooshpasha and Shirvani, 2015). Mitchell (1981) made a relationship between unconfined compressive strength and curing time as follows:

$$q_u(t) = q_u(t_0) + K\log(t/t_0) \qquad (2.2)$$

Where:

$q_u(t)$ = unconfined compressive strength at t days, in kPa

$q_u(t_0)$ = unconfined compressive strength at t_0 days, in kPa

$K = 70C$ for coarse grained soils and $K = 10C$ for fined grained soils (C: cement content, % by weight)

A study on soil cement showed that addition of cement increases the effective cohesion significantly (Lo and Wardani, 2002). There are two components of the strength, namely

frictional angle or frictional resistance and cohesion. The frictional resistance takes place with the aggregation of hydrated cement particles and soil particles forming a skeleton. This procedure contributes to form a significant amount of particle interlocking and enhances the frictional component of the strength. The cohesion component results from the reaction of pozzolanic forming cementitious to bind particles together, creating the inter-particle bond strength. Mitchell (1976) showed the effect of cement content on effective cohesion of coarse grain and fined grain in Fig 2.12. From Fig 2.12, the increase in cohesion can be expressed as a function of unconfined compressive strength directly.

$$c = 7.0 + 0.225\ (\sigma_c) \qquad (2.\ 3)$$

Where:

σ_c is unconfined compressive strength

c is effective cohesion

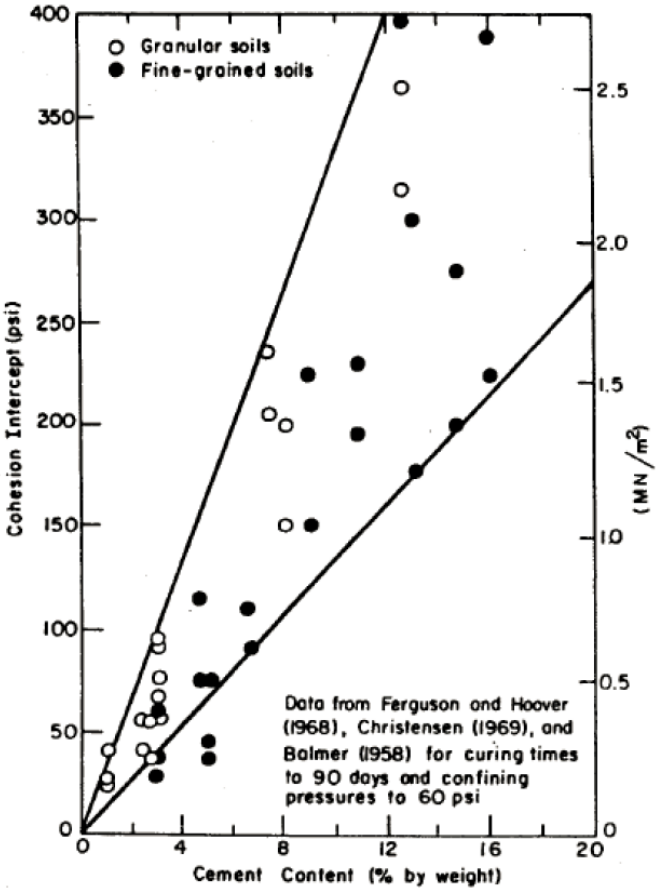

Fig 2. 12 Effect of cement content on effective cohesion for coarse and fined grained soils at curing time 90 days (Mitchell, 1976)

Internal friction angle remains relatively constant for cement treated soils regardless cement content and curing time (Clough et al., 1981). However, Uddin et al. (1997) described that cement stabilization leads to significantly increase in internal friction angle and cohesion; meanwhile the friction angle increase with increasing curing time and cement content. These contradicted idea might be related to the different types of experimental soils. Soil mixing procedure can effect on soil strength. White and Gnanendran (2005) pointed out that a delay between mixing and compaction of soil cement leads to significant reduction in strength. In a particular research showed that the reduction in strength was 10% to 20% and possibly up to 40% for 4 and 24 hour delay. The unconfined compressive strength increases with increasing relative compaction as well.

2.5 Concluding remarks

Most studies on soil erosion have focused on the mechanism of soil erosion by using untreated soil. Clay, sand and coarse grain soil were frequently used in experimental studies. Regarding to assessment of the soil cement resistance to erosion, a small sample size was commonly used, which could not provide a big aspect of effectiveness of soil cement application against erosion. Even soil cement has been used for erosion protection, the effectiveness of soil cement was frequently experimented at fields which sometimes causes some errors for analysis. In addition, a little comprehensive study on soil cement was conducted, in particular shear strength under consolidated drained triaxial compression test. In previous studies, an unconfined compressive strength is usually shown, which is not strong enough for erosion study to associate compressive strength. It would be better to relate the shear strength of soil to erosion study due to soil erosion mainly associated with shear force not only axial forces. As mentioned, there are many studies on cement treated clay, sand and coarse; whereas, there is little research on cement treated silt. Silt is also commonly found in irrigation project. It is the most sensitive soil to erosion. Thus, it might be so useful to have a detail investigation on strength improvement on silt.

Chapter 3 Erosion on Earth Irrigation Structures in Cambodia

This chapter describes the field situation and eroded earth irrigation facilities in Cambodia. Two irrigation sites in paddy farming regions were selected for field investigation, Kandal Steung and Thomney irrigation schemes.

3.1 Background

Cambodia economic largely depends on the agricultural sector that contributes 33 percent of the nation. The agricultural sector contributes 26.7 percent to the national Gross Domestic Product (GDP) and employs more than 42 percent of the national labour force (Netherland, 2018). Improving water management in agricultural systems is one of the main priorities of Cambodia government to meet the ambition of being a rice exporting country in the international market. In the last decades, Royal Government of Cambodia (RGC) has made a strong commitment to enhance the subsistence agricultural practice to commercial agriculture through constructing the agricultural infrastructures such as roads, irrigations, and reservoirs. Enhancing the irrigation system, farmers will be less reliant on rainfalls and they can cultivate more than one time per year with more certainty and predictability. The government has strongly emphasized the importance of water management to increase agricultural productivities through rehabilitating and enhancing irrigation facilities. The irrigated area and supplemental irrigation are predicted to increase 20% to 25% due to the national strategic development plan set to increase the production in the rice sector (De silva et al., 2014).

Despite the importance given to irrigation in the development strategies of Cambodia, there is a lack of study information regarding to irrigation protection techniques. Most irrigation facilities in Cambodia are earthworks, thus erosion on earth irrigation structures is commonly found. Sithirith (2017) described that the maintenance and operation of large scale and smaller canals used to distribute water falls to the local level, but local governments and communities do not have the capacity to handle it. In addition, due to financial constraint, the rehabilitation of those irrigation structures is hardly achieved, which make adverse impacts on the irrigation management (Sam and Shinogi, 2015).

3.2 The degradation of irrigation structures in Cambodia

Deteriorated irrigation facilities have become one of the most concerns for government. Most part of the irrigation system in Cambodia was constructed during Pol Pot regime, about 14,000 km in total length was constructed almost by manpower (MoWRAM, 2008). According to the inventory in 1997, there are 950 irrigation schemes in the countries identified mostly built during Pol Pot regime, only 20% are still functional, 14% are not functional, and the rest is partly functional. In another case of irrigation facilities degradation around Tonle Sap Basin, of around 570 schemes, only 195 schemes are fully operational. The last updated of irrigation development in Cambodia showed that Cambodia has 2,403 irrigation systems throughout the country including the old facilities that constructed in Pol Pot regime and the new facilities that constructed from 1980s to 2004; however, most systems are not well functional due to improper maintenance and operation. The updated inventory data compiled by Ministry of Water Resources and Meteorology shows that there are 2,403 irrigation system in the country extending 1.05 million irrigated area. Of the total of 2,403 systems, 1, 415 (59%) are small scale, 955 schemes (40%) are medium scale, and 33 schemes are categorized into large scale irrigation systems.

Two irrigation sites in paddy farming regions were selected for field investigation. These irrigation schemes were rehabilitated and supported by JICA fund cooperated with Ministry of Water Resource and Meteorology, Cambodia. First irrigation site named Kandal Steung shown in Fig 3.1 is located in Kandal province, about 30 km far from Phnom Penh city. The total area in Kandal Steung site is approximately 1,950 ha including 31 villages. There are 3,499 households benefited from this irrigation project (JICA, 2010). The main sources of income are rice production, labour and livestock. The primary water supply sources in wet season are rain water and irrigation water from the Kandal Steung channels. The secondary water sources in dry season are shallow wells and ponds. Another investigation site is Thomney located in the north of Daun Keo town about 13 km far from the Takeo city in Takeo province (Fig 3.2). The total irrigation area in Thomney site is approximately 301 ha including two beneficiary administrative villages. The main water supply sources in the wet season are rain water and Thomney reservoir. The secondary water sources in dry season come from the existing channels constructed during Pol Pot regime.

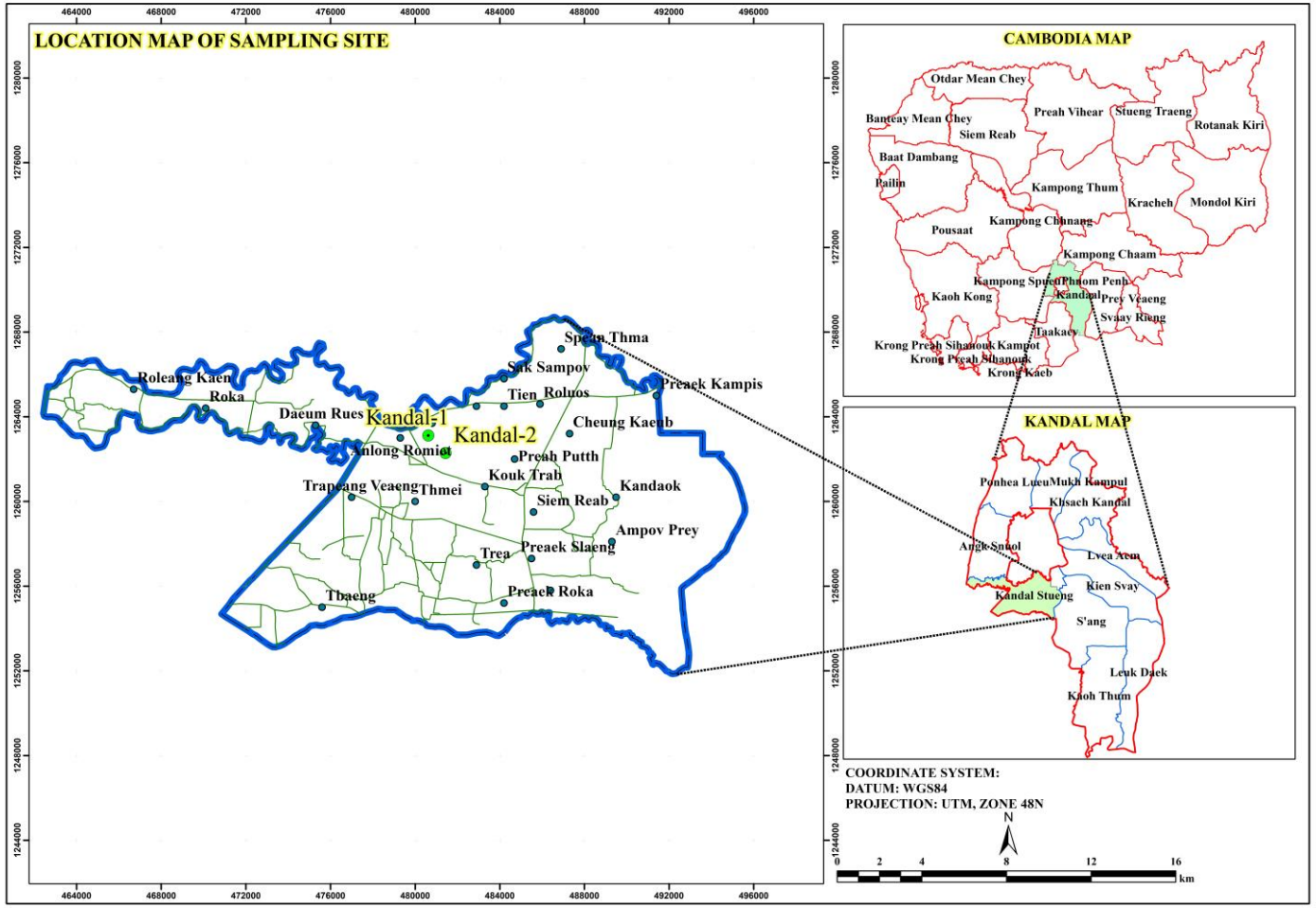

Fig 3. 1 The location of Kandal Steung irrigation site, Kandal province, Cambodia

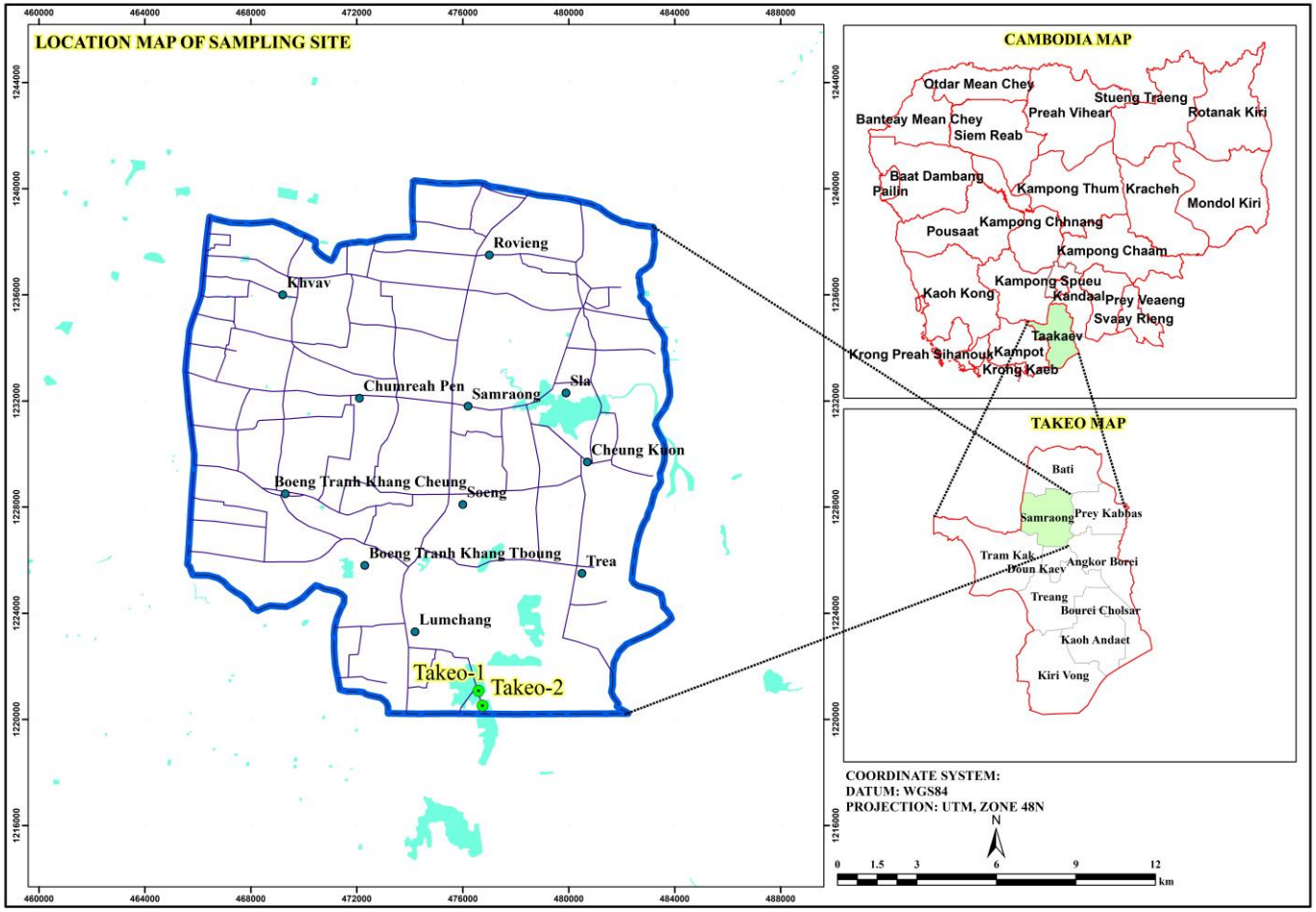

Fig 3. 2 The location of Thomney irrigation site, Takeo province, Cambodia

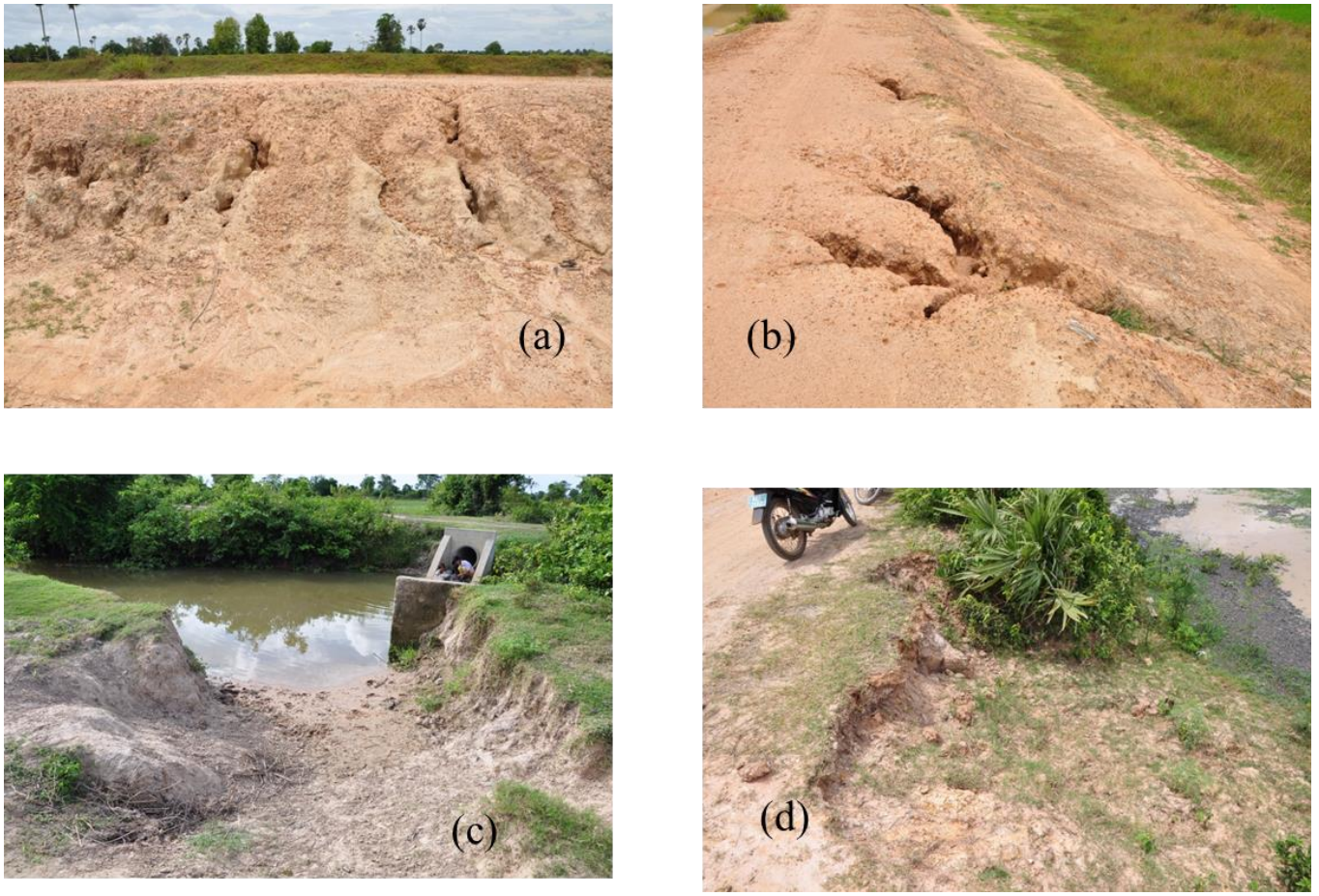

Fig 3. 3 Situations of field investigation sites (a), (b) embankment of Kandal Steung main channel, (c) a situation of channels constructed in Pol Pot regime, and (d) upstream slope of the Thomney reserviour embankment

Most people are farmers and rice production is their main income source. At the investigation sites in Kandal Steung, erosion along the channel embankments was observed. The typical situations along the Kandal Steung main channel are shown in Fig 3.3(a) and 3.3(b). A soil named Kandal 1 was sampled from the embankment shown in Fig 3.1. Figure 3.3(c) shows a situation of channels constructed in Pol Pot regime and many channels were constructed at that time, but a lot of them are not in function as channels, and they are eroded and do not remain original figures. At this place shown in Figure 3.1, we sampled a soil named Kandal 2 and in-situ density tests were conducted.

In Thomney, the typical situation of upstream slope of the Thomney reservoir embankment is shown in Fig 3.3(d). Both upstream and downstream slopes of the embankment were eroded. Soils named Takeo 1 and 2 were respectively sampled from upstream and downstream slopes. The in-situ density tests were also conducted.

3.3 Erosion measurement

Soil erosion is one of the most concerns in sustainable irrigation development in Cambodia. There is no study on soil erosion occurred on earth irrigation facilities; however, some lessons learned of irrigation deteriorated are drawn from many irrigation project sites in Cambodia. We selected a typical 30 m length along the earth embankment in Kandal Steung to investigate the width, length, and depth of each eroded trench by using digital photos and manual measure. Some erosion with big holes were found on the surface embankment. In order to capture the real erosion condition, many photos were taken. The JWD program was used to modify the photos as shown in Fig 3.4. The gradual surface erosion on embankment might be one among the possible consequences to a severe seepage flow. It was found that the area eroded was about 9.8 m^2 and about 9% of the area measured.

In Thomney irrigation site, 43 m length along the reservoir embankment was selected to investigate the eroded trench. The similar method was applied in this measurement (Fig 3.5). The erosion condition on the surface embankment in Thomney was not so different from Kandal Steung. On the surface of the embankment, many eroded cracks were observed. The results showed that the area eroded was about 30 m^2 and about 6% of the area measured.

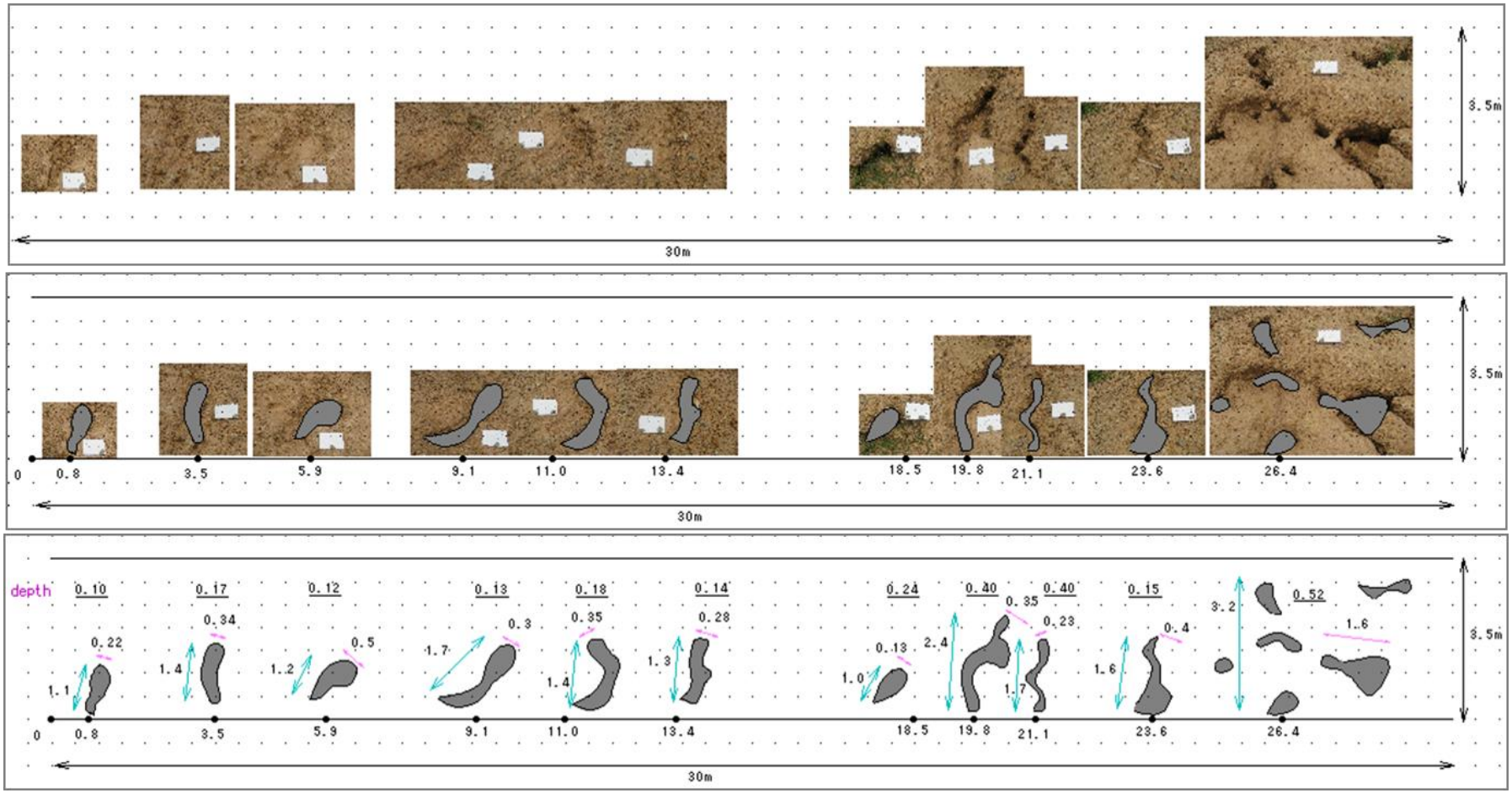

Fig 3. 4 The schematic diagram of erosion measurement in Kandal Steung site, Kandal province, Cambodia

Fig 3. 5 The schematic diagram of erosion measurement in Thomney site, Takeo province, Cambodia

3.4 Laboratory tests

The physical properties of the four soils (Kandal 1, 2, Takeo 1, 2) are summarized in Table 3.1. The grading curves are shown in Fig 3.6. It was found that these soils had similar grading curves and the contents of sand, silt, and clay were almost 40%, 50% and a few percent, respectively. So these soils were classified as CL or ML according to Japanese unified soil classification system. The values of permeability of the soils of Kandal 1 and 2, Takeo 1 and 2 were 2.24×10^{-8} m/sec, 3×10^{-8} m /sec, 2.8×10^{-7} m/sec and 2.3×10^{-7} m/sec. The results of compaction tests are shown in Fig 3.7 and Table 3.2. The compaction energy is proctor's 100% and the volume of the mould used is 1,000 cm^3. These four soils had similar maximum dry densities and optimum water contents and they were around $\rho_{d\,max}$ = 1.9 g/cm^3 and w_{opt} = 12 %. The results of in-situ density tests are also summarized in Table 3.2. The mean field dry densities of Kandal 1 and 2, Takeo 1 and 2 were 1.57 (maximum 1.64, minimum 1.52), 1.62 (1.69, 1.58), 1.56 (1.65, 1.45) and 1.61 (1.66, 1.55) g/cm^3, respectively. The associated mean field water contents were 5.8, 5.7, 5.0 and 6.6 %. The values of compaction degree D (= 100 ρ_{fd}/ρ_{dmax}, (%), ρ_{fd} = field dry density; ρ_{dmax} = maximum dry density obtained from standard Proctor method) were between 81 - 88%. Comparing with the Japanese compaction standard for embankment dam; D value should be around 95%, the compaction situations of earth embankment at investigation sites were not sufficient and under loose conditions.

In order to investigate the dispersibility of the soils, a series of crumb tests were conducted. In the test, the dispersibility was identified by observing the hydration of cubical specimens (Maharaj, 2011). The tendency that colloidal size particles deflocculate, is observed by suspending the soils into 250 ml distilled water. The diameters of crumbs used in this test were approximately 6-10 mm. The guideline for observation of the crumb test is shown in Table 3.3 in which four grades are set. The results of the crumb tests showed that Kandal 1 was categorized G1, Kandal 2 and Takeo 1 as G2 and they were non-dispersive soils. Takeo 2 was only identified as dispersive soil and the grade was G3.

3.5 Concluding remarks

The overall results from field investigations suggested that the erosion on earth embankment was serious. The compaction situation of the earth embankment was not

sufficient causing a strong sensitivity to erosion. In addition, the grading curves of soil samples showed that 50% are silt contents. These soil samples were classified as non-plastic, which were so sensitive to dispersion and erosion.

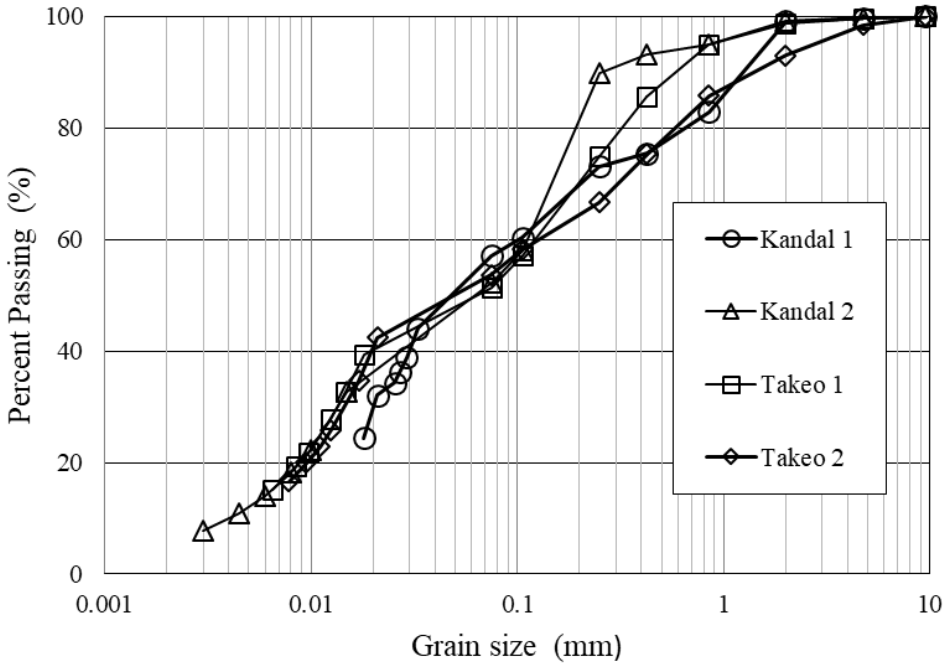

Fig 3. 6 The grain size distribution of soil sampled from irrigation project sites

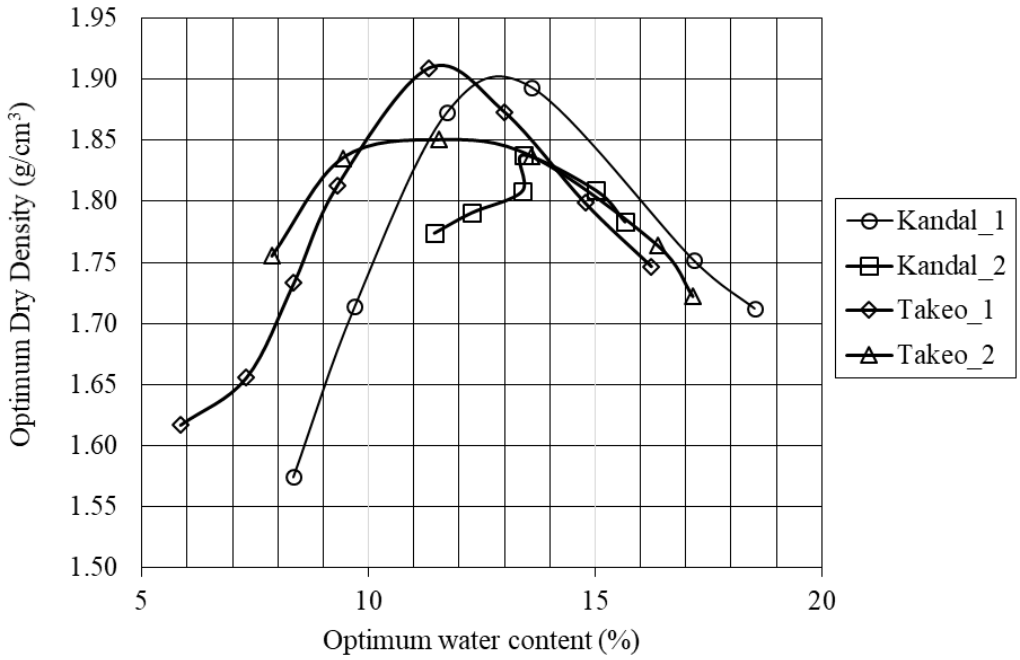

Fig 3. 7 The results of compaction test of four soils sampled in Cambodia

Table 3. 1 Physical properties of the four soils sampled in Cambodia

Materials		Kandal 1	Kandal 2	Takeo 1	Takeo 2
Density of soil particle	ρ_s (g/cm^3)	2.589	2.648	2.629	2.674
Liquid limit	w_L (%)	27.4	22.5	26.3	25.2
Plastic limit	w_P (%)	16.5	-	14.4	16.3
Plastic index	IP (%)	10.9	NP	11.9	8.9
Coef. of Permeability	k (m/s)	2.24×10^{-8}	3×10^{-8}	2.8×10^{-7}	2.3×10^{-7}
Soil Classification based on JGS standard		CL	ML	CL	CL

Table 3. 2 Results of in-situ density tests and standard compaction tests

Materials		Kandal 1	Kandal 2	Takeo 1	Takeo 2
Average field dry density	ρ_{df} (g/cm^3)	1.57	1.62	1.56	1.61
Average field water content	w_f (%)	5.83	5.68	4.97	6.59
Maximum dry density	ρ_{dmax} (g/cm^3)	1.90	1.84	1.91	1.85
Optimum water content	w_{opt} (%)	14.0	13.0	11.3	12.0
D value	D (%)	82.6	88.0	81.7	87.0

Table 3. 3 The guidance for observation of the crumb test, which conducted in Cambodia

Grade	Reaction	Description	Categories
1	No reaction	Crumbs may slake or run out to form a shallow heap on the bottom of the beaker but there is no sign of cloudiness caused by colloidal in suspension.	Non-dispersion
2	Slight reaction	A very slight cloudiness can be seen in water at the surface of the crumb.	Non-dispersion
3	Moderate reaction	There is easily recognizable cloud of colloidal in suspension, usually spreading out in thin streaks at the bottom of the beaker.	Dispersion
4	Strong reaction	A colloidal cloud covers most of the bottom of the beaker, usually as a thin skin.	Dispersion

Chapter 4 Research Methodologies

In the research methodology chapter, some main experimental tests are described. First, physical and mechanical soil properties tests were conducted to obtain bulk density, maximum dry density, optimum water content, grain size distribution, and soil strength. Then, the rain erosion resistance test was conducted to assess the effectiveness of soil cement application against erosion processes under rainfall intensity 50 and 100 mm h^{-1}. DL clay and ordinary Portland cement were used for this study.

4.1 Physical soil properties tests

4.1.1 Soil density

The soil density, also known as dry density, is the weight of dry soil divided by the total soil volume. By following the testing standard JGS 0191, bulk density of experimental soil (DL, clay) was obtained. The minimum dry bulk density of DL-clay was 1.3 g/cm^3, and the maximum dry density was 1.5 g/cm^3.

4.1.2 Grain size distribution test

The grain size analysis is widely used in classification of soils. Determination of particle size is more important because the particle size determines bulk density, physical stability, permeability and many more (Hogg, 2008). Sieving and hydrometer tests were used to determine the distribution of particles. Sieve analysis is a laboratory test in which particles remove through the sieve mesh. Sieving test is conducted to determine the distribution of the coarser, larger sized particles, and the hydrometer test is used to determine the distribution of the finer particles. As soil particle used in this experimental study was fine particles, hydrometer test was conducted by following the standard of this test, JGS 0131. The data obtained from grain size distribution curves was also used in the gabion design for slope model test.

4.1.3 Compaction test

The proctor compaction test is usually used to determine the optimal moisture content of soils. This test is profoundly useful when determining the relationship between water content and dry unit weight of soils. These values are often determined before starting earthwork to provide reference values for field practice. The compaction is necessary in constructions. If compaction is not performed properly, soil settlement can occur. Kumar et al. (2007) described that compacting soil can increase load capacity and stability.

To carry out a laboratory compaction test, JIS A 1210 standard was used. In the laboratory, processing of soil samples started with air-drying. After drying, soil was weighted to ensure enough compacted volume to properly fill the mould. Then water was added incrementally to increase the individual moisture content by about 2% for each specimen and mixed thoroughly. In case of DL clay mixed with cement, an appropriate amount of soil and cement for each sample was first mixed in an air-dry state, the necessary amount of water was then added to the mixture. Each prepared specimen was placed in a compaction mould (with collar attached) and compacted in layers by dropping the hammer (about 2.5 kg) onto the specimen in the mould in a certain uniform 25 dropping.

Kumar et al. (2007) also mentioned that for each of the initial points of compaction, the mass and unit weight of the soil would increase and allowed them to be consolidated into a denser state from the same compactive effort. By about fourth or fifth point, the mass of the sample would decrease as the volume of water reached a point where it displaced soil particles in a given volume. This indicated that optimum moisture had been exceeded and having another point beyond that would make it a bit easier when constructing the final compaction curve.

The weight of each specimen was used to calculate wet unit weights and the oven-dried moistures were used to determine a dry unit weight for each point. The results were plotted on a graph as dry unit weight versus moisture content. This relationship allowed the maximum dry weight and optimum moisture for each type of soil to be established.

4.2 Hydraulic properties test

Soil hydraulic properties represent the basis for understanding flow and transport processes of water in soils (Vereecken et al., 2007). In this focus, moisture/water retention

characteristic and hydraulic conductivity are always presented. For erosion study, it is very important to understand the hydraulic property of soil and the characteristic of soil water retention. In this study, two main hydraulic property tests were conducted.

4.2.1 Hydraulic conductivity test

Laboratory investigations were carried out on a DL clay soil and DL clay treated with ordinary Portland cement, 0, 3, 5, and 7% by dry weight of soil. Table 4.1 shows the physical properties of cement. In case of DL clay, three different densities were tested. However, DL clay mixed with cement was tested with dry density 1.3 g/cm^3. The curing time of specimens were 7, 14, and 28 days.

Table 4. 1 Chemical compositions of ordinary Portland cement

Chemical components	Symbol	Ordinary Portland cement (%)
Lime	CaO	64
Silica	SiO_2	21.3
Alumina	Al_2O_3	5.6
Iron Oxide	Fe_2O_3	3.36
Magnesia	MgO	2
Sulphur Trioxide	SO_3	2.14

The falling head hydraulic conductivity test was conducted with a permeability cell (Fig 4.1). The permeability cell is made of plated steel. The base and the top are clamped with stainless steel rods. Soil samples were saturated for 24 hours before placing into the cell. The test was performed with a permeability cell with a specimen 5 cm in diameter and 10 cm in high, which had to be connected to a manometer stand. During the test the cell was placed in a soaking tank fitted with overflow tube. The coefficient of permeability was calculated by equation 4. 1.

$$k_{s,T} = \frac{2.3aL}{A(t_2 - t_1)} log_{10}\left(\frac{h_1}{h_2}\right) \quad (4.\ 1)$$

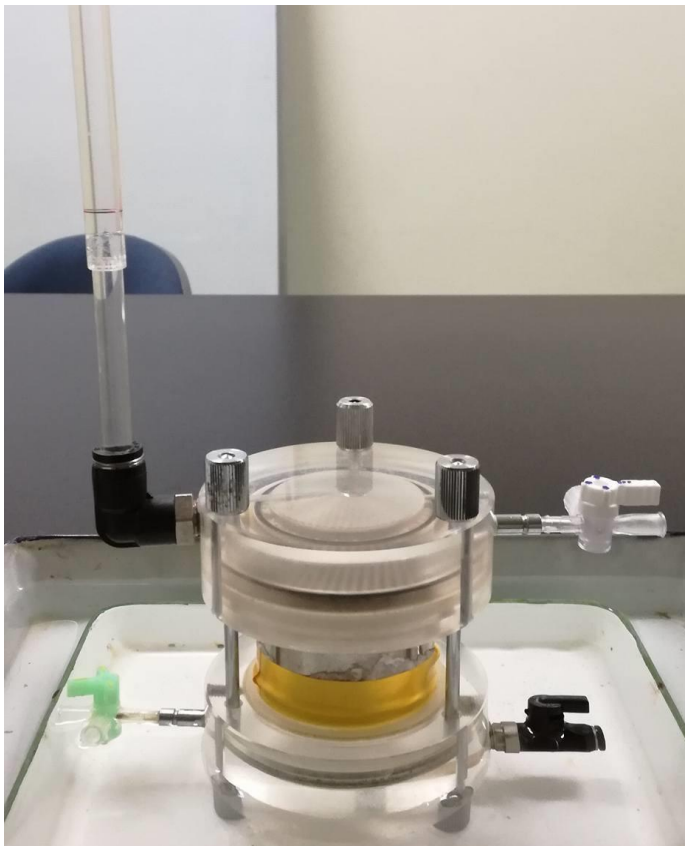

Fig 4. 1 Hydraulic conductivity apparatus

4.2.2 Soil water retention test

It is important to understand soil water characteristic in erosion study. Soil water characteristic curve can describe the amount of water retained in a soil under equilibrium at a given matric potential (Tuller and Or, 2004). In addition, soil water characteristic is an important hydraulic property which can be demonstrated the effects of soil texture and structure on water retention in soils. In this study, suction controlled triaxial system was used to obtain a soil water retention curve of soil cement and DL-clay. The wetting and drying curves were attempted to derive from this test. The layout of the suction controlled triaxial system is shown in Fig 4.2.

Specimen preparation

DL clay was mixed with three different cement contents, 0, 3, and 5%. The water content of the soil specimen was 17% and dry density was 1.3 g/cm^3. The soil specimens were cured for 28 days. The specimen size was 6 cm in diameter and 2 cm in high. After curing for

28 days, the soil specimens were de-aired in the vacuum chamber for 24 hours. During de-air specimens, water were added to the specimen container to ensure the specimens can reach to the maximum saturation. During set up for testing, the specimens were continued to saturate for 48 hours by capillary forces, using flowing water through ceramic disk. When the saturation process was finished, the drying process was firstly started. The minimum suction of drying curve was 20 kPa, and the maximum suction was 100 kPa. Then, the wetting curve was continually obtained by reducing the suction from 100 kPa to 20 kPa.

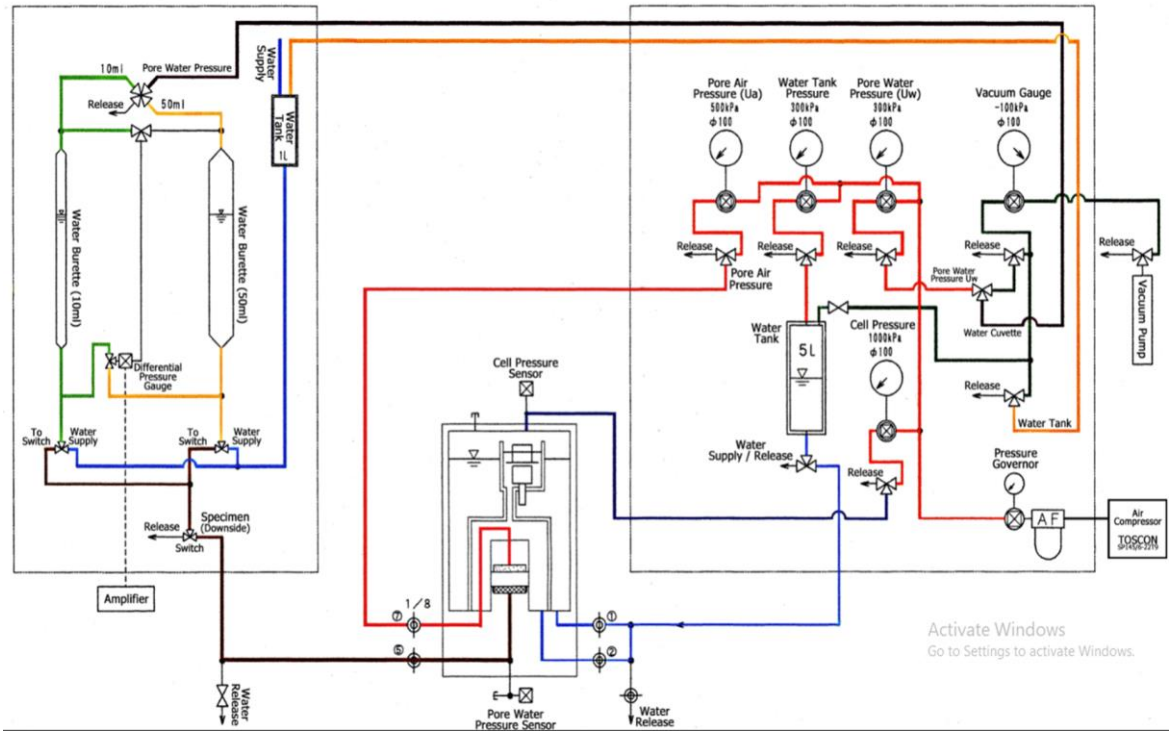

Fig 4. 2 Layout of suction control triaxial apparatus

4.3 Enhance crumb test

The susceptible soils easily disperse in water. Crumb test, a new rapid test, is proposed to characterize the sensitivity of soils to water. It is practicable with the interpretation based on visual observations, and the results are qualitative (Haghighi et al., 2012). Even this simple and quick test is qualitative, it strongly depends on visual observation by an operator. It is possible that the results affected by human reading, but it is the most convenient test. Thus, the crumb test was used to assess the sensitivity of experimental soils; DL clay and soil cement. The test involved with placing a small cube of remoulded soil into 250 ml of distilled water or tap water.

Specimen preparation

The specimens were prepared at the same water content, 17%, as other specimens in physical properties tests. The soil was compacted into a paper mould 15 mm in diameter and 20 mm in high. The curing time of soil cement specimens for crumb test was 7 days; it was mainly set to the same curing time of the soil slope models in rain erosion resistance test. This crumb test was conducted with 0, 3, and 5% of cement content. Table 4. 2 shows the mixing proportion of soil specimens.

Table 4. 2 The proportion of soil and soil cement specimen for crumb test

Cement content (%)	DL-clay (g)	Cement (g)	Water (g)
0	4.59	0.00	0.78
3	4.45	0.14	0.78
5	4.36	0.23	0.78

The specimens were placed in a rectangular container, 21 x 34.7 x 5.8 cm, then filled with the tap water. To observe the tendency of soil particles to disperse, one camera equipped with a tripod was set up to capture the photo of the specimens, locating 28 cm from the rectangular container (Fig 4.3). The interval of shooting range of 0 minutes, 1 minute, 5 minutes, 15 minutes, 30 minutes, 45 minutes, 60 minutes, 24 hours, and 48 hours.

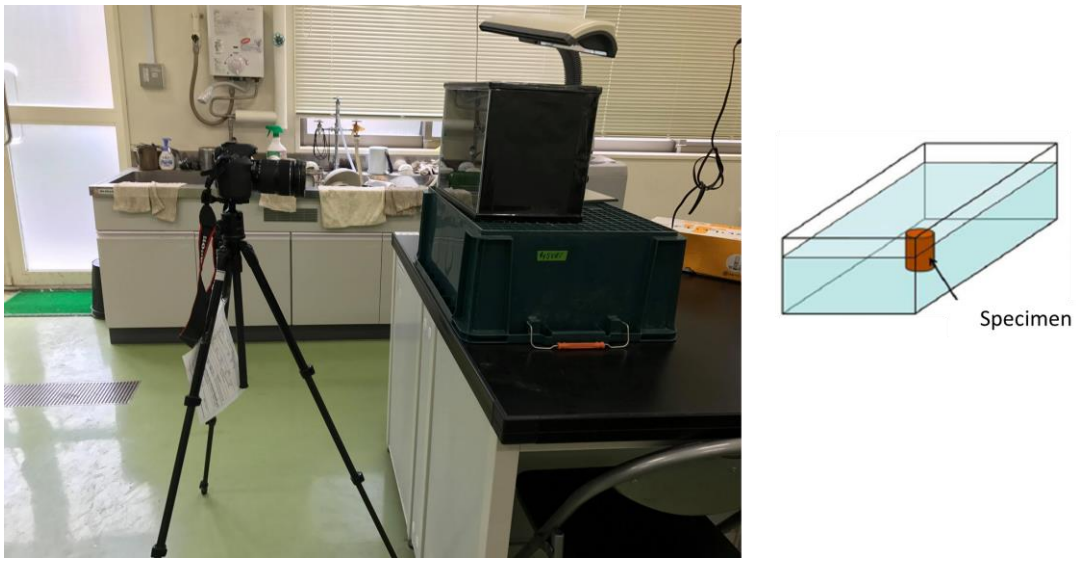

Fig 4. 3 Schematic of specimen setup for crumb test

4.4 Consolidated drained triaxial compression test

Consolidated drained triaxial compression (CD test) is a testing method to shear a soil specimen under drained condition where a given lateral confining pressure is applied. The triaxial compression test apparatus used in this study was a conventional one with double triaxial cells to measure the volume change of the specimen by measuring water levels of the inner and outer cell. The outer cell has 17 cm in diameter and 32 cm in high while the inner cell has 6 cm in diameter and 17 cm in high. The schematic of the experimental apparatus is shown in Fig 4.4. The standard consolidated drained triaxial compression test JGS 0524 was used.

4.4.1 Soil sample preparation

The cylindrical specimens, 5 cm in diameter and 10 cm in high, were used for triaxial test. The mixture of soil sample was compacted into a metal mould with a dry density 1.3 g/cm^3 and 17% of water content. All the specimens were sealed with plastic bag and cured in the constant temperature room for 7, 14, and 28 days. Before starting shearing test, the specimen was subjected to consolidation process. After finishing consolidation process, axial load was applied through an electric motor, the strain rate was about 0.3 %/min. The test was stopped when the axial strain excess 15%. During applying axial stress, the confining pressure was kept constant. Three confining pressures were used 50, 100 and 200 kPa.

4.4.2 Data analysis

A basic computer program DC3100 was set up to control data accumulation on the computer. The data were recorded within 1 minute interval. The deviator stresses can be obtained by equation below:

$$\sigma_a - \sigma_r = \frac{P}{A_c} \times \frac{1-\frac{\varepsilon_a}{100}}{1-\frac{\varepsilon_v}{100}} \times 10 \qquad (4.2)$$

P: Axial load (N) applied to the specimen at the axial strain ε_a

σ_a: Axial stress acting on the specimen (kN/m^2)

σ_r: Lateral stress acting on the specimen (kN/m^2)

The displacement can be determined by the Linear Variable Differential Transform (LDVT's) which attached to the top cap of the chamber. This probe measures axial deformation. The axial strain can be computed by dividing the deformation of the specimen with the initial length of the soil sample (Eq 4.3).

$$\varepsilon_a = \frac{\Delta H}{H_0} \times 100 \qquad (4.3)$$

Where ΔH (cm): Axial displacement of the specimen during compress. It is obtained by

$$\Delta H = \varepsilon \times \mathrm{C} \qquad (4.4)$$

ε : is the strain of pressure sensor and C is the coefficient of displacement.

The volumetric strain is calculated by:

$$\varepsilon_v = \frac{\Delta V}{V_0} \times 100 \qquad (4.5)$$

4.4.3 Strength parameter calculation

There are two methods to estimate the value of c and ϕ under consolidated drained triaxial test. To calculate the cohesion and friction angle for this study, Method (I) was used.

(I) Method number one

$q_f = (\sigma_1 - \sigma_3)_f$

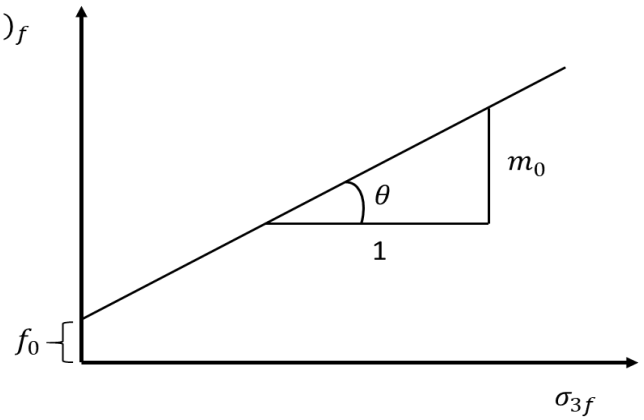

$$\sin\theta = \frac{m_0}{2 + m_0} \qquad c = \frac{f_0}{2\sqrt{1 + m_0}}$$

(II) Method number two

$$q_f = \frac{(\sigma_1 - \sigma_3)_f}{2}$$

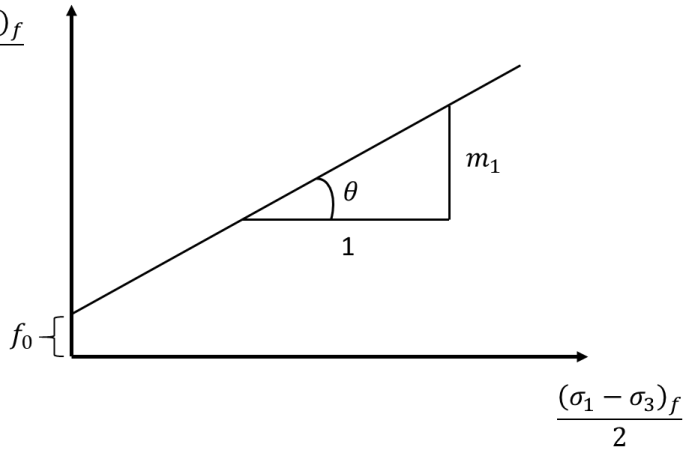

$$\sin\theta = m_1 \qquad c = \frac{f_1}{\sqrt{1 - m_1^2}}$$

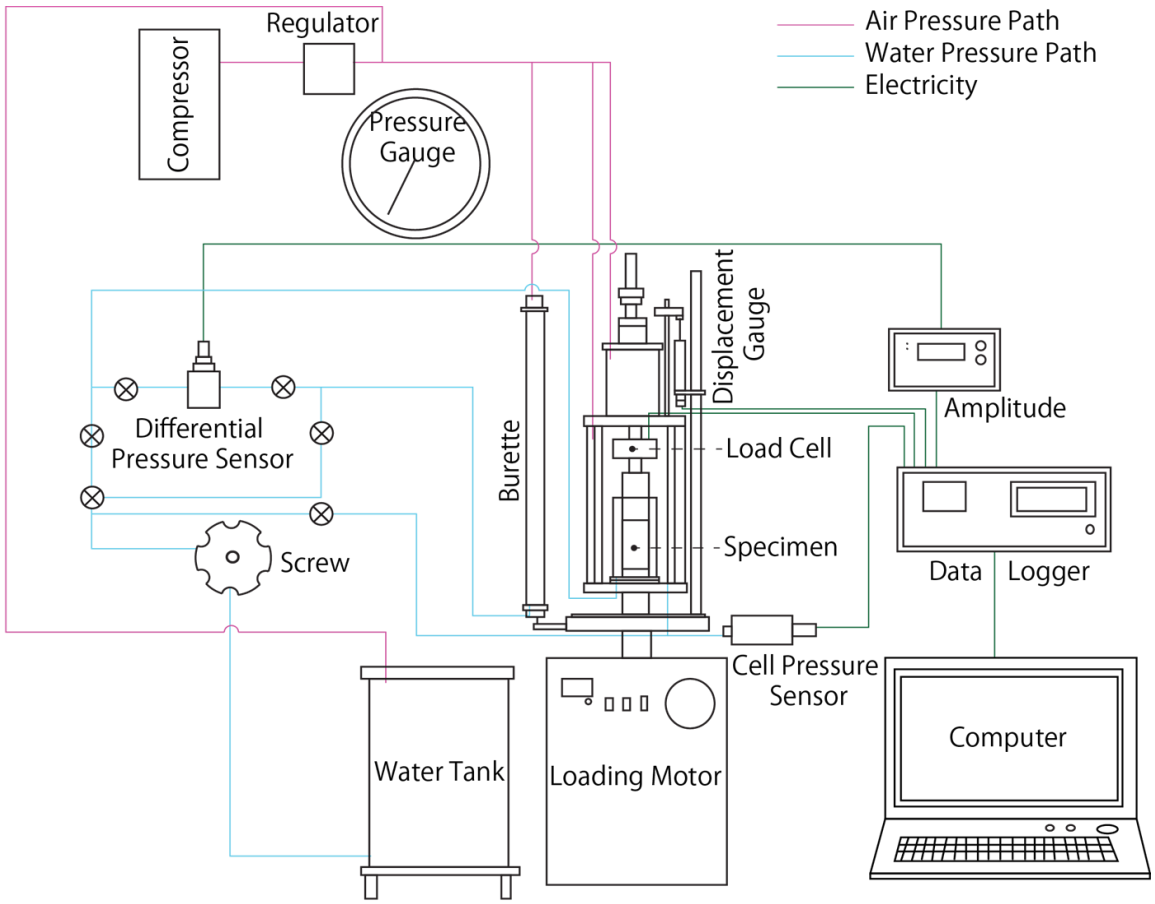

Fig 4. 4 The conventional triaxial apparatus

4.5 Rain erosion resistance test

In rain erosion resistance test, rainfall simulator was used to create a specific characteristic of rain event. In this experimental test, two different rainfall intensities, I = 50 and 100 mm h^{-1}, were applied. Before starting test, rainfall was calibrated to get a good distribution of rainwater on the surface slope models. The procedure and equipment of the rain erosion resistance test were described as follows:

4.5.1 Adjustable slope apparatus

A slope adjustable equipment was used for the rain erosion resistance test. This equipment consisted of a soil box, which had dimension 200 x 50 x 55 cm. The angle 20-degree (about 36% slope) of this equipment was assigned to this experimental test (Fig 4.5).

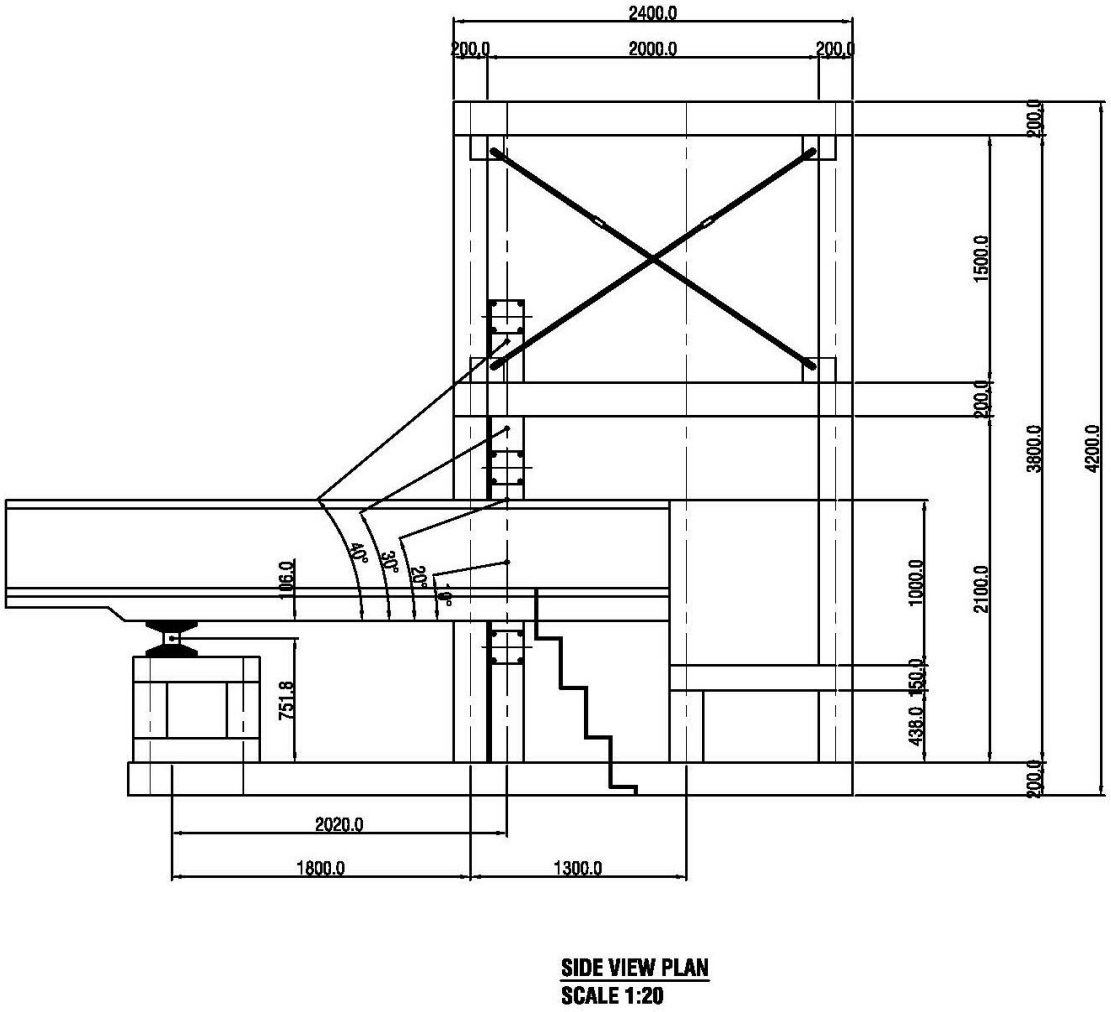

Fig 4. 5 Layout of adjustable slope apparatus for rain erosion resistance test

4.5.2 Rainfall simulator

A rainfall simulator was used to delivery an artificial rainfall (Fig 4.6). It was set about 3 meters over the top of the adjustable slope equipment. Two square spray nozzles from Ikeuchi Co., Ltd were used to supply rainwater (Fig 4.7). The mean raindrop diameters were about 0.5 mm and 0.7 mm for rainfall intensity 50 mm h^{-1} and 100 mm h^{-1}.

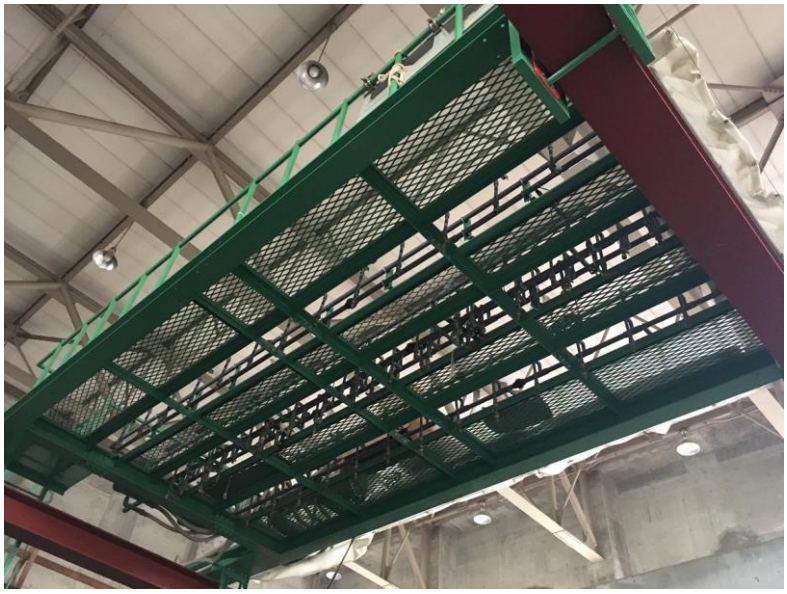

Fig 4. 6 Rainfall simulator used to supply rainwater over the surface soil slopes

Fig 4. 7 Spray nozzle used in soil slope model erosion resistance test (Chueasamat, 2018)

A wire mesh sheet with 1 cm thickness was placed in the bottom of the soil box to reinforce the compacted soils. The gabion filled with 2 mm gravels was used to hold and prevent the soil sample to slide down when the soil box was lifted the up to the desired 20-degree. The schematic of the experimental apparatus is shown in Fig 4.8.

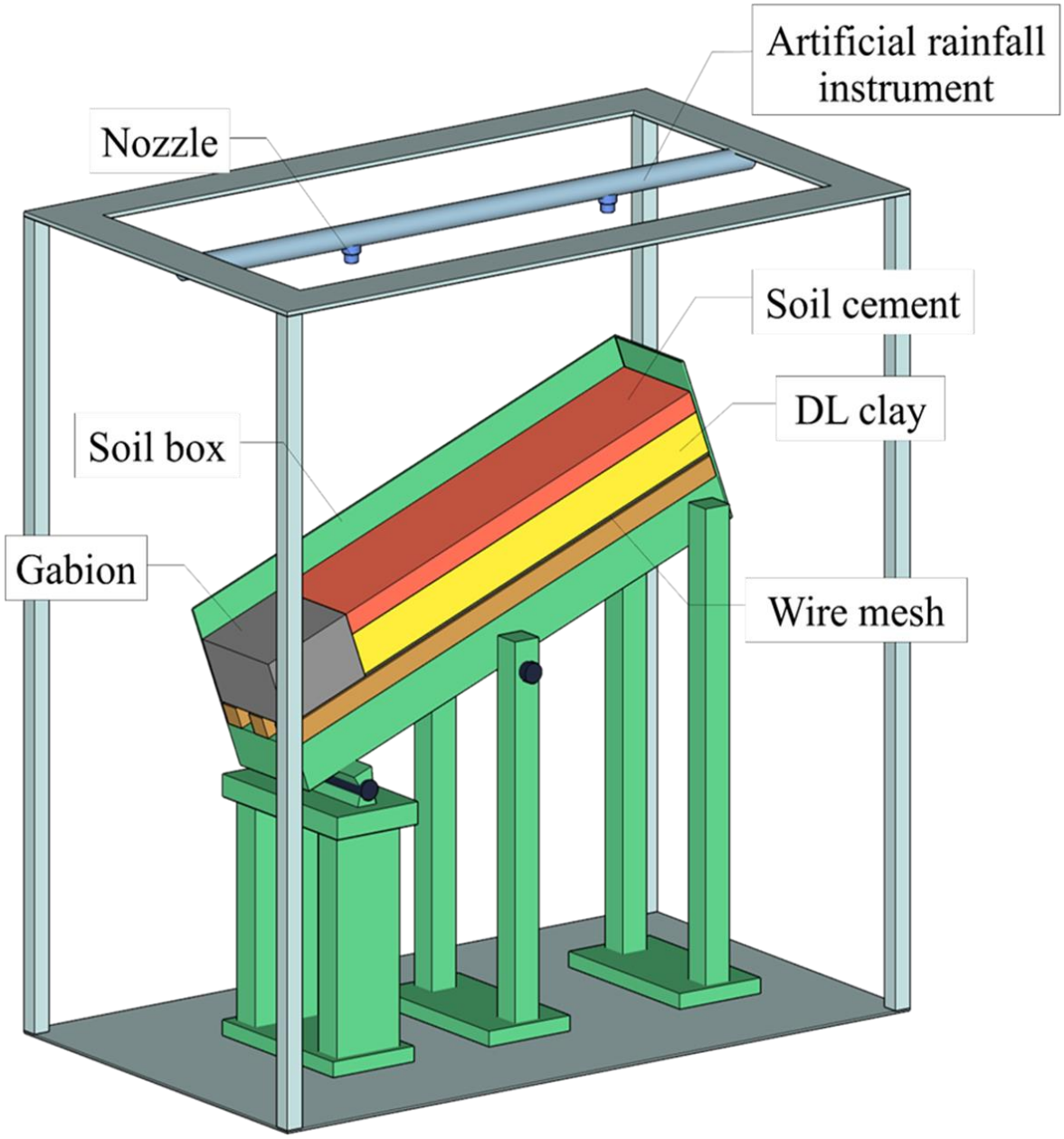

Fig 4. 8 Schematic of rain erosion resistance test apparatus

4.5.3 Pore water pressure transducers

Pore water pressure transducers from Da Instrument Co. Ltd were used to measure pore water pressure within the soil slopes. The maximum capacity of the transducer was about 100 kPa. Transducers were connected to ceramic chip with a tiny tube filled with de-aired water (Fig 4.9). Pore water pressure transducers were connected to a data logger and a switch box to detect pore water pressure in every 10 second interval (Fig 4.10). Before installing, transducers were calibrated to determine the coefficient factor for data conversion (Fig 4.11).

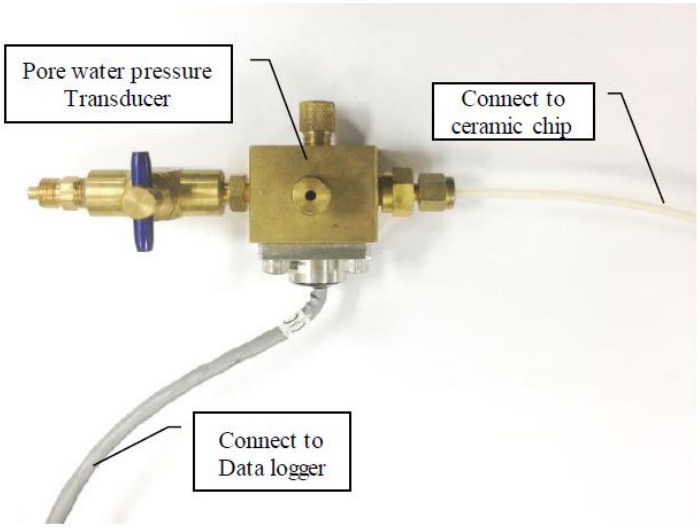

Fig 4. 9 Transducer body and cable functions (Chueasamat, 2018)

Fig 4. 10 Data logger and switcher to record the pore water pressure (Chueasamat, 2018)

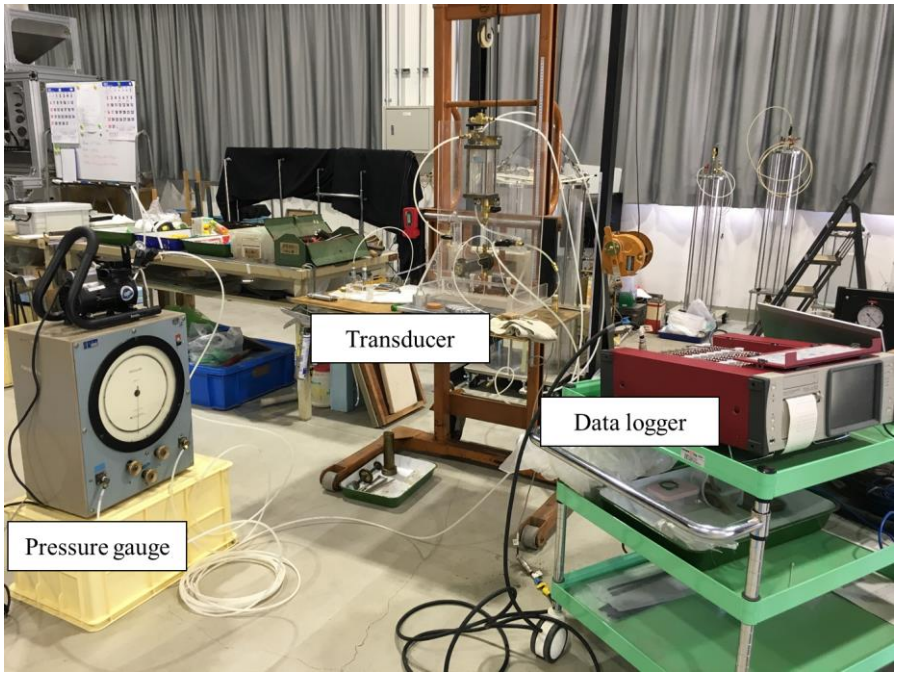

Fig 4. 11 Calibration of pore water pressure transducers

There were 7 PWPs transducers installed for Case 1, 2, and 3 under rainfall intensity 50 mm h^{-1}. To get more data, additional 6 transducers were inserted in Case 4, 5, and 6. Thus, the total of transducers were 13 PWPs transducers for rain erosion resistance test under 100 mm h^{-1}. The position of the transducers is shown in Fig 4.12 and Fig 4.13. The calibration coefficient of PWPs transducers is shown in Table 4. 3 and Table 4. 4. In case of ceramic chip, it was saturated with de-aired water in a vacuum chamber before attaching to the transducer and installing inside the soil slopes.

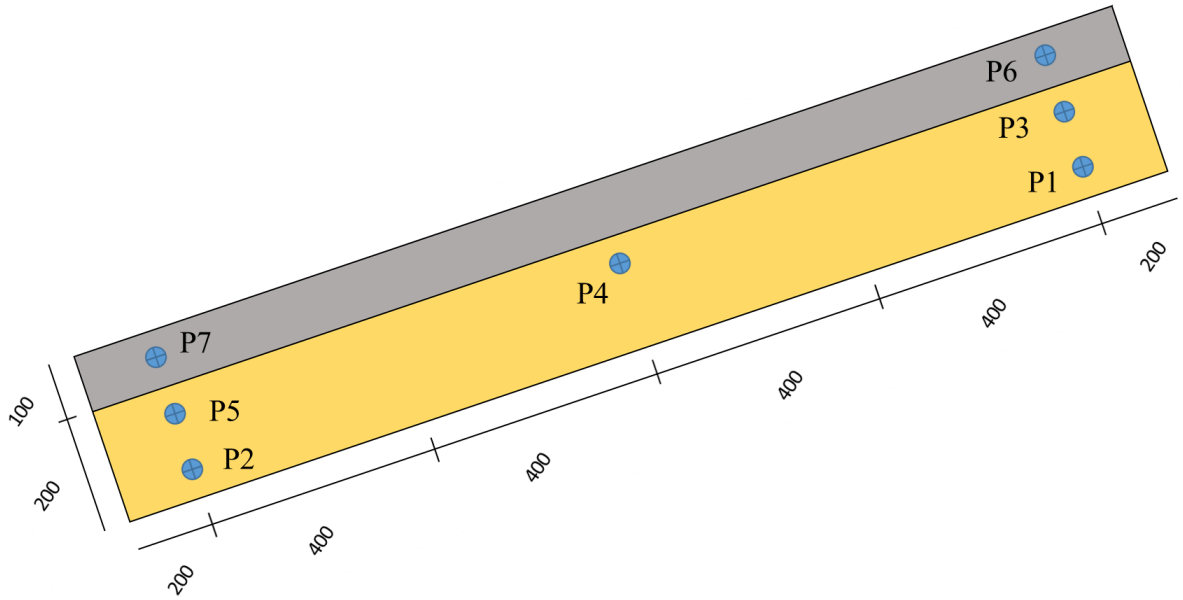

Fig 4. 12 Position of PWPs transducers for Case 1, 2, 3 under rainfall intensity 50 mm h^{-1}

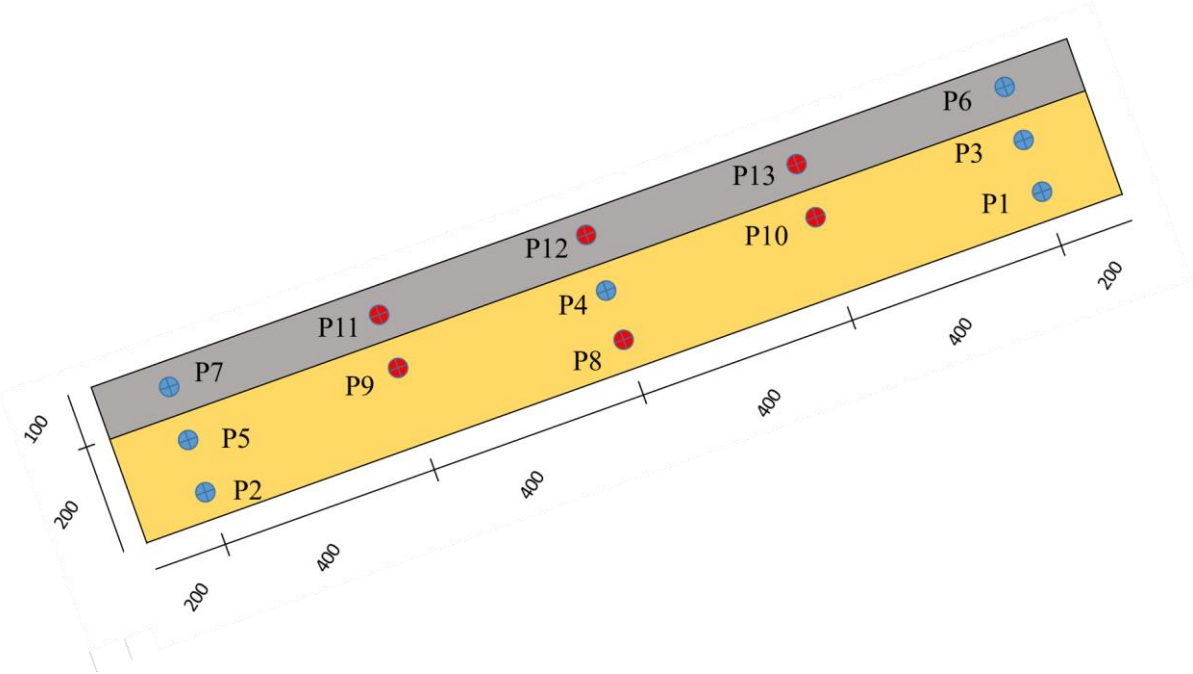

Fig 4. 13 Position of PWPs transducers for Case 4, 5, 6 under rainfall intensity 100 mm h^{-1}

Table 4. 3 Calibration coefficient of pore water pressure transducers 50 mm h^{-1}

Number	Coefficient (kPa/μ)	Zero-Value (μ)
1	0.0172418	-1874
2	0.0171140	-90
3	0.0170948	-1533
4	0.0169964	-960
5	0.0172375	170
6	0.0171694	254
7	0.017183	-3141

Table 4. 4 Calibration coefficient of pore water pressure transducers 100 mm h^{-1}

Number	Coefficient (kPa/μ)	Zero-Value (μ)
1	0.017857	72.4
2	0.017938	487.8
3	0.017881	412.3
4	0.01788	-1210.6
5	0.018034	61.9
6	0.001406	-5287.9
7	0.002588	-119.6
8	0.017788	51.3
9	0.00259	2840.9
10	0.017859	-1640.8
11	0.017982	-571.9
12	0.002593	-433.5
13	0.00253	568.3

4.5.4 Data collection and analysis

To evaluate the effectiveness of soil cement on surface soil erosion, the following properties were measured and calculated. In addition, photos of surface soil conditions were taken to trace the differences.

4.5.4.1 Surface topography and volume change

A grid method was used to determine the surface eroded volume of the soil slopes. On the surface soil slope was first divided into 5 cm by 5 cm square grids (Fig 4.14(a)). A depth sampler fixed at a given height was used to measure changes in the distance between the sampler and the grid node (i.e., depth) at all grid nodes (Fig 4.15). At each grid node, the initial (h_1 to h_4 in Fig 4.14(b)) and final (h_1' to h_4') depths were measured (Fig 4.14(c)). The differences between the initial h_I and the final h_I' were used to compute the eroded volume per grid using the following equation.

$$\Delta V = L^2 \times \left(\frac{(h_1 - h_1') + (h_2 - h_2') + (h_3 - h_3') + (h_4 - h_4')}{4} \right) \qquad (4.\ 6)$$

Where L is the grid size (= 5 cm), h is the elevation height.
After the eroded volume change for each grid was obtained, a total eroded volume was computed by summing them up:

$$\Delta V = \sum_{i=1}^{n} \Delta V_i \ , \qquad (4.\ 7)$$

4.5.5.2 Runoff and sedimentation collection

During the experiment, surface runoff with sedimentation was collected in every 15 minutes interval. The collected runoff was left overnight to settle the sediment down. Then, the sediment was extracted for oven dry (24 hours). The amount of sediment collected with runoff was considered as a part of soil losses from erosion processes. Apart from collecting sediment with runoff, the soil losses, which were estimated from surface eroded volume, were considered as soil losses from surface erosion too. In case of rain erosion resistance test under rainfall intensity 100 mm h^{-1}, the surface runoff and sub-flow were separated for soil cement.

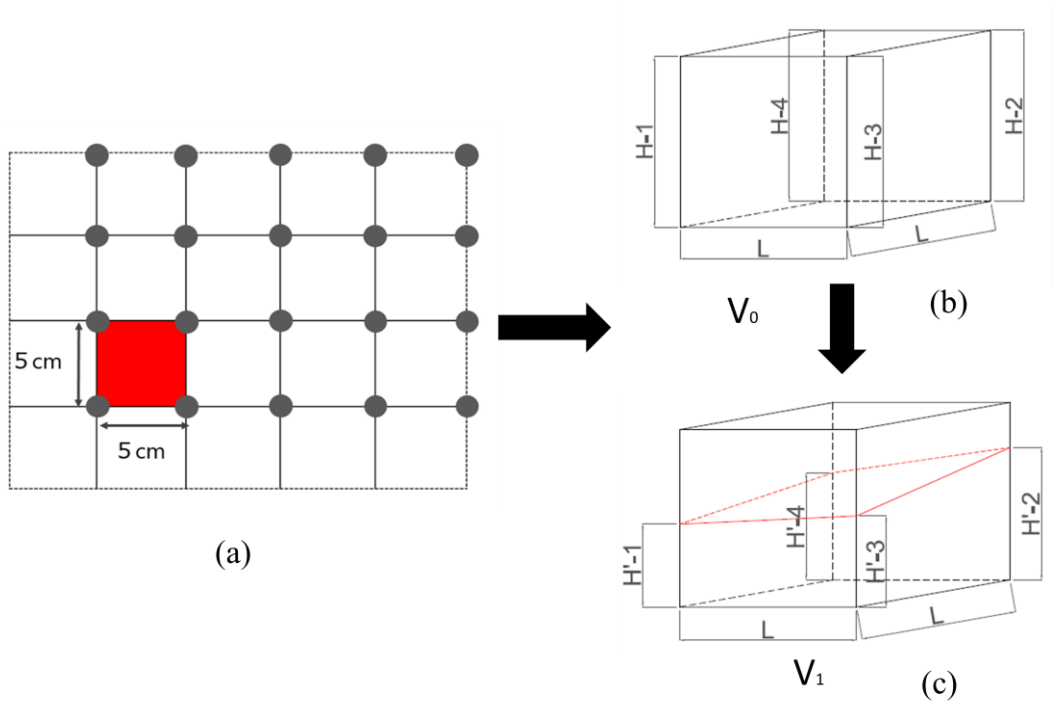

Fig 4. 14 The conceptual diagram of surface volume change calculation, (a) a grid space on the surface soil, (b) an initial h_1 measuring before test, (c) a measuring h_1' after testing

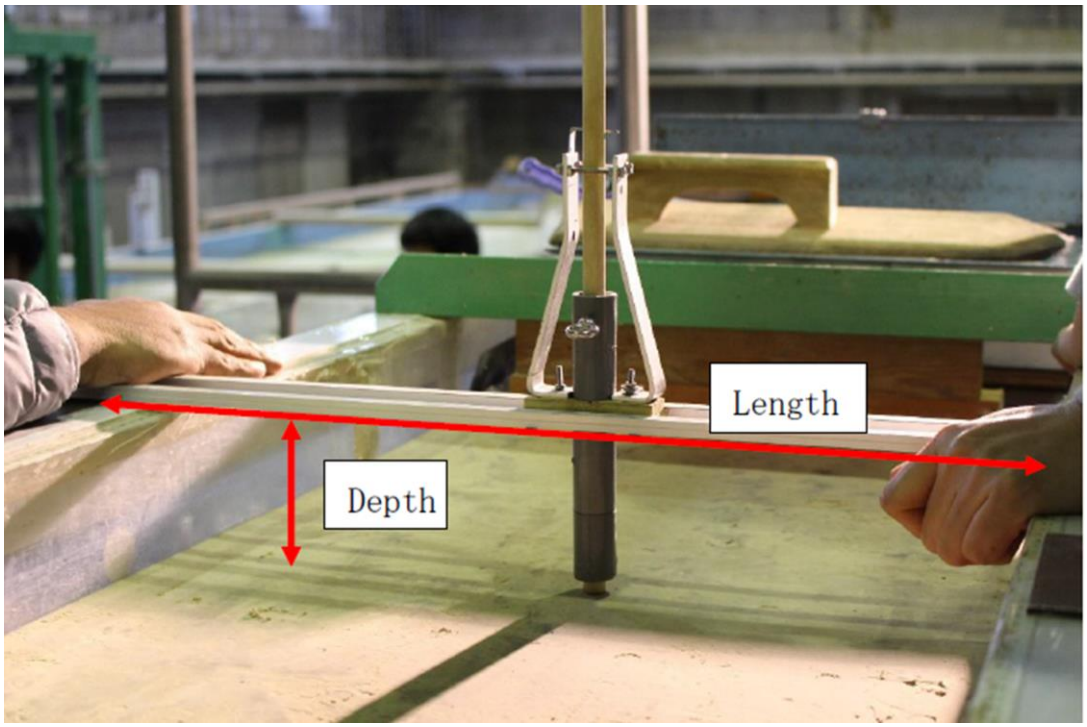

Fig 4. 15 Depth sampler uses to measure the surface changes

Chapter 5 Physical and Mechanical Properties of DL clay and Soil cement

In this chapter, the element test results are discussed. A series of experimental tests were conducted to study the characteristics of cemented silt soils. The element test consists of 1) Physical properties test; 2) Hydraulic properties test and 3) Consolidated drained triaxial compression test.

5.1 Density and grain size test results

To obtain the basic information of experimental soil, DL clay and cemented DL clay, various test methods were used. The summary of standard test methods used to investigate physical and mechanical properties of the soil cement is shown in Table 5.1. The composition of ordinary Portland cement, which is used for this study, is summarized in Table 5.2. The physical property of DL clay is shown in Table 5.3.

Table 5. 1 Standard test method used for physical property of DL clay

Test method	JGS standard number
Density of soil particle	JGS 0111
Liquid limit and plastic limit of soils	JGS 0141
Particle size distribution of soils	JGS 0131
Permeability of saturated soils	JGS 0311
Consolidated-drained triaxial compression test	JGS 0524

Table 5. 2 Chemical compositions of ordinary Portland cement

Chemical components	Symbol	Ordinary Portland cement (%)
Lime	CaO	64
Silica	SiO_2	21.3
Alumina	Al_2O_3	5.6
Iron Oxide	Fe_2O_3	3.36
Magnesia	MgO	2
Sulphur Trioxide	SO_3	2.14

Table 5. 3 Physical property of DL-clay

Materials	Unit	DL-Clay
Density of soil particle	ρ_s (g/cm^3)	2.653
Maximum dry density	ρ_{dmax} (g/cm^3)	1.52
Optimum water content	w_{opt} (%)	21
Maximum particle size	d_{max} (mm)	0.039
Coefficient of permeability	k_s (m/s)	6.68×10^{-7}

DL clay is an artificial soil material made from silica, kaolin, and pyrophyllite. From the liquid and plastic limit test results, it is classified as non-plastic silt. The density of DL clay (ρ_s) is about 2.65. The component of particle size distribution is sand = 0.1%, silt = 90.4%, clay = 9.5% as shown in Fig 5.1.

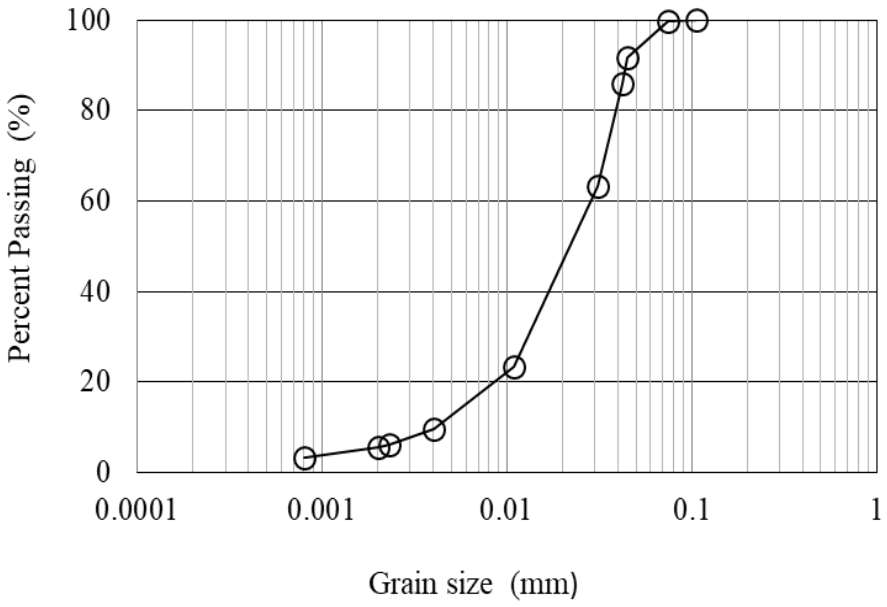

Fig 5. 1 Grain size distribution curve of DL clay

5.2 Compaction test results

Prior to decide the condition of soil specimens for consolidated drained triaxial compression test, it is necessary to determine the optimum moisture content for soil cement. Standard laboratory compaction test (JIS A 1210) was used to obtain the maximum dry density and optimum water content of soil cement.

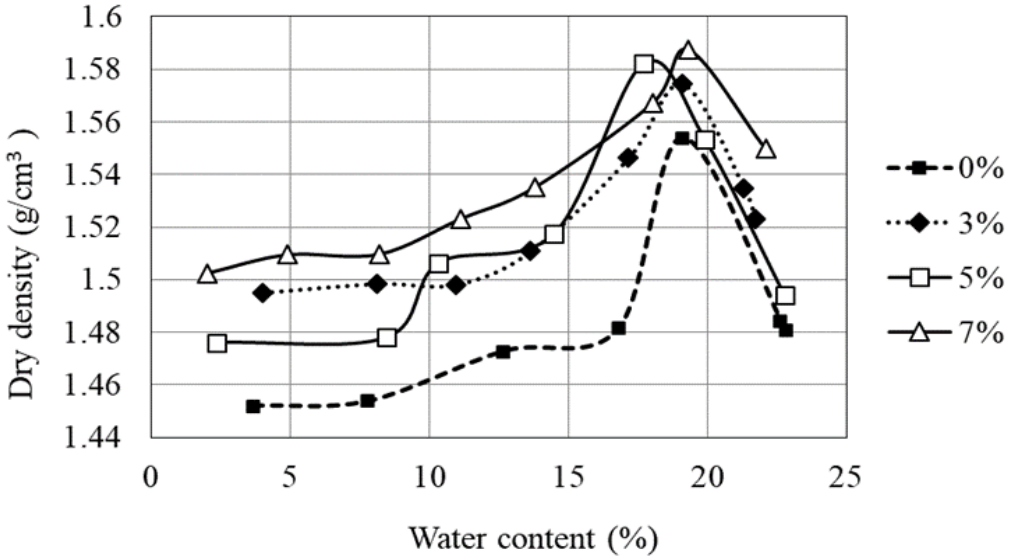

Fig 5. 2 Compaction curves of DL-Clay and Cemented DL clay

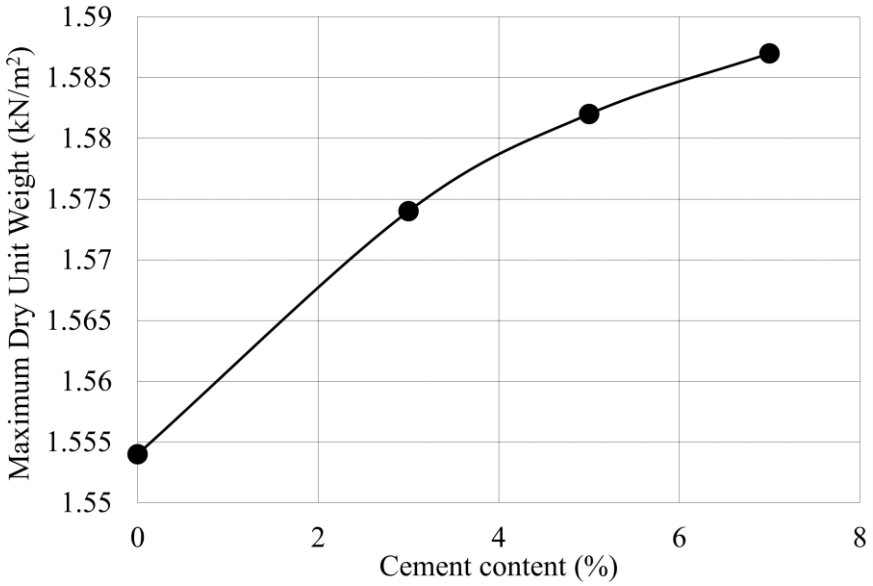

Fig 5. 3 Effect of cement content on maximum dry unit weight

The optimum water content and the maximum dry density relation of soil cement are shown in Fig 5.2, and the variation in maximum density due to the change in cement content is shown in Fig 5.3. Dry densities of the soil specimens increased at higher cement content. However, the optimum water content of the soil specimens slightly decreased while the more cement added. Based on the test results, the moisture content slightly below the optimum water content is most desirable for other testing. In Fig 5.3 shows the relationship between maximum density and cement content. It depicts that the maximum dry density of soil cement increases with the addition of cement content. This behaviour might be related to the chemical reaction of cement; soil and water.

5.3 Hydraulic conductivity test results

Twelve soil samples mixed with different cement contents, 0, 3, 5, and 7%, were tested. In case of soil cement, soil samples were cured for 7, 14, and 28 days before testing. The results are shown in Fig 5.4 to Fig 5.7. For DL clay, three different densities were tested. The results showed that density effected on the hydraulic coefficient (k). The dense density reduced the k value, while the loose density had a higher k value (Fig 5.4). For DL clay mixed with 3% of cement content, the k value started to decrease with increasing curing time (Fig 5.5). For soil cement 5%, the k value was fluctuated at various curing times, 7 and 14 days; but k value increased at curing time 28 days (Fig 5.6). The k value of soil cement 7% increased significantly, the k value was higher than soil cement 3 and 5% at curing time 28 days (Fig 5.7). This might be related to the hydration process of cement within the soil. The hydration of cement at high cement content might create more porosity inside the soil samples, so the water can be permeable more into the soil samples. The larger pore sizes are associated with higher permeability. When cementation products formed by the pozzolanic reaction fill mainly the intra-aggregate pores or cemented several small aggregates into a larger one, but the entire sample is not yet bound together (Quang and Chai, 2015). Thus the k value of soil cement became bigger than untreated soils in case of adding a small amount of cement. Quang and Chai (2015) also mentioned that the k value might decrease considerably when the cement content is higher than 8%. However, in the hydraulic conductivity test of this study, the cement content was less than 8% by dry weight. It might not be able to give a complete view of the k value at higher cement content.

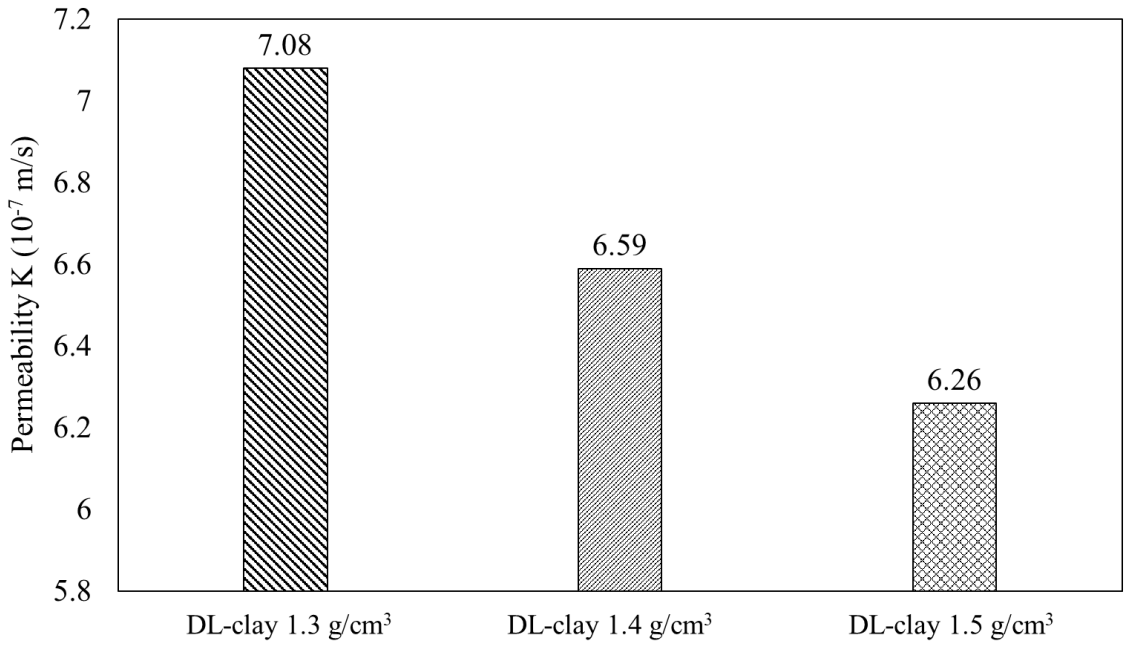

Fig 5. 4 Hydraulic conductivity of DL clay at different densities

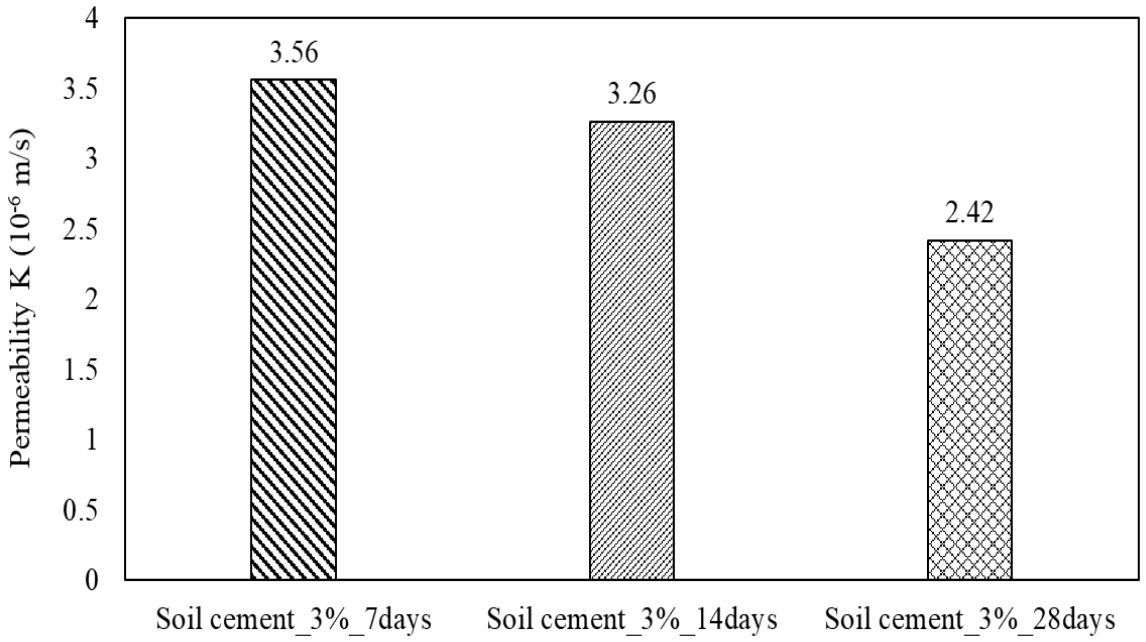

Fig 5. 5 Hydraulic conductivity of soil cement_3% at different curing times

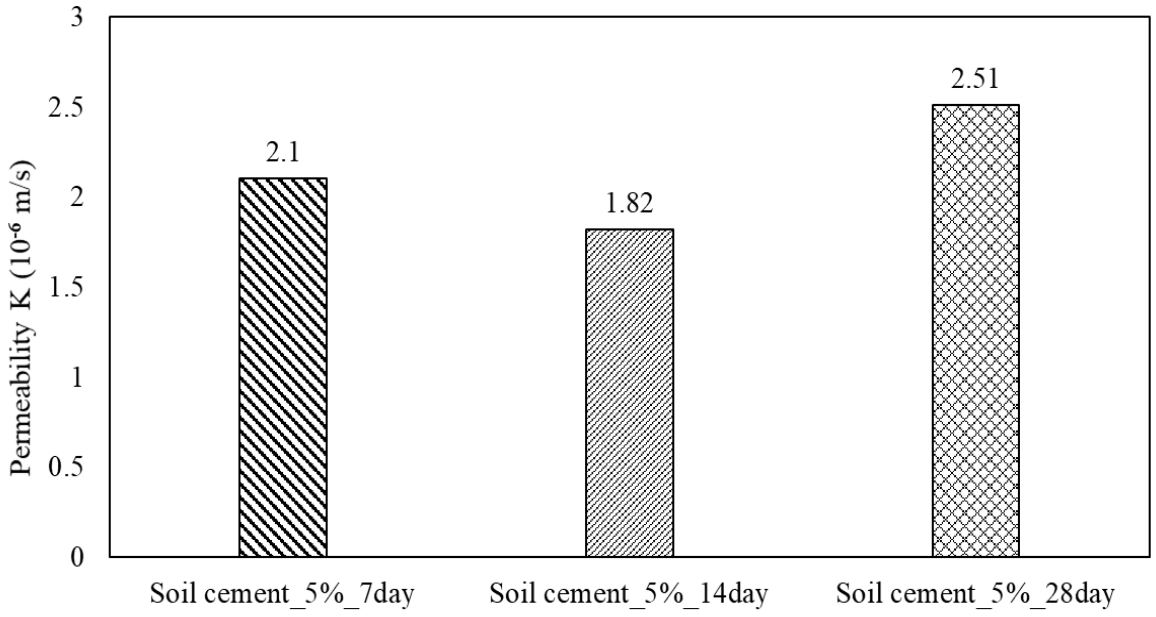

Fig 5. 6 Hydraulic conductivity of soil cement_5% at different curing times

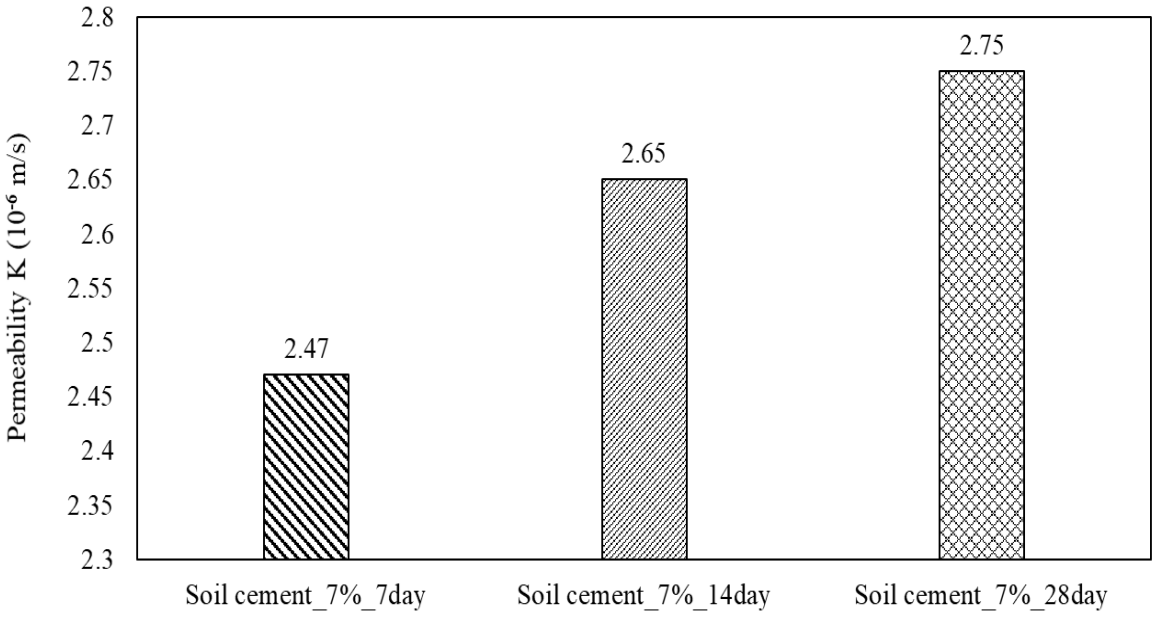

Fig 5. 7 Hydraulic conductivity of soil cement_7% at different curing times

5.4 Soil water retention curve (SWRC) test results

Estimating the unsaturated soil hydraulic properties at sub-surface, or near surface is essential for hydrological analysis (Sakai et al., 2015). An increase of water content in the soil, causing by rain, makes the loss of matric suction and the decrease of shear strength will promote soil erosion. The relationship between water content and matric suction is usually defined as the soil water characteristic curves (SWRCs). The SWRCs is widely used in geotechnical, geo-environmental, and agricultural engineering.

The initial condition soil specimens for soil water retention test is shown in Table 5.4. The saturation volumetric water content of soil cement was greater than DL clay (Fig 5.8). The hydration of cement with soil created the small aggregate; therefore, the soil cement had a larger volumetric water content than DL clay. In case of cement treated soils, the volumetric water contents decreased when the percentage of cement increased for a given suction.

Hysteresis exerts a considerable effect on the state and mobility of soil water in unsaturated porous media. The majority of SWRC hysteresis uses information on the basic wetting and drying curves. It is often necessary to use the wetting curve along with the drying curve for irrigation mode calculations and research on the soil moisture migration problem (Shein and Mady, 2018). The occurrence of hysteresis is usually observed in laboratory studies of SWRCs. Parlange (1976) stated that there are four major causes of the hysteretic effects: (1) geometrical non-uniformity of individual pores; (2) differences in the spatial interconnections and geometry of the pores during drying and wetting; (3) changes in the liquid and solid contact angle during drying and wetting; and (4) the presence of trapped air.

The wetting and drying curves of DL clay and DL clay mixed with cement are shown in Fig 5.9. Before applying suction, confining pressure, 10 kPa, was applied to all the specimen during the saturation process. The initial water content of 0%, 3% and 5% were 89%, 97% and 96.6%. The drying curve was constructed for the following suction values: 20; 40; 60; 80 and 100 kPa, and the wetting curve was constructed from the suction values of 80; 60; 40 and 20 kPa. The experimental wetting curve showed that soil water content under these conditions was lower than recorded during the drying. The width of the hysteresis loop, which is also known as the degree of hysteresis, can be defined as the ratio of moisture content values for the same water pressure

value. This value depends on the grain size composition, density, initial moisture content, and contact angle for wetting drying (Rafraf et al., 2016; Shein and Mady, 2018). The degree of hysteresis was higher for soil cement and lower for untreated soil (Fig 5.9). The overlapped points were not found in drying and wetting curves of 0% (Fig 5.9(a)). Because the drying process changes the original soil sample properties, soil specimen cannot return to the original state during the wetting process. In soil cement cases, two points were overlapped when the suction was reduced (Fig 5.9(b, c)). Due to the hard soil specimen, the original state of the soil specimens was not changed much. During wetting process, all specimens formed a hysteresis loop, but these hysteresis was not described by closed loop with fixed end points.

Table 5. 4 Initial condition of soil specimens

Water content (%)	17
Density	1.3 g/cm^3
Cement (%)	0, 3 and 5
Curing time	28 days
Height	2 cm
Diameter	6 cm
Suction Range	20, 40, 60, 80 and 100 kPa

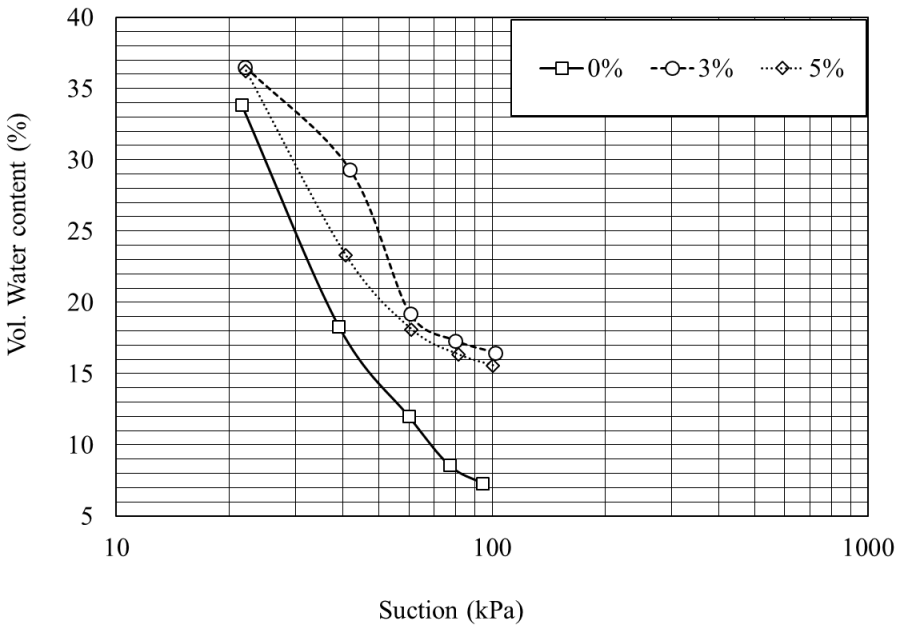

Fig 5. 8 The relationship between volumetric and suction

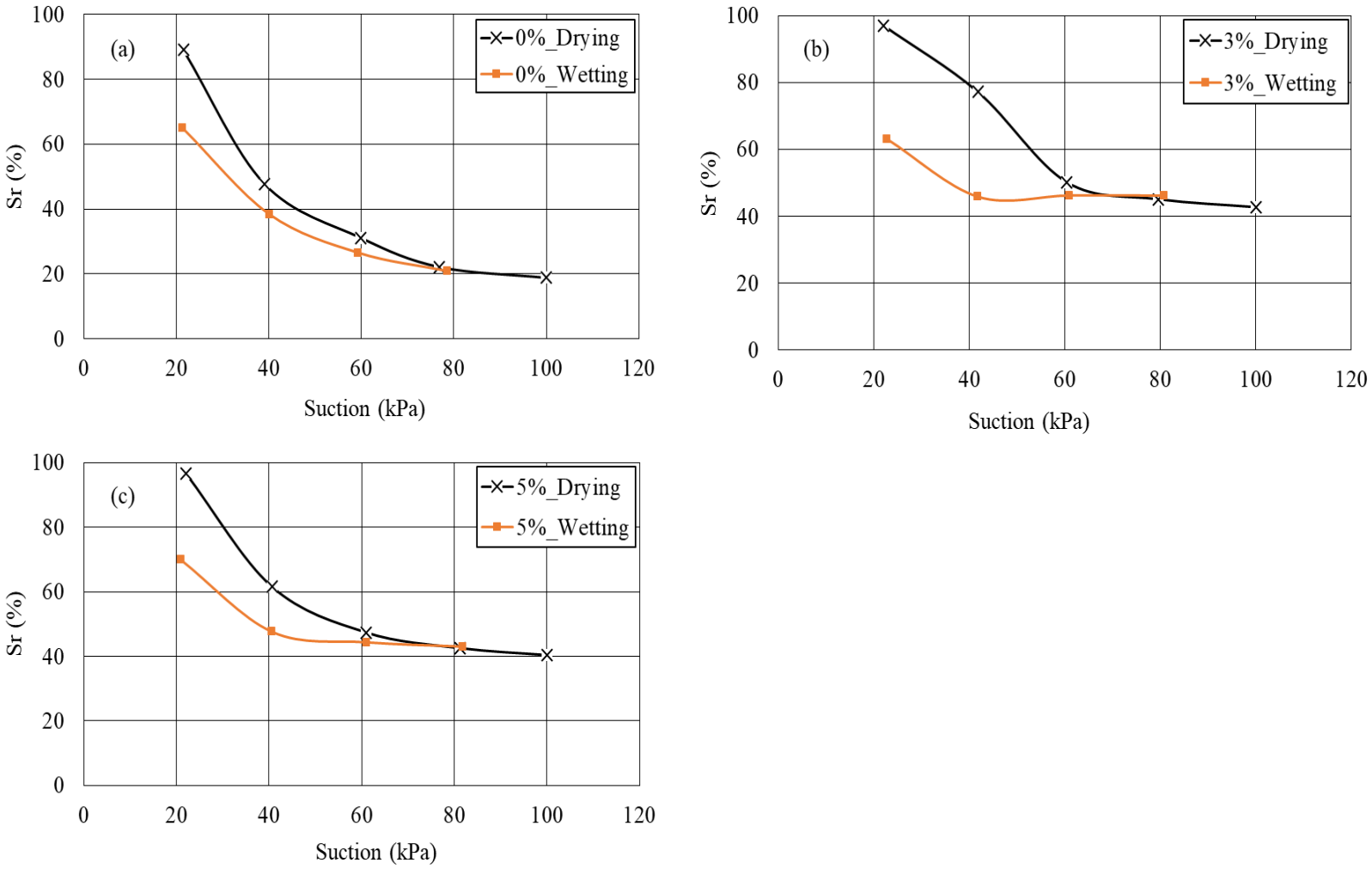

Fig 5. 9 Wetting and drying curves of DL clay and cemented DL clay

5.5 Crumb test results

The characteristic of dispersed soil was investigated through a crumb test, which was the simplest and most economical test. The soil sample used for the crumb test was 1.5 cm in diameter and 2 cm in high. Fig5.10 illustrates the crumb test results of DL clay. The dispersion process of DL clay was quickly observed, but there was no cloudiness caused by colloidal in suspension. The cylinder specimen was collapsed in 30 seconds after immerging into water due to the cohesionless of the soil specimen. In case of soil cement, two cement contents, 3 and 5%, were used.

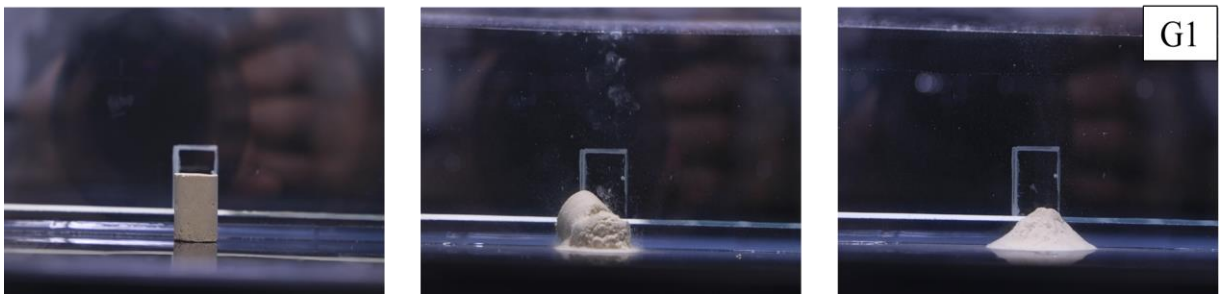

Fig 5. 10 The crumb test result of DL clay, the soil specimen collapsed very fast (30 second)

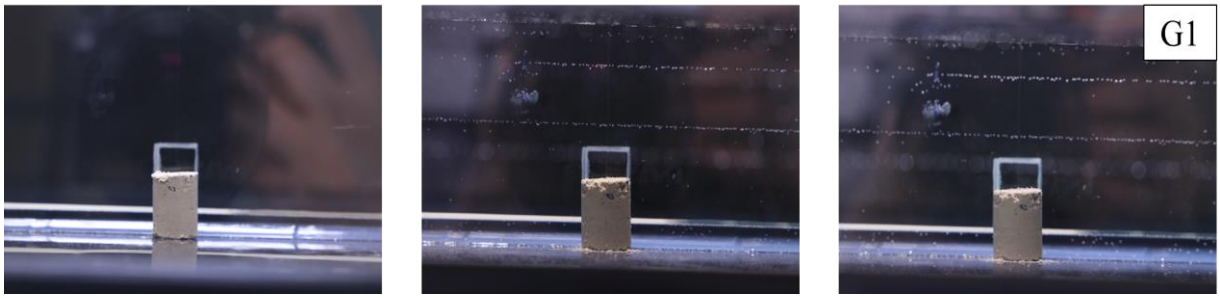

Fig 5. 11 The crumb test result of soil cement 3%_7 days

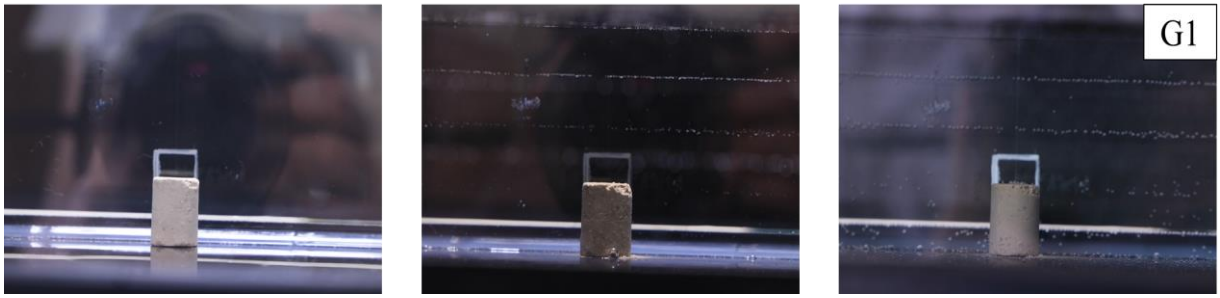

Fig 5. 12 The crumb test result of soil cement 5%_7 days

The results of crumb test showed that there was no degradation occurs on the soil cement samples, even after 48 hours immersion (Fig 5.11 and Fig 5.12). However, there were some visual changes, in particular on the crumble of the surface soil samples. In Table 5.5 shows the categories of the dispersion level and the detail description of observation in crumb test. The dispersion grade of soil specimens 0%, 3% and 5% were all graded into G1.

Table 5. 5 The categories of soil dispersion level

Grade	Reaction	Description	Categories
1	No reaction	Crumbs may slake or run out to form a shallow heap on the bottom of the beaker but there is no sign of cloudiness caused by colloidal in suspension.	Non-dispersion
2	Slight reaction	A very slight cloudiness can be seen in water at the surface of the crumb.	Non-dispersion
3	Moderate reaction	There is easily recognizable cloud of colloidal in suspension, usually spreading out in thin streaks at the bottom of the beaker.	Dispersion
4	Strong reaction	A colloidal cloud covers most of the bottom of the beaker, usually as a thin skin.	Dispersion

5.6 Mechanical properties of soil cement

Soil cement has been used in the field of geotechnical engineering for decades, considering as a recycling technique which helps to reduce the cost of construction. The strength of soil cement mainly depends on the mixing design and curing time. Soil cement mixing condition and curing is similar to concrete. For the consolidated drained triaxial compression test (CD test), the saturated soil specimen was subjected to a confining pressure (σ_3) firstly. The connection to the drainage was open for complete drainage. Then the deviator stress $\Delta\sigma$ increased at a very slow rate to complete dissipation of water. The confining pressures were 50 kPa, 100 kPa, and 200 kPa. The detail of the initial condition of all specimens for CD test is shown in Table 5.6. The typical test results of deviator stress (q) - axial strain (ε_a) and axial strain-volumetric strain (ε_v) relationships are discussed as follows.

Table 5. 6 Initial condition of soil specimens for CD test

Specimen No.	Confining pressure (kPa)	Cement content (%)	Curing time (day)	Water content (%)	Dry density (g/cm^3)	Void ratio	Degree of saturation (%)
1	50	0	0	17.6	1.282	1.069	43.7
2	50	3	7	15.7	1.306	1.031	40.4
3	50	3	14	17.7	1.283	1.068	44.0
4	50	3	28	17.5	1.274	1.082	42.9
5	50	5	7	16.6	1.298	1.044	42.2
6	50	5	14	15.7	1.302	1.038	40.1
7	50	5	28	16.6	1.292	1.053	41.8
8	50	7	7	16.6	1.305	1.033	42.6
9	50	7	14	16.6	1.295	1.049	42.0
10	50	7	28	16.7	1.298	1.044	42.4
11	100	0	0	16.5	1.270	1.089	40.2
12	100	3	7	16.7	1.277	1.078	41.1
13	100	3	14	15.9	1.278	1.076	39.2
14	100	3	28	15.7	1.312	1.022	40.8
15	100	5	7	15.8	1.277	1.078	38.9
16	100	5	14	18.4	1.238	1.143	42.7
17	100	5	28	17.3	1.280	1.073	42.8
18	100	7	7	15.9	1.270	1.089	38.7
19	100	7	14	16.7	1.264	1.099	40.3
20	100	7	28	16.7	1.292	1.053	42.1
21	200	0	0	17.6	1.289	1.058	44.1
22	200	3	7	17.3	1.278	1.076	42.7
23	200	3	14	17.3	1.280	1.073	42.8
24	200	3	28	17.7	1.284	1.066	44.1
25	200	5	7	17.2	1.297	1.045	43.7
26	200	5	14	16.2	1.278	1.076	39.9
27	200	5	28	16.7	1.289	1.058	41.9
28	200	7	7	16.2	1.305	1.033	41.6
29	200	7	14	16.2	1.297	1.045	41.1
30	200	7	28	16.5	1.295	1.049	41.7

5.6.1 Stress strain relationship of soil cement

Before starting discussion, we will define stress variable q. The stress variable is

$$q = \sigma_1 - \sigma_3 \qquad (5.\ 1)$$

Where q is deviator stress, σ_1 is maximum principal stress, and σ_3 is minimum principal stress.

Fig 5.13 shows the results of specimens with the same curing time t = 28 days, the different cement contents; C_c = 0, 3, 5 and 7%, and different confining stresses; σ_3 = 50, 100 and 200 kPa. It was observed that the addition of cement to soil could substantially improve shear strength. As Das et al. (1995) concluded that the strength of cemented sand increases with increase in cement content. The peak strength of soil cement noticeably increased, but the brittle stress-strain behaviour was observed, especially of the soil mixed with cement 7%. Schniad et al. (2001) and Consoli et al. (2009) reported that the brittle stress-strain behaviour occurs at the higher cement contents. In addition Sariosseiri and Muhunthan (2009) also described that the utilization of cemented specimens changes soil behaviour to a noticeable brittle behavour. Park (2011) described that the brittle behaviour can cause the sudden failure of soil structures.

All the cemented specimens with σ_3 = 50 kPa expressed strain softening and dilation (Fig 5.13(a)). The behaviour of softening became weaker with an increase in confining stresses (Fig 5.13(b, c)). The amounts of dilations and the peak shear strengths almost increased with an increase in cement contents, but the influence of cement contents to ultimate shear strengths was rather smaller than the peak shear strengths. The tendency is similar to those of cemented sands (Wang and Leung 2008). Gao and Zhao (2012) proposed a constitutive model where the cemented effects are referred as a bonding effect. The bonding effect may be similar to the second suction effect in unsaturated soils. In unsaturated soils, we have to consider two suction effects (Kohgo et al. 1993a, b); (i) An increase in suction increases effective stresses, and (ii) An increase in suction enhances the yield stresses and affects resistance to plastic deformations. The second effect is induced by capillary forces that act at contact points of soil particles and draw soil particles together. Thus the capillary force acts as a water-soluble bond. The bonding effect disappears at the critical state (ultimate state) because it induces internal confinements and all the internal confinements may disappear at the critical state. The bonding effect due to cement may also disappear at the ultimate state.

However the first suction effect can still remain in unsaturated soils. This point is only different between the behaviors of cemented soils and unsaturated soils.

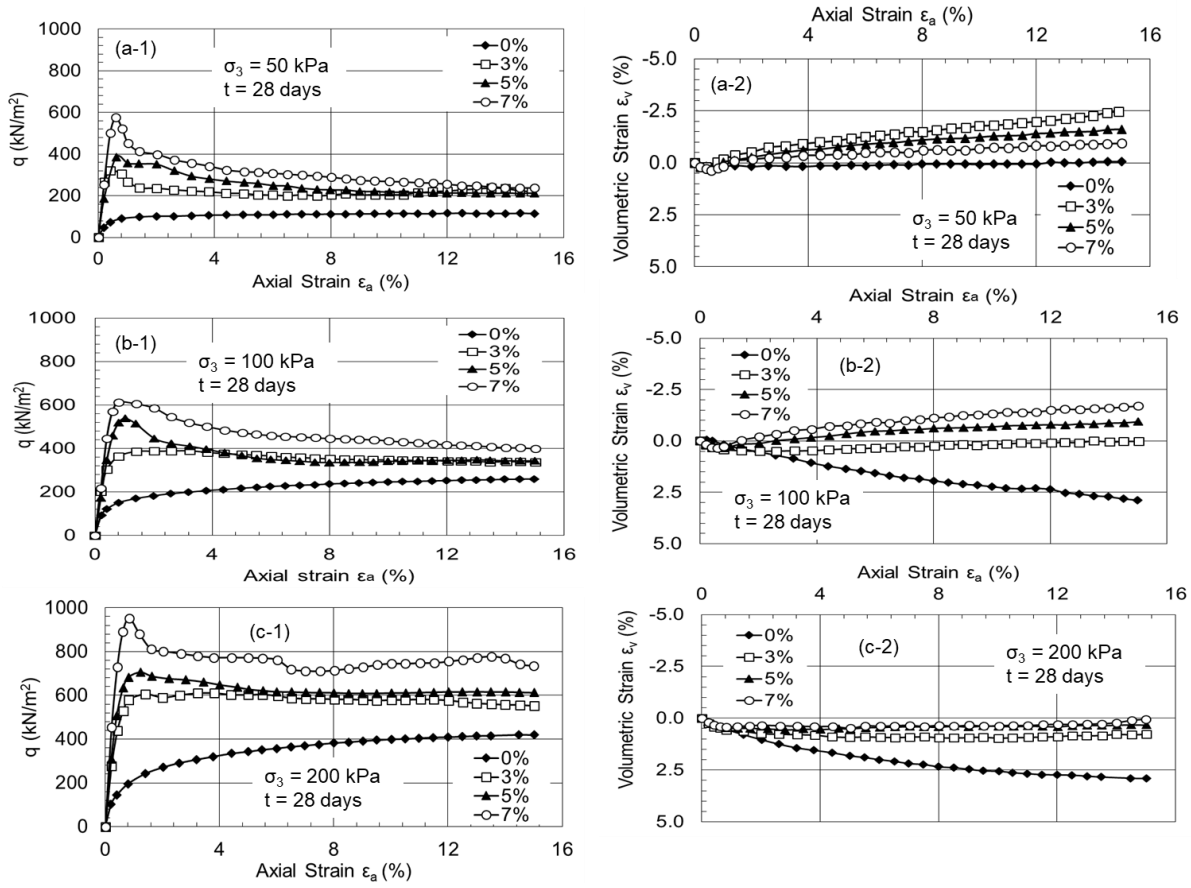

Fig 5. 13 Results of CD tests for cemented DL clay specimens, curing time 28 days

The influences of curing times to stress - strain and axial strain - volumetric strain relationships for σ_3 = 50 kPa and 200 kPa are shown in Fig 5.14 and 5.15, respectively. The shear strength values at the peak depended on the curing times, namely those increased with an increase in curing times, but there were a little influences of curing times to the strength values at the ultimate (Fig 5.14). Al-Aghbari et al. (2009) investigated on the shear strength of cemented sandy soils also agreed that the shear strength increased with curing time. All the specimens expressed larger dilations as curing times progressed (Fig 5.14). Fig 5. 14 and Fig 5.15 shows that the specimens with C_c = 7 % have clearer peak shear strengths than other specimens. Though there were scatters at the ultimate strength, the specimens with the same cement contents were likely to have the similar strength values (Fig 5.15(c-1)).

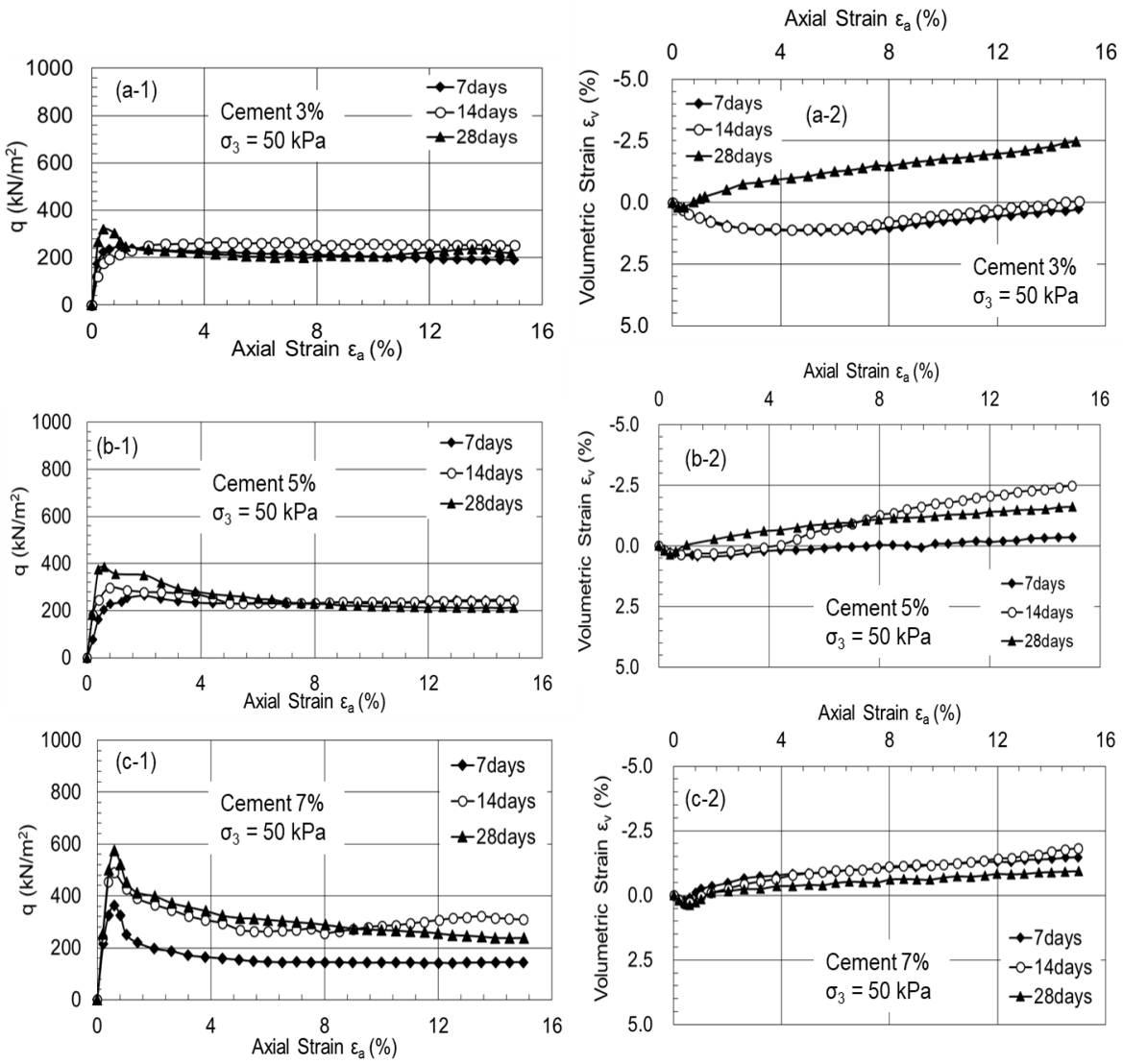

Fig 5. 14 Influence of curing time to stress-strain relationship and axial strain-volumetric strain relationships in specimens with σ_3 = 50 kPa

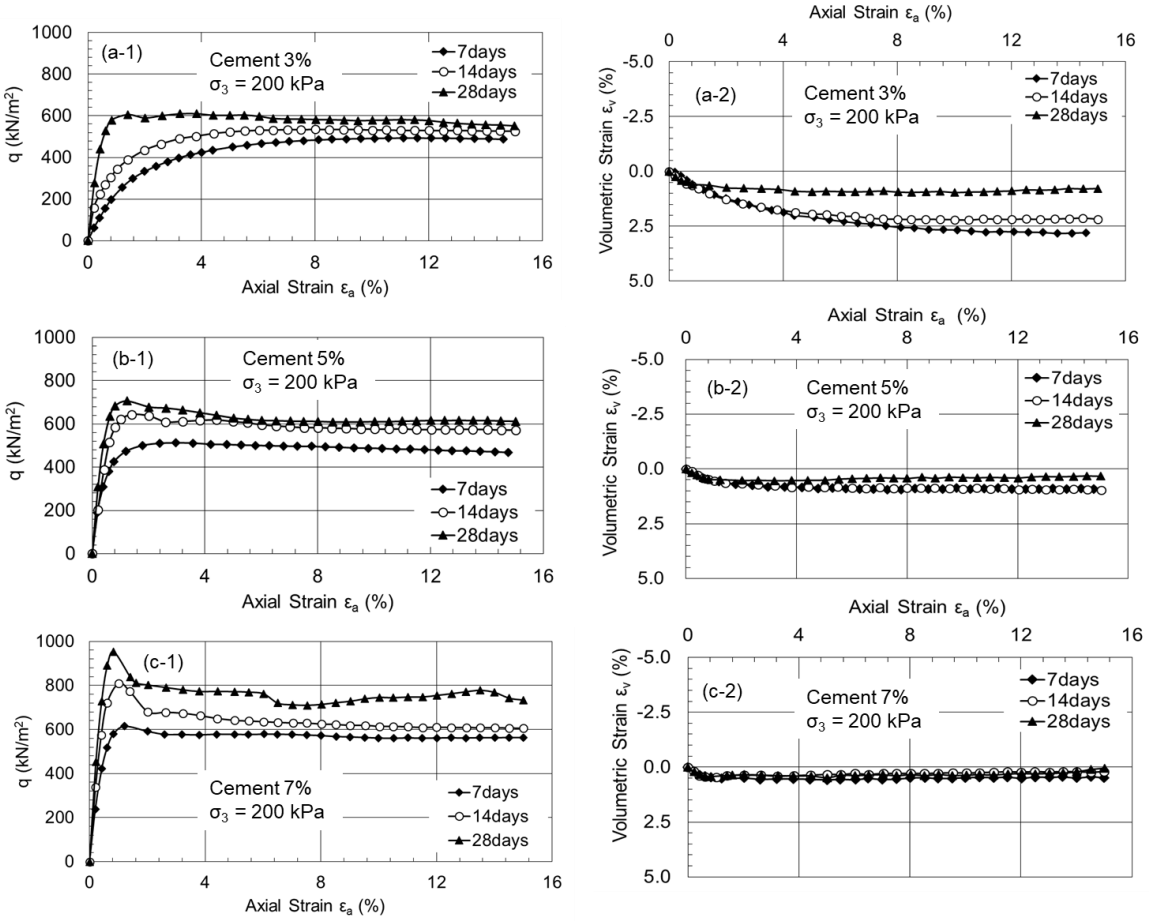

Fig 5. 15 Influence of curing time to stress-strain relationship and axial strain-volumetric strain relationships in specimens with σ_3 = 200 kPa

5.6.2 Relationship between shear strength values at peak and curing times

In measures of erosion, it is one of the important design factors to know the relationship between shear strength values at peak and cement contents. Fig 5.16 to Fig 5.18 shows deviator stress $q_f - \sigma_3$ relationships obtained from the specimens with different curing time at t = 7; 14 and 28 days. These data were obtained from both triaxial compression and unconfined compression tests. Though the estimated failure lines had the same slope degrees; the lines showed good estimations for all the cases. Thus, the differences of cement content values (C_c) affected strongly to the cohesion values (c), and c values increased with an increase in C_c values. The similar findings were confirmed by Mitchell (1976) that a stabilizing agent increased the effective cohesion (c). Fig 5.19 to Fig 5.21 shows the relationship between cohesion c and C_c. Symbols are values calculated from the estimated failure lines shown in Fig 5.16 to Fig 5.18. The relation almost expressed linear. In case of curing time 28 days, the

relation precisely expressed R^2=0.98. The cohesion of soil cement also increased with curing time.

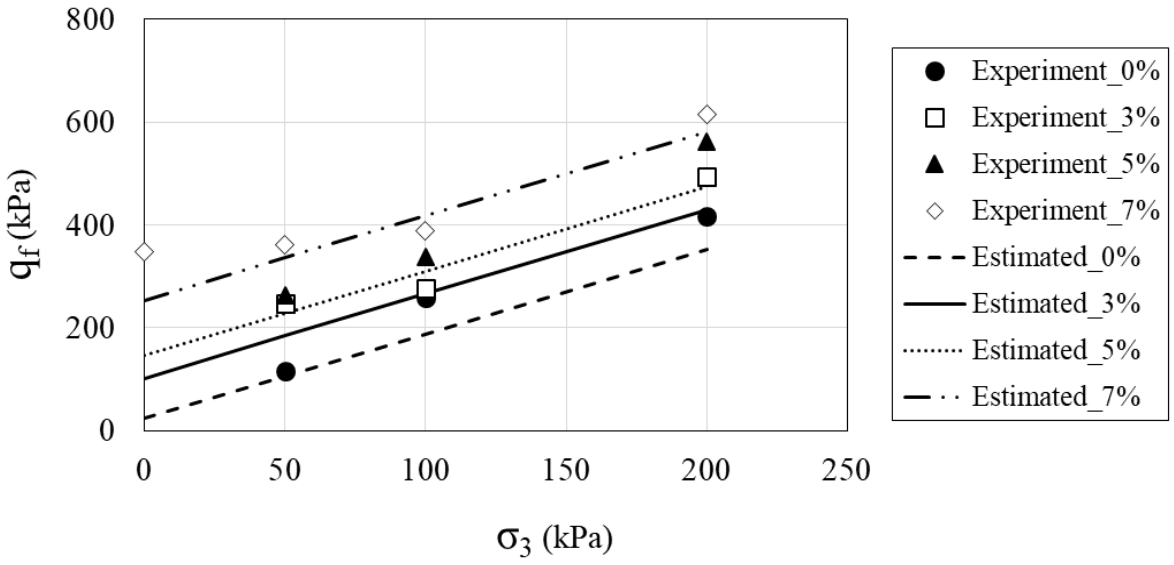

Fig 5. 16 Relationships between normalized shear strength values and curing times _ 7 days

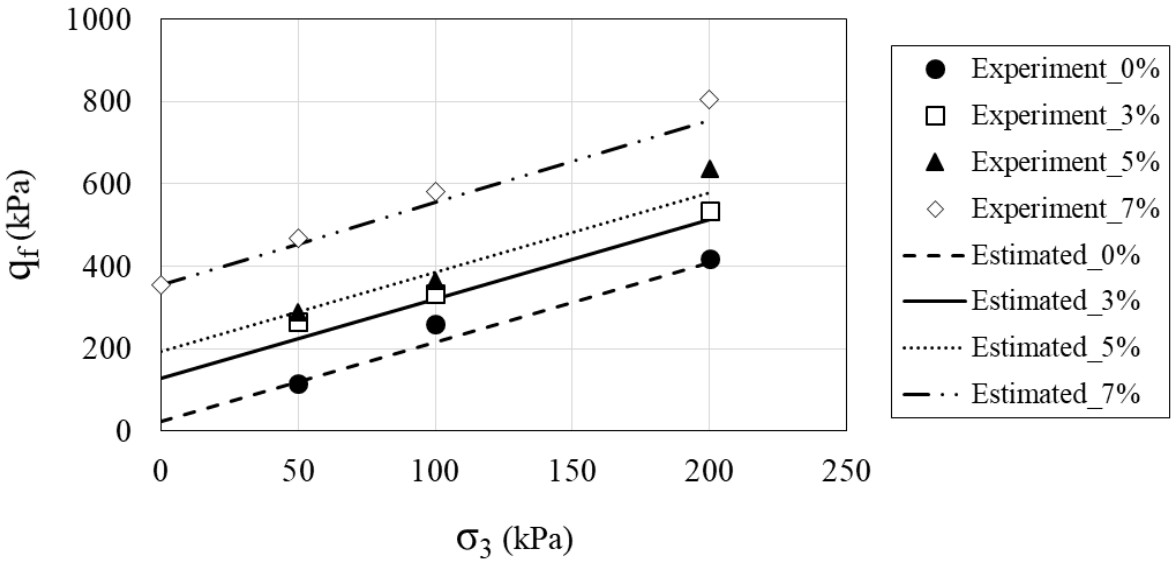

Fig 5. 17 Relationships between normalized shear strength values and curing times _ 14 days

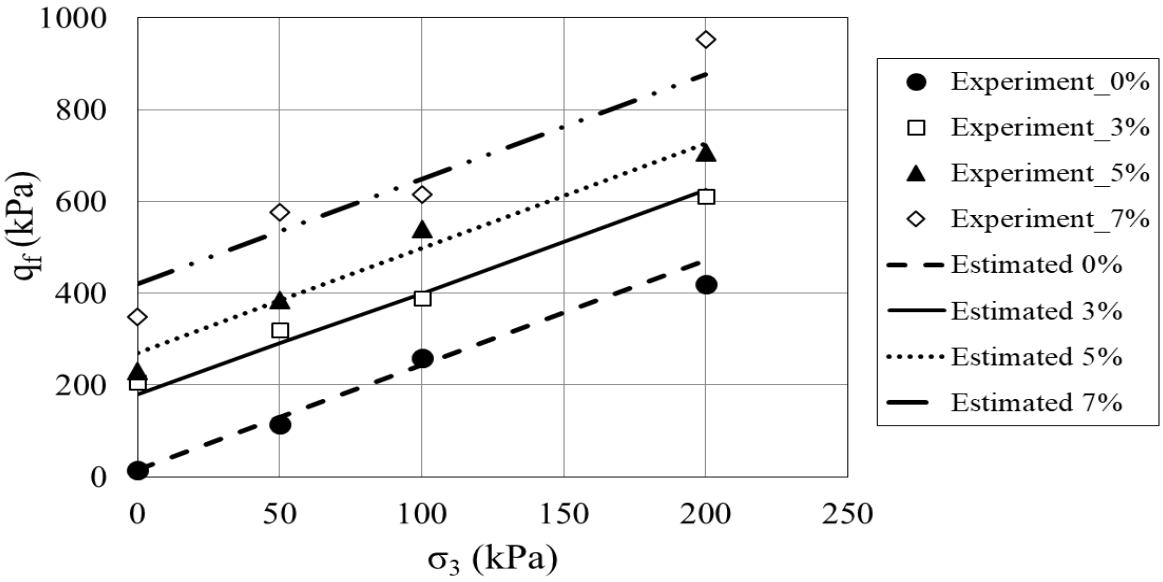

Fig 5. 18 Relationships between normalized shear strength values and curing times _ 28 days

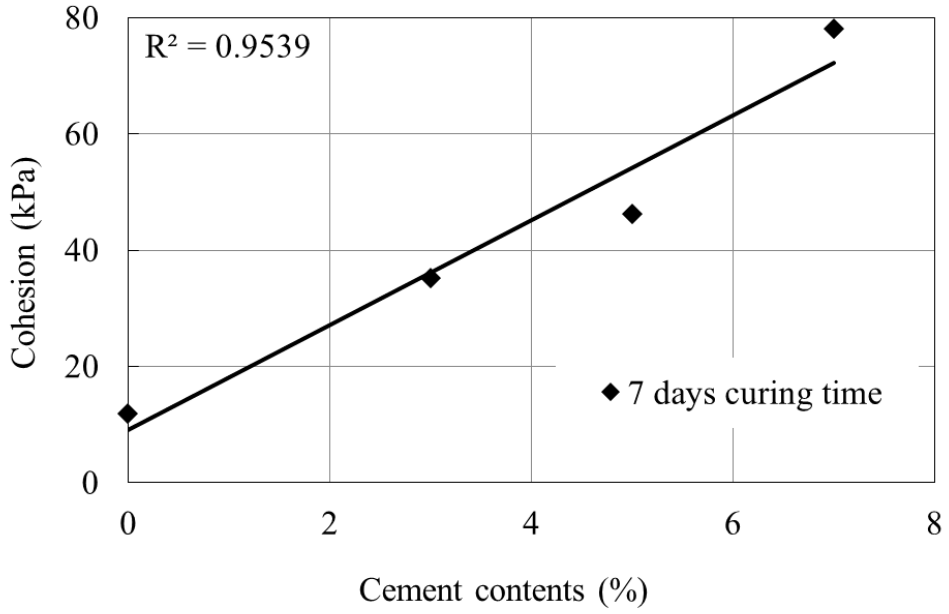

Fig 5. 19 Relationships between cohesion *c* and cement contents C_c _7 days

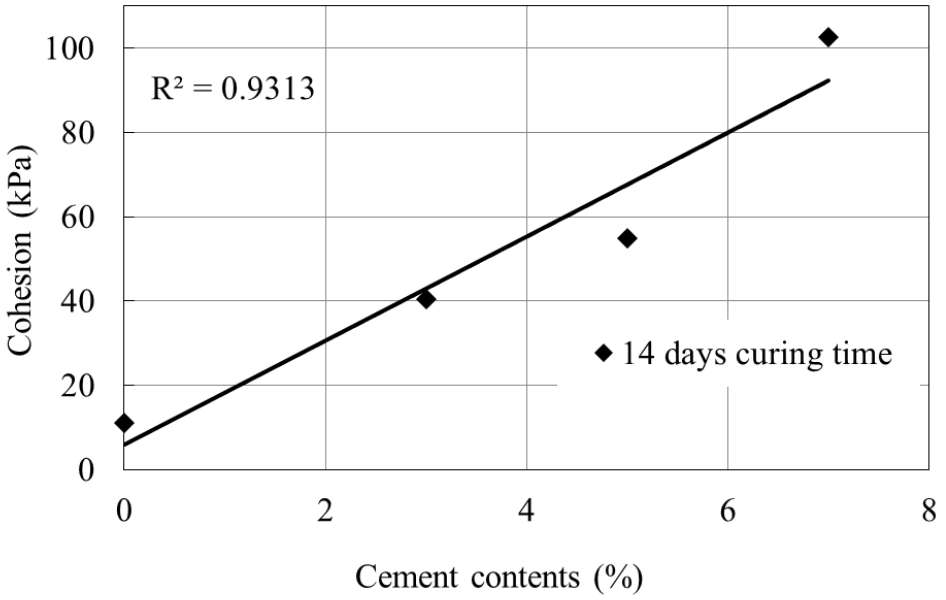

Fig 5. 20 Relationships between cohesion *c* and cement contents C_c _ 14 days

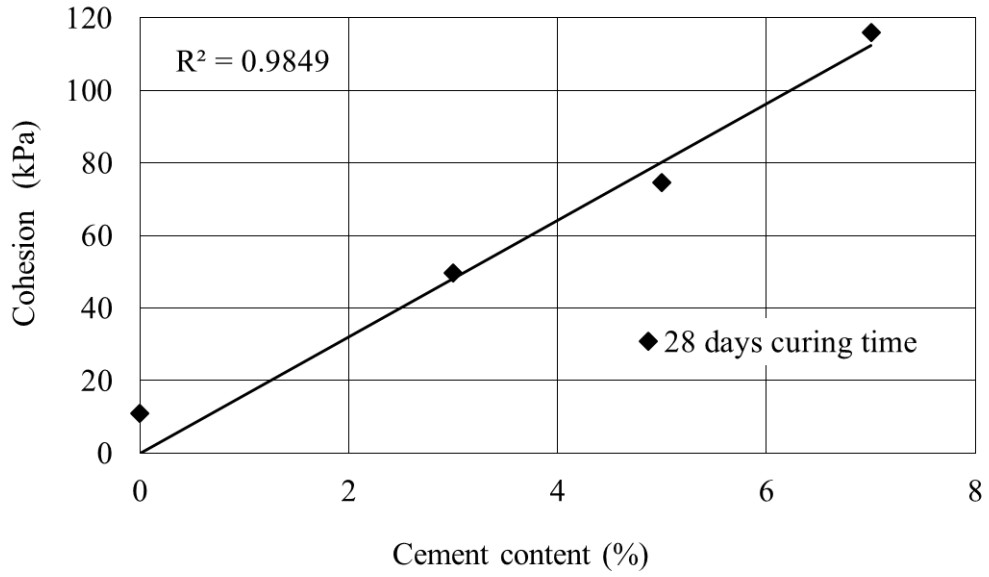

Fig 5. 21 Relationships between cohesion *c* and cement contents C_c _ 28 days

5.6.3 Estimation for a long-term performance of soil cement

The long-term performance of soil cement application against erosion is very important. In this section, the long-term shear strength is evaluated until 91 days. The following hyperbolic equation is assumed in order to estimate the peak shear strength values q_{ft} for each confining pressure at curing time t by using the associated q_{f7} at curing time t = 7 days:

$$\frac{q_{ft}}{q_{f7}} = \frac{t}{a+bt}, \qquad (5.2)$$

or

$$\frac{t}{(q_{ft}/q_{f7})} = a + bt, \qquad (5.3)$$

where a and b are parameters, $q_f = \sigma_1 - \sigma_3$ at failure (the peaks).

Fig 5.22 shows the relationship between normalized shear strength values and curing times. It was found that Equation (5. 3) may almost be valid. The estimated parameters are shown in Table 5.7. The values of a and b ranged within 2.577 - 3.446 and 0.518 - 0.677, respectively. Then as the variations were small, the values of q_{ft} might be estimated by using the mean values $\bar{a}$ and $\bar{b}$. The lines estimated with each a and b values and the line with the mean values $\bar{a}$ and $\bar{b}$ are plotted in Fig 5.22. The estimated lines have good agreements, and the line with the mean values has also a good one. Thus it is available to use an estimated line with mean values $\bar{a}$ and $\bar{b}$.

Table 5. 7 Estimated parameters for equation (5. 2)

Cement content (%)	a	b	R^2
3	2.577	0.677	0.9806
5	3.446	0.589	0.9399
7	3.208	0.518	0.9951
Mean values	3.077	0.595	

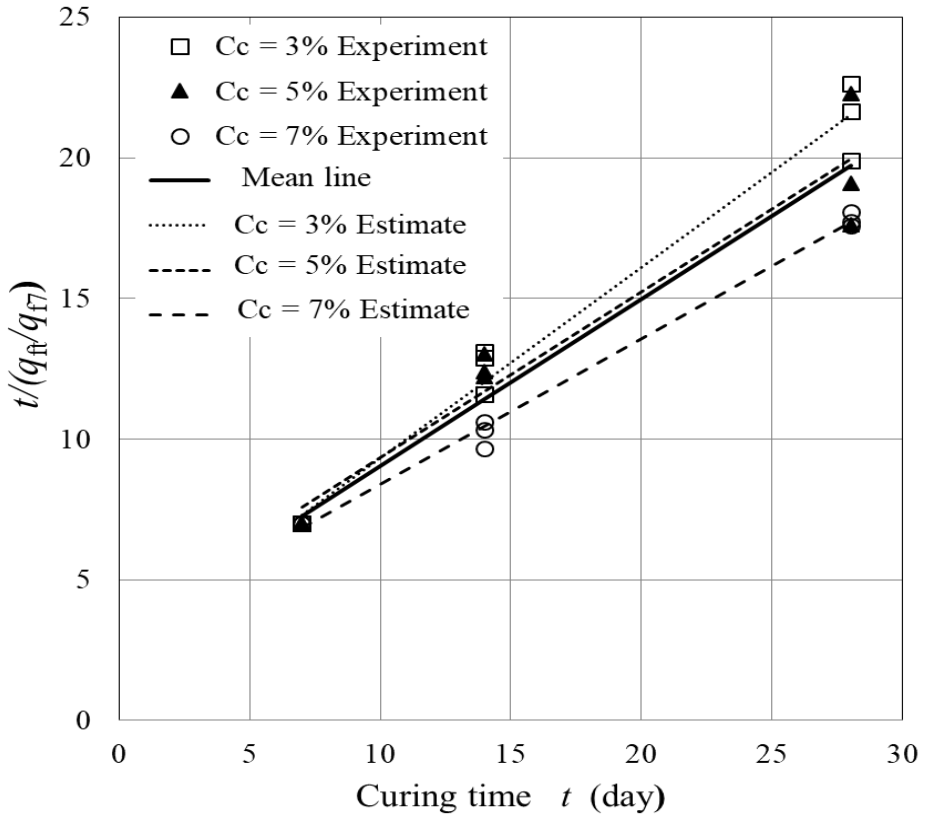

Fig 5. 22 Relationships between normalized shear strength values and curing times

The relationships between q_f and curing time t estimated by Equation (5. 2) are shown in Fig 5.23, where the values of q_f are estimated until t = 91 days. In these figures the symbols, the dashed lines, and the solid lines express experimental data, the values estimated by Equation (5. 2) with each a and b, and the values estimated by Equation (5. 2) with mean values $\bar{a}$ and $\bar{b}$, respectively. In confining pressures σ_3 = 50 kPa and 100 kPa, there are almost high agreements between the values estimated with each a and b and with $\bar{a}$ and $\bar{b}$; but in higher confining pressure σ_3 = 200 kPa, the difference between the estimations is larger. When cemented soils are used as measures of erosion, the confining pressures are generally low. Then the estimation line with mean values $\bar{a}$ and $\bar{b}$ may be applicable to estimate peak shear strength for long period. Concerning to long-term performance and degradation of soil cement, several research groups found that the strength of soil cement increases with time (Hayashi et al., 2003; Kitazume et al., 2003; Ikegami et al., 2005). Hayashi et al. (2003) conducted a practical experiment on the long-term strength of in-situ cement treated soil, which aged more than 10 years, confirmed that the shear strength, in particular the strength inside the treated soil, continued to increase with time. At the same time, the deterioration at

the outer boundary of soil cement samples was observed, but the extent of degradation (strength reduction) of the outer boundary of soil cement was very small (Hayashi et al., 2003; Ikegami et al., 2005). As mentioned before, the main goal of this study is to propose measures, which are low cost, easy construction and easy repair, to protect embankments of irrigation facilities against surface erosion. If deterioration on the surface of the embankment treated with cement occurs, the repair may be easily conducted and the deterioration may not be serious problems.

5.7 Concluding remarks

It was found from the crumb test that the DL clay sample easily broke into pieces, but there were no clouds in suspension. The dispersion rate of DL clay mixed with cement content 3% and 5% was also low. The DL clay and DL clay mixed with cement were graded in grade 1. The hydration of cement content of soil strongly affected on the soil water retention curves and hydraulic conductivities. At the low cement content, the hydration of cement, soil and water created more pores inside the soil specimens which leaded to the fluctuation of the hydraulic conductivities at various curing times. The degree of hysteresis of soil cement was much bigger than DL clay. It indicated the ratio of moisture containing in soil cement specimens was much more than DL clay. The strength of soil cement increased at the low cement contents. The cement content 7% showed the largest shear strength; however, the significant brittle failure was also found in 7% of the cement content soil specimen, which made the big concern for construction. In case of 3% and 5% specimens, it showed the sufficient strength. The shear strength of soil cement continued to increase for a long curing time 28 days as well as the cohesion of the soil specimens.

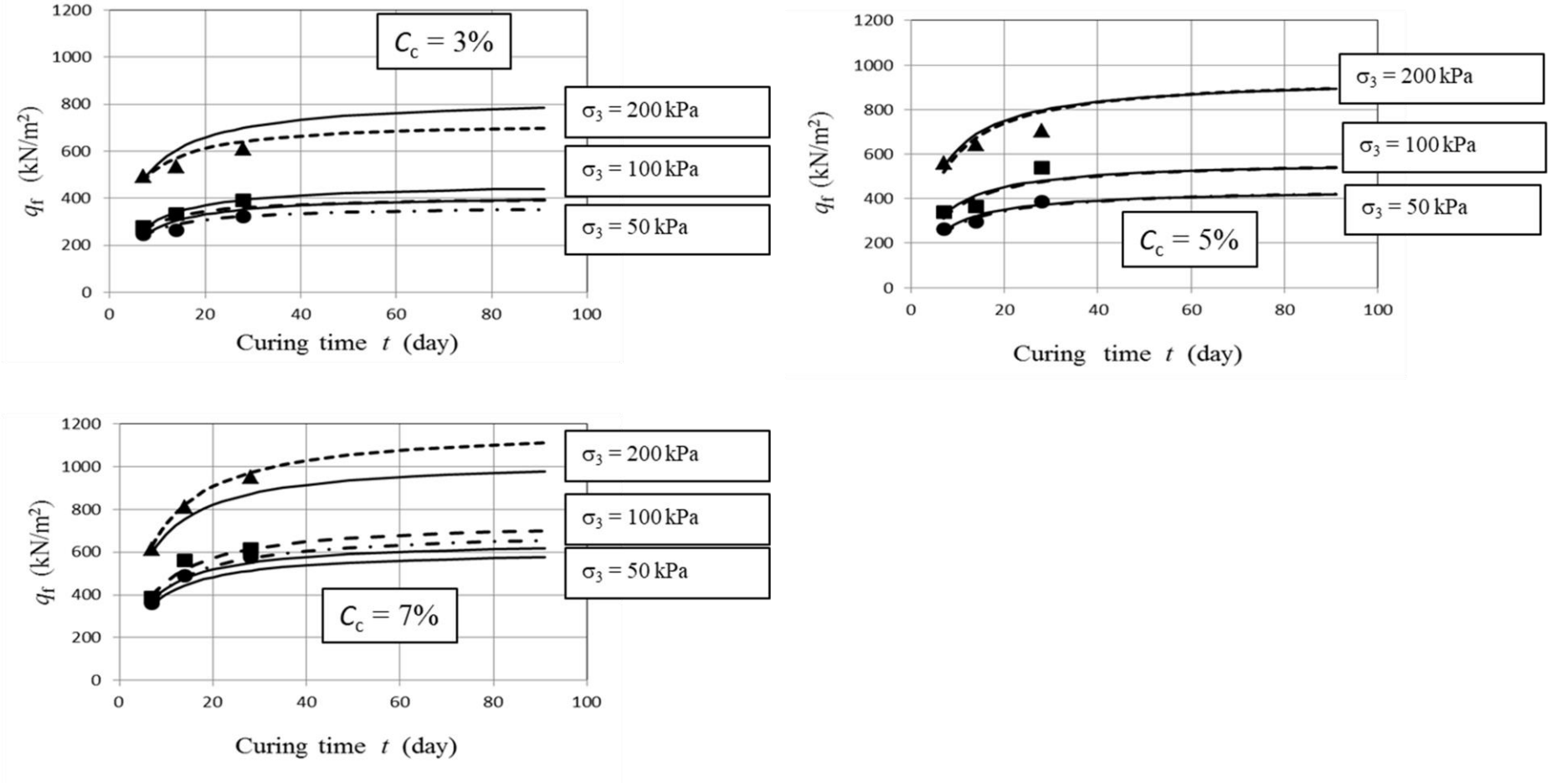

Fig 5. 23 Relationships between q_f vs. curing time t estimated by Equation (2); Symbols: Experimental data, Dashed lines: Estimations with each a and b, Solid lines: Estimations with mean a and b

Chapter 6 Rain Erosion Resistance Test

In order to evaluate the resistance of soil cement to surface erosion, simulated rainfall equipment was used to deliver a rainfall at a specific rainfall intensity to six slope models covering the surface soil with different cement contents 0, 3, and 5%. Two types of rainfall intensities were used to assess the efficiency of soil cement materials as a precaution against surface erosion, 50 and 100 mm h^{-1}. Thus, surface soil conditions and surface eroded volume of slope models were mainly determined in this test by using the grid method and a depth sampler to measure the vertical change of each grid cell. In this part, the result of surface changes, surface runoff, soil losses, and the relationship between soil shear strength, hydraulic conductivity of soil are described.

6.1 Test procedures

6.1.1 Rainfall calibration

To calibrate rainfall, 3,000 ml measuring buckets were placed in two rows to capture the rainwater on the surface slope equipment. There were 8 foam platforms designed to form an accurate slope, 20-degree, and arranged 16 measuring buckets over it (Fig 6.1). During the rainfall calibration process, it is necessary to control and carefully check the arrangement of the nozzle direction, falling pressure adjustment, and water discharge capacity. The nozzle arrangement was optimized to get the most effective rainfall distribution on the surface slope. Rainfall intensity was calculated by the amount of trapped water in the buckets divided by time. The distribution of rainwater over the surface soil slopes is shown in Fig 6.2 and Fig 6.3.

To check the uniformity of the rainfall distribution over the surface soil slopes, the Christiansen's uniformity coefficient (CU) formula was used to calculate for the uniformity of rainfall distribution. The uniformity coefficient is given by:

$$C_U = \left[1 - \frac{\sum_{i=1}^{n} |R_i - M|}{nM} \right] \quad (6.1)$$

Where C_U = Christiansen's coefficient of uniformity (%)

R_i = Average absolute deviation from the mean

M = mean application

n = number of individual application amounts

Little et al. (1993) reported that if the Christensen Uniformity Coefficient value is = 90%, between 80-89%, between 70-79% and > 69%, it is considered as very good, good, poor and worst. The CU value of 50 mm h^{-1} is 86% and 83% for 100 mm h^{-1}, thus the uniformity of two rainfall intensities is in good condition.

Fig 6. 1 Rainfall Calibration process by using measuring cups to capture the rainwater at the specific duration

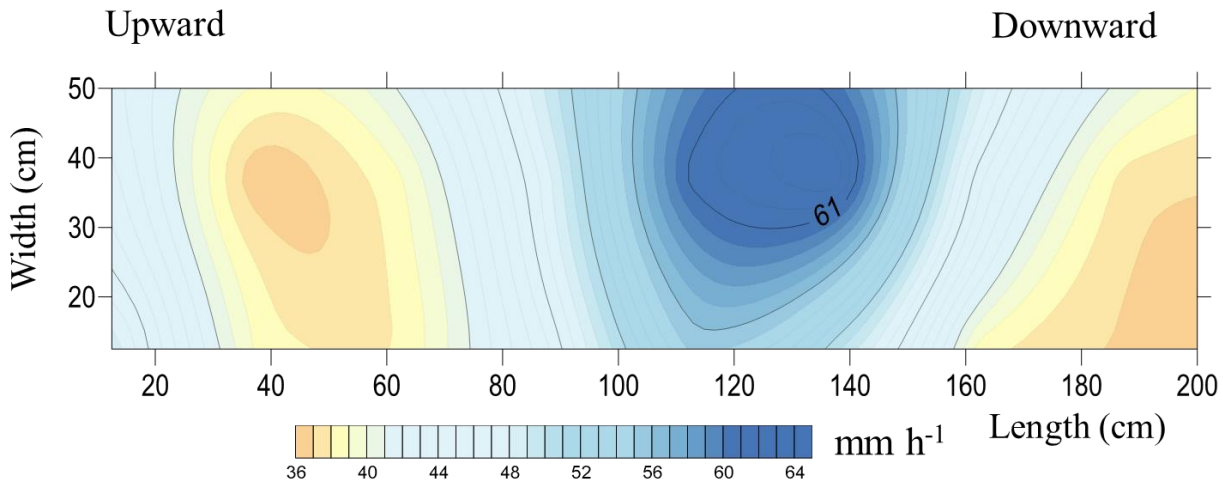

Fig 6. 2 The distribution of the rainfall on the surface slopes_50 mm h^{-1}

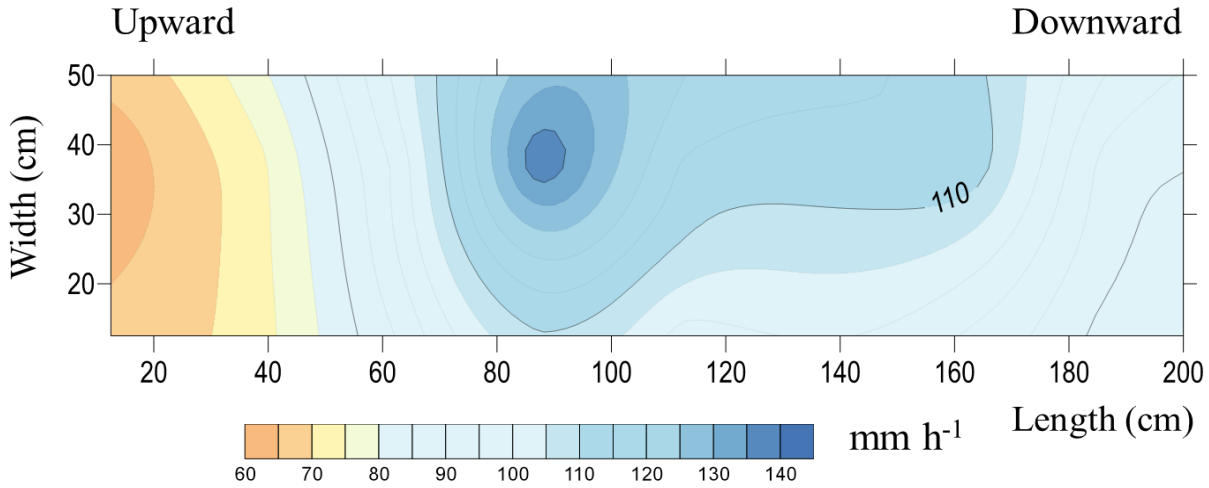

Fig 6. 3 The distribution of the rainfall on the surface slopes_100 mm h^{-1}

6.1.2 Soil slope model and preparation

The experimental soil slope model consists of two layers of soils as shown in Fig 6.4. Soil box (200 x 50 x 55 cm) was filled with a 30-cm thick soil. A top layer filled with soil treated with cement at a given cement content was placed on a 20-cm thick base DL-clay layer. A top 10-cm layer of soil treated with cement was used in a surface erosion protection measure for earth embankment. The dry density was set to 1.3 g/cm^3 for both top and sub-layers. DL-clay, cement,

and water were mixed by using an electrical soil mixer at the desired water content of soils 17% (Fig 6.5).

The compaction of soils was performed in a horizontal plane before lifting up to the angle of 20-degree. Six 5-cm layers of the soils were compacted to obtain 30-cm thickness. For each layer, compacting was done in a careful and systematic manner to achieve a uniform density and smooth surface. First, an amount of mixed soils necessary for a 5-cm layer were weighted and uniformly spread inside the soil box. Then, surface soils were scraped to a uniform thickness and tamped with a wooden block. The soil was compacted by dropping a 5.5 kg wooden block on a 30 x 23 cm wooden plate placed on the surface soils (Fig 6.6). After finishing compaction, the surface elevation was checked, the accepting error was less than 2 mm. For the next layers, it was done in a similar manner. In case of soil treated with cement 3% and 5%, soil samples were covered with a plastic sheet for 7 days for curing. Then, we lifted the soil box to 20-degree of slope. The detail of soil slope construction is shown in Table 6.2, Table 6.3 and Table 6.4.

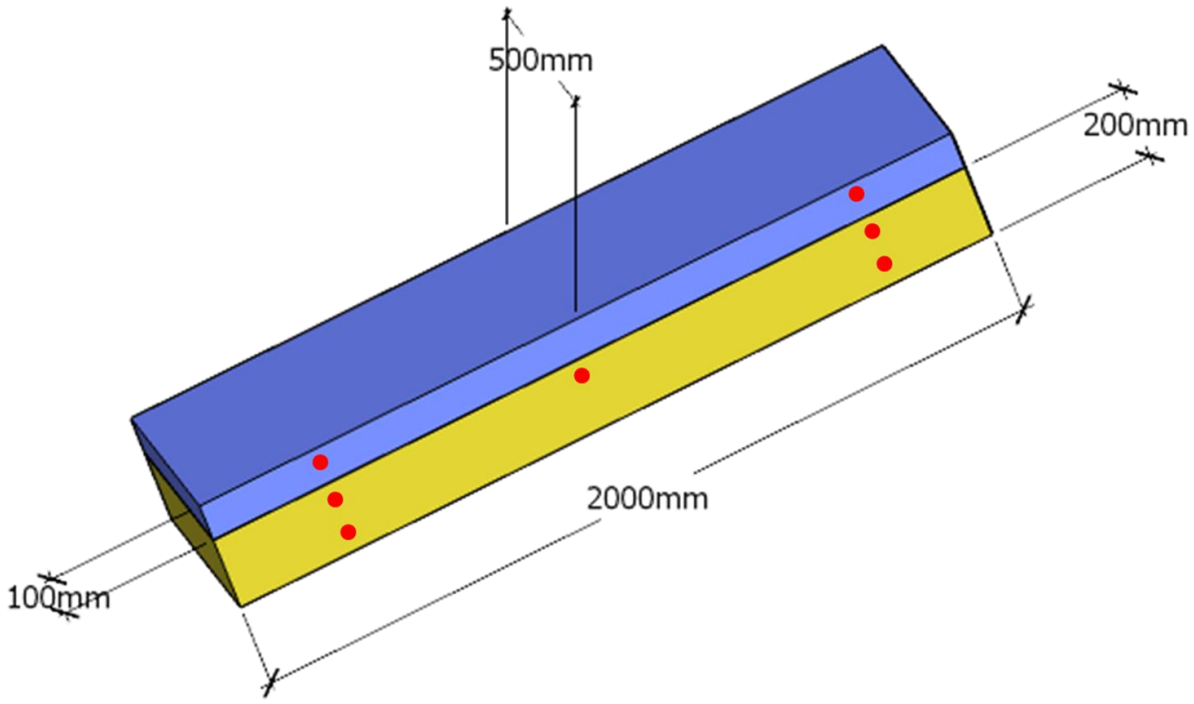

Fig 6. 4 Dimension of soil compacted into soil box, the lifting up degree of this compacted soil was 20-degree

Fig 6. 5 Electric mixer uses to mix soil cement

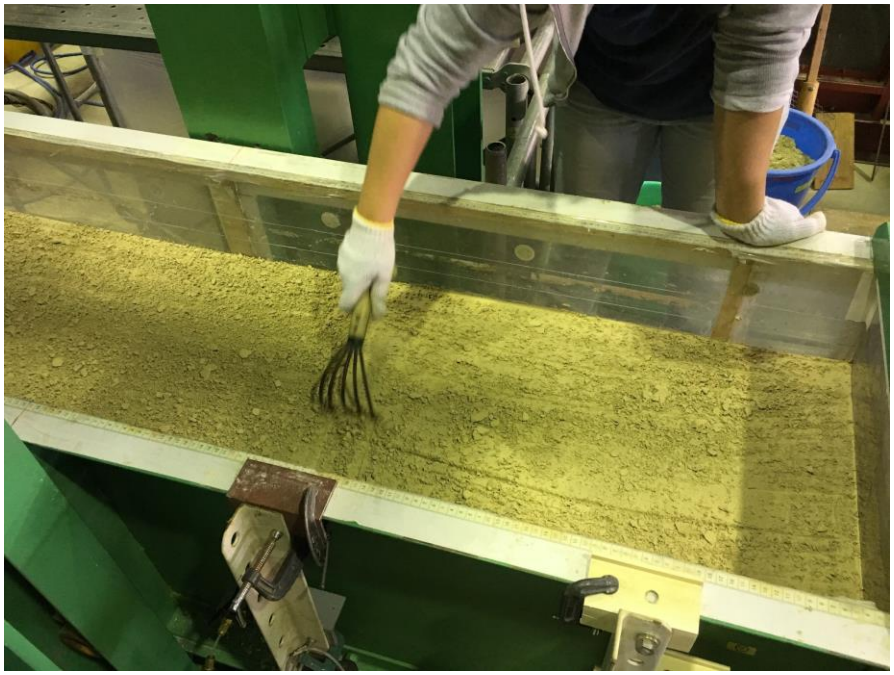

Fig 6. 6 The compaction procedure of soil slope

Table 6.1 shows the number of cases with different cement contents and rainfall durations of all the soil slope model tests. Note that the duration of rainfall in Case 1 and Case 4 was shorter than other cases due to the entire slope models in Case 1 and Case 4 severely eroded after applying rainfall for 210 minutes.

Table 6. 1 Experimental condition of soil slope models and duration of rainfall tests

No	Cement Content (%)	Rainfall duration (minutes)	Rainfall intensity (mm h^{-1})	Curing time (day)	Water content (%)	Dry density (g/cm^3)
Case 1	0	210	50	0	17	1.3
Case 2	3	240	50	7		
Case 3	5	255	50	7		
Case 4	0	210	100	0		
Case 5	3	240	100	7		
Case 6	5	240	100	7		

Table 6. 2 Construction layer of untreated soil slope_0% of cement content

Layer	Thickness (cm)	Total Thickness (cm)	Volume (cm^3)	Dry Density (g/cm^3)	Water Content (%)	Wet Density (g/cm^3)	Mass Input Wet Soil (kg)	Mass Input Cement (kg)	Total Input (kg)
1	5	5	50000	1.3	17.08	1.521	76.05	0	76.05
2	5	10	50000	1.3	17.08	1.521	76.05	0	152.1
3	5	15	50000	1.3	17.08	1.521	76.05	0	228.15
4	5	20	50000	1.3	17.08	1.521	76.05	0	304.2
5	5	25	50000	1.3	17.08	1.521	76.05	0	380.25
6	5	30	50000	1.3	17.08	1.521	76.05	0	456.3

Table 6. 3 Construction layer of treated soil slope_3% of cement content

Layer	Thickness (cm)	Total Thickness (cm)	Volume (cm^3)	Dry Density (g/cm^3)	Water Content (%)	Wet Density (g/cm^3)	Mass Input Wet Soil (kg)	Mass Input Cement (kg)	Total Input (kg)
1	5	5	50000	1.3	16.9	1.521	76.05	1.95	76.05
2	5	10	50000	1.3	16.9	1.521	76.05	1.95	152.1
3	5	15	50000	1.3	16.9	1.521	76.05	0	228.15
4	5	20	50000	1.3	16.9	1.521	76.05	0	304.2
5	5	25	50000	1.3	16.9	1.521	76.05	0	380.25
6	5	30	50000	1.3	16.9	1.521	76.05	0	456.3

Table 6. 4 Construction layer of treated soil slope_5% of cement content

Layer	Thickness (cm)	Total Thickness (cm)	Volume (cm^3)	Dry Density (g/cm^3)	Water Content (%)	Wet Density (g/cm^3)	Mass Input Wet Soil (kg)	Mass Input Cement (kg)	Total Input (kg)
1	5	5	50000	1.3	17.5	1.521	76.05	3.25	76.05
2	5	10	50000	1.3	17.5	1.521	76.05	3.25	152.1
3	5	15	50000	1.3	17.5	1.521	76.05	0	228.15
4	5	20	50000	1.3	17.5	1.521	76.05	0	304.2
5	5	25	50000	1.3	17.5	1.521	76.05	0	380.25
6	5	30	50000	1.3	17.5	1.521	76.05	0	456.3

6.2 Results of rain erosion resistance test under rainfall intensity 50 mm h^{-1}

6.2.1 Surface changes under rainfall intensity 50 mm h^{-1}

In this section, the results of the rain erosion resistance test under rainfall intensity 50 mm h^{-1} are discussed, firstly. Three cases in the rain erosion resistance test were conducted by changing the cement content ratio of the surface layer. The initial condition of the slope surfaces is shown in Fig 6.7(a, c). The elevation error of the initial surface was less than 2 mm. Fig 6.8(a, c) shows the soil surface taken at the end of each experiment illustrating the differences of surface conditions. In Case 1, the characteristic surface soil was evidenced by sinuous ridges and formed deep furrows. At first, the sheet erosion was observed on the surface soil, and it developed rill erosion. The serious erosion was observed at the downward part of the slopes; the deepest erosion was 10 cm in Case 1 (Fig 6.8(a)).

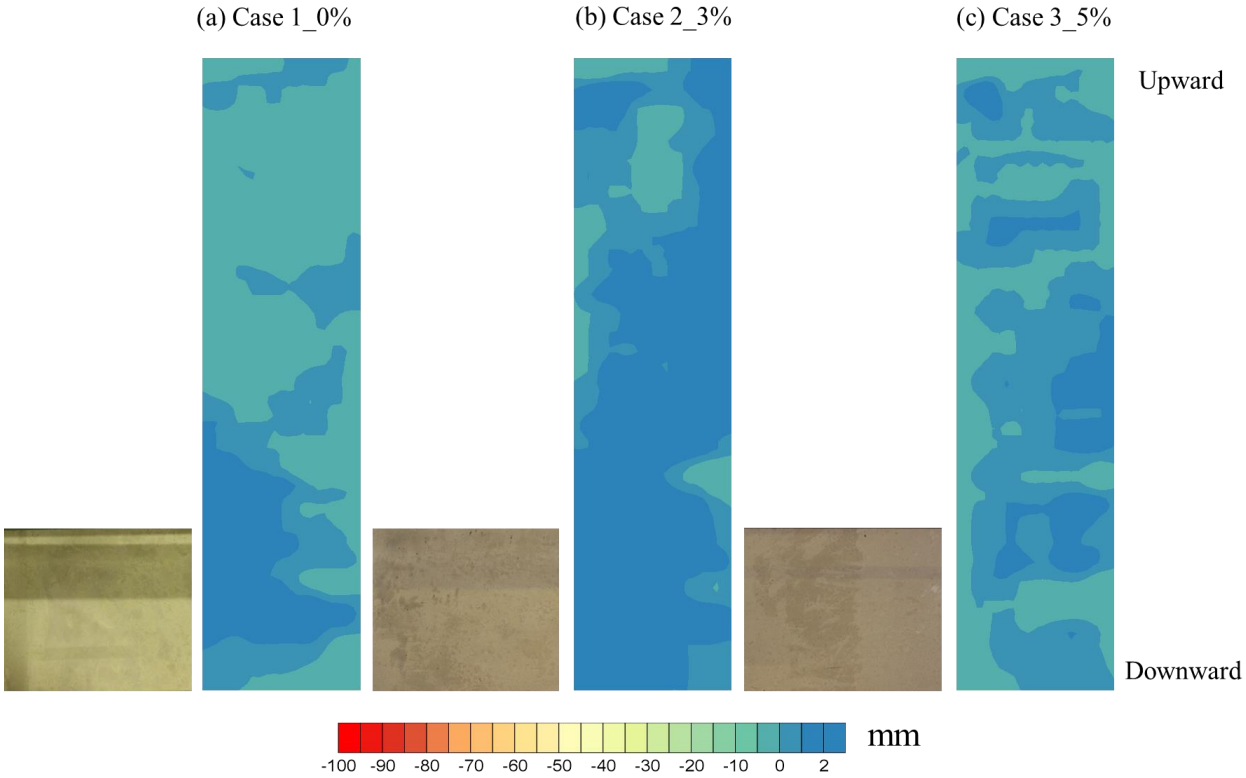

Fig 6. 7 The initial condition of slope surface_50 mm h^{-1}

Even no serious damages were observed on the surface slopes in Case 2 and 3 of soil treated with cement, there were some small crusts observed on the surface slopes. Rainfall

detached the surface soils, and rainwater abraded the surface soil cement. However, there were very shallow abrasions. The maximum erosion depth was around 1 to 2.5 cm. Case 3, soil treated with 5% of cement content, remarkably displayed a better resistance to rainfall in term of surface detachment based on the visual figures shown in each left side of Fig 6.8.

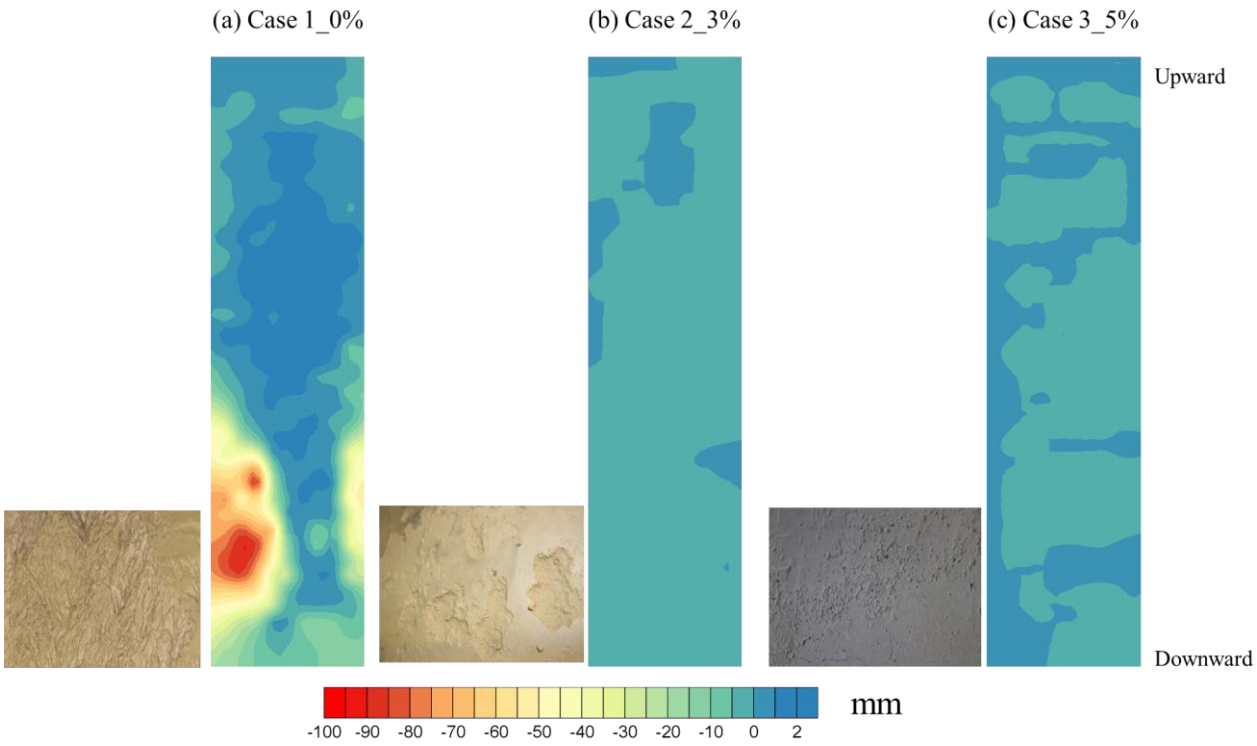

Fig 6. 8 Surface conditions of soil slope after testing 50 mm h^{-1}; pictures of surface conditions shown in each left side and each right figure shows distributions of surface displacements. (unit = mm)

6.2.2 Volume changes and soil losses_50 mm h^{-1}

The surface eroded volumes are shown in Fig 6.9. By using the grid method, the total surface eroded volume was estimated. It was shown that Case 1 had the largest eroded volume compared with the other two cases. The eroded volume of Case 1 was 8 times larger than Case 2 and almost 26 times larger than Case 3 (Fig 6.9). The eroded volume of Case 3 was much smaller than Case 2. In Table 6.5 shows the estimated surface volume and soil losses. The huge amount of soil loss, about 8.35 kg, was found in Case 1 of untreated soil slope. The surface eroded soil

from Case 2 was about 1.09 kg, while the soil treated with cement at 5% content showed a very little soil loss.

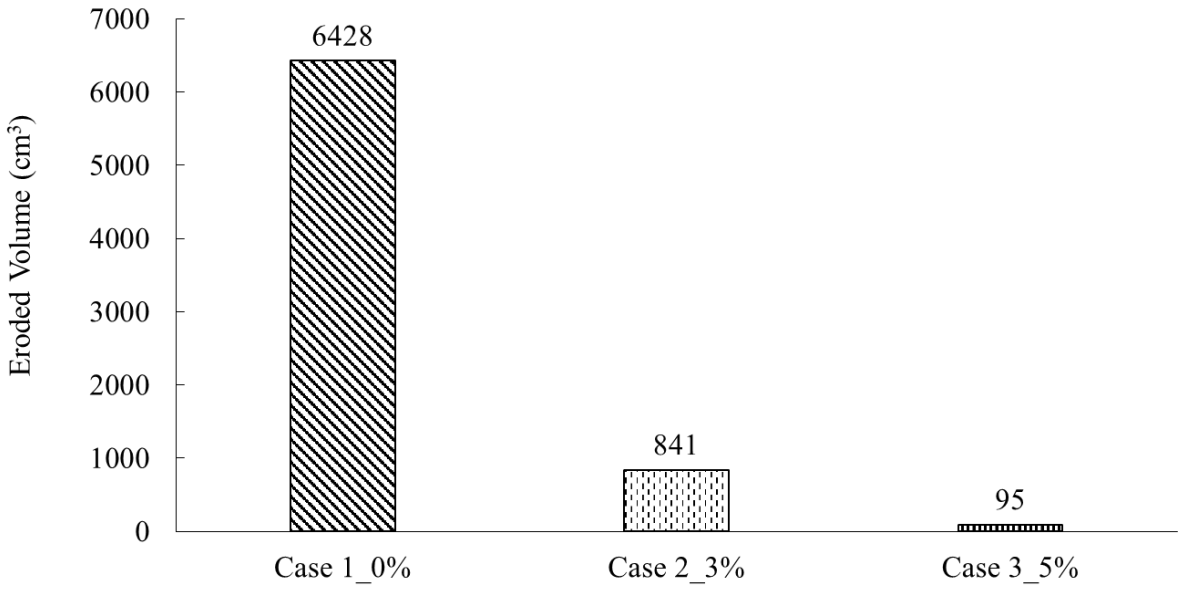

Fig 6. 9 The estimated surface eroded volume under 50 mm h^{-1}

Table 6. 5 Surface eroded volume and estimated soil losses under rainfall intensity 50 mm h^{-1}

No	Cement Content (%)	Eroded Volume (cm^3)	Soil losses (kg)
Case 1	0	6428	8.35
Case 2	3	841	1.09
Case 3	5	95	0.12

6.2.3 Runoff and sediment collection under rainfall intensity 50 mm h^{-1}

During the experiment, surface runoff was collected in every 15 min interval. There was no separation between surface runoff and sub-flow under 50 mm h^{-1}. The amount of cumulative runoff water for three soil slopes are shown in Fig 6.10. The runoff in all three cases continued to

increase with time. In case 3% and 5%, there was no big significant difference between the amounts of cumulative runoff. However, the amount of runoff of untreated soil sloped (0%) showed the largest amount compared to 3% and 5%. It might imply that the amount of rainwater may store more inside cemented soil slopes than untreated slope.

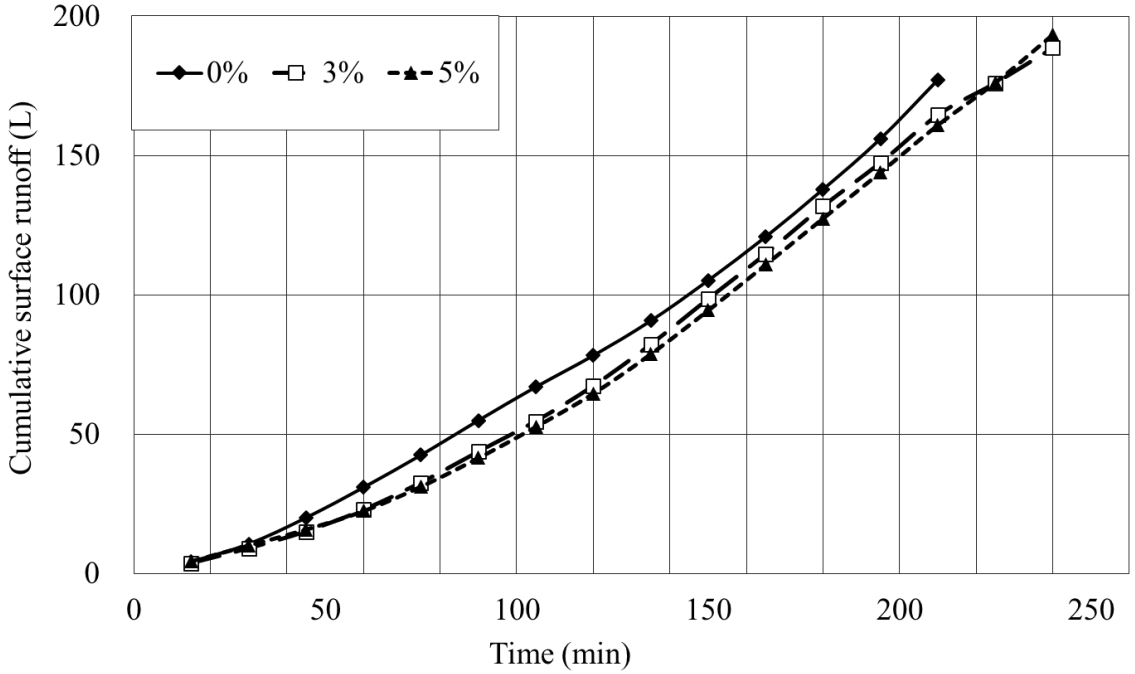

Fig 6. 10 Cumulative runoff under rainfall intensity 50 mm h^{-1}

Fig 6.11 shows the relationship between soil loss collected with runoff and cement contents. The eroded soil was started to measure from 150 minutes when the soil slopes were almost saturated for 100 minutes after applying rainfall. In case 0%, untreated soil slope, the amount of eroded soil was about 7.35 kg, which was much larger soil losses compared to 3% and 5%. The largest soil loss measured with 3% was 0.15 kg, while 5% was 0.13 kg. Note that the estimation of eroded soil loss determined from surface eroded volume showed much larger amount than the eroded soil collected with runoff. Due to the fact that some amount of eroded soil might be trapped inside the gabion.

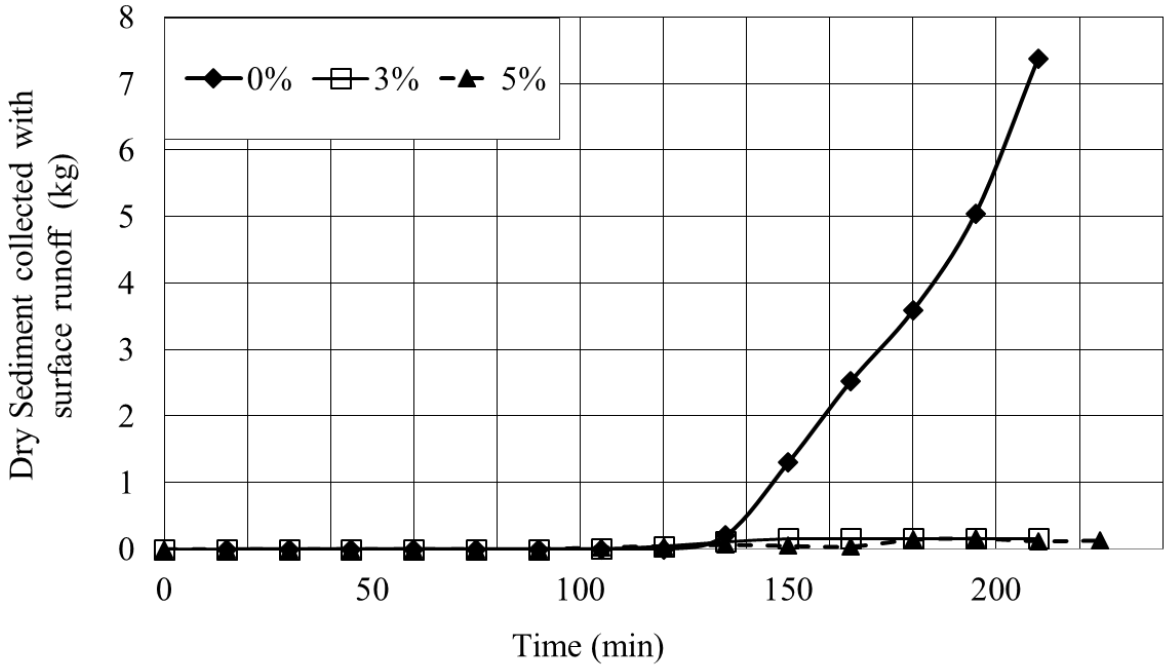

Fig 6. 11 Eroded soil loss collected with runoff under rain erosion resistance test_50 mm h^{-1}

6.2.4 Pore water pressures under rain erosion test 50 mm h^{-1}

The variation of pore water pressure in soil slopes is monitored at the points as shown in Fig 6.12 (a, d). There were 7 pore water pressure transducers inserting inside the soil slopes to detect the presence of water under rain erosion resistance test at rainfall intensity 50 mm h^{-1}. However, four pore water pressure transducers were selected to show in this section. The pore water pressure (PWPs) values were detected in every 10 second interval. The tensiometers were inserted at the downward, at the middle and upward part of the soil slopes. At first, the PWPs values were negative in all the cases. At the initial stage, the PWPs value of soil cement in Case 2 and Case 3 was around -21 and in Case 1 was between -17 to -18 (Fig 6.12(a, d)). For 60 minutes after applying rainfall, the PWPs values in Cases 2 and 3 simultaneously started to increase. As shown in Fig 6.12(a, c), the PWPs at position P2 and P4 in Case 2 and Case 3 started to increase more rapid than in Case 1. The increase commenced at 70 minutes in Case 1. The values in Cases 2 and 3 became positive in 120 minutes, while it took around 140 minutes in Case 1. The similar observations were also found for PWPs transducers at position P3 and P5; all the values of PWPs of soil cement increased quicker than those in untreated soil.

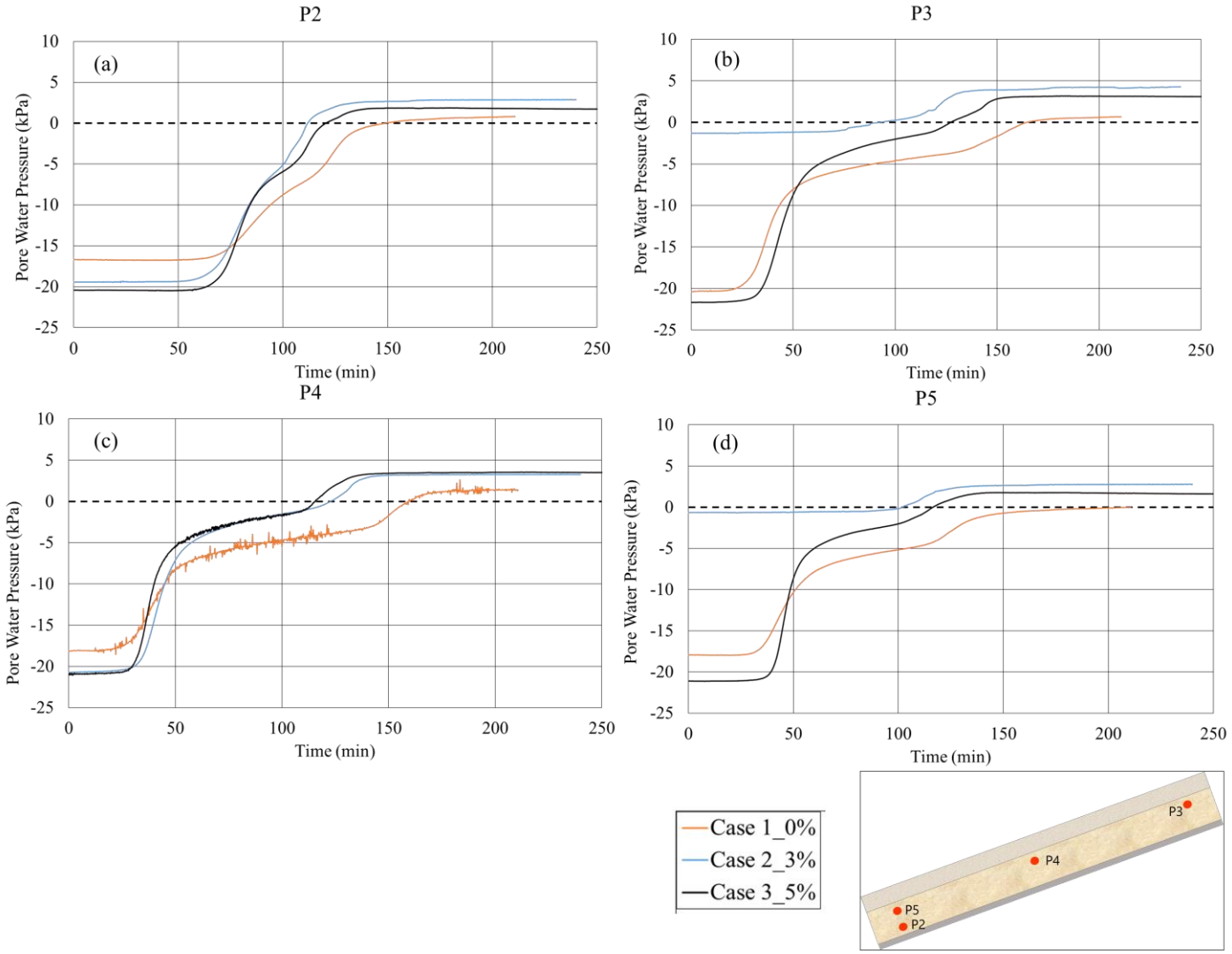

Fig 6. 12 Pore water pressure changes during rainfall applied at position P2, P3, P4, and P5 under rainfall intensity 50 mm h^{-1}

The rapid changes of PWPs values inside soil slopes showed that the soil cement layer (top layer) could have higher permeability than the DL clay layer (0%). Morgan (2005) described that soils with high capacity of infiltration (high permeability) could reduce runoff; therefore, it minimizes soil erosion caused by surface runoff. The higher infiltration capacity could be attributed to larger pores of soil. The cement hydration process might not only create larger pores, but it also increases the porosity as soil cement can create macro-pores (Bellezza and Fratalocchi, 2006; Nimmo, 2013).

6.3 Results of rain erosion resistance test under rainfall intensity 100 mm h^{-1}

As mentioned earlier in this chapter, the rain erosion resistance tests were conducted under two different rainfall intensities. To get more detail on the resistance of soil cement application against water erosion, another heavy rainfall was applied, 100 mm h^{-1}. In this section, the results of the surface eroded volume of soil slopes, soil losses, and pore water pressure values of three soil slopes are discussed. Note that the initial condition of soil slope model for heavy rainfall was kept the same as 50 mm h^{-1}. In addition, surface runoff and sub-flow of the three soil slope models were separately collected.

6.3.1 Surface changes under rainfall intensity 100 mm h^{-1}

In Fig 6.13 shows the initial surface elevation of Case 4, Case 5 and Case 6. The elevation error of surface soil was between 1 to 2 mm. Fig 6.14 shows the final surface condition of the soil slopes after applying rainfall. The severe erosion was observed in Case 4, mainly from the middle part of the soil slope down to the toe. Many deep furrows were appeared on the surface of untreated soil in Case 4. The concentration of rainwater were too much around the middle part of Case 4 to the downward of the slope. Not only the surface soil was seriously affected; but also the base layer. The rill erosion developed very quickly for the untreated soil slope. The deepest erosion was measured about 30 cm, which the rainwater likely washed away the entire of untreated soil slope (Fig 6.14a).

The slope covered with soil cement on the surface showed less damage on the surface slope (Fig 6.14(b, c)). The physical observation in Case 5 and Case 6 showed that there were many soil crusts on the surface slope. The mechanism of crust formation on the surface soil under 100 mm

h^{-1} was not different from the rainfall intensity 50 mm h^{-1}. Soil crust formation could result from the beating action of rainfall on the hard surface of treated soil. However, due to the heavy rainfall the surface crust appeared earlier and deeper than the test with rainfall intensity 50 mm h^{-1}. The variation of the deepest erosion was measured around 1-3 cm for Case 5 and Case 6. Not different from Case 2 and Case 3, the swell of a compacted treated soil was also found. This swelling phenomenon of Case 6 was much greater than other cases due to the amount of rainwater was much more than 50 mm h^{-1}.

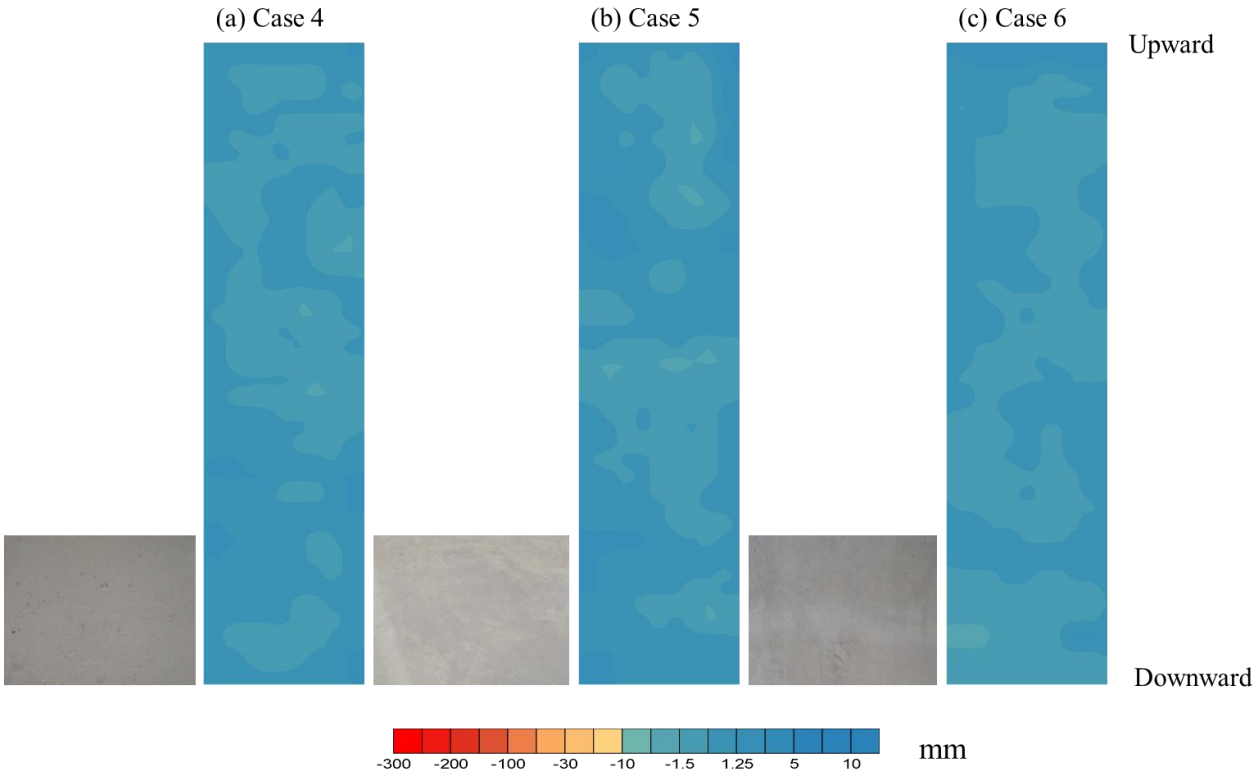

Fig 6. 13 The initial surface condition of soil slope before testing 100 mm h^{-1}; pictures of surface conditions shown in each left side and each right figure shows distributions of surface elevation.

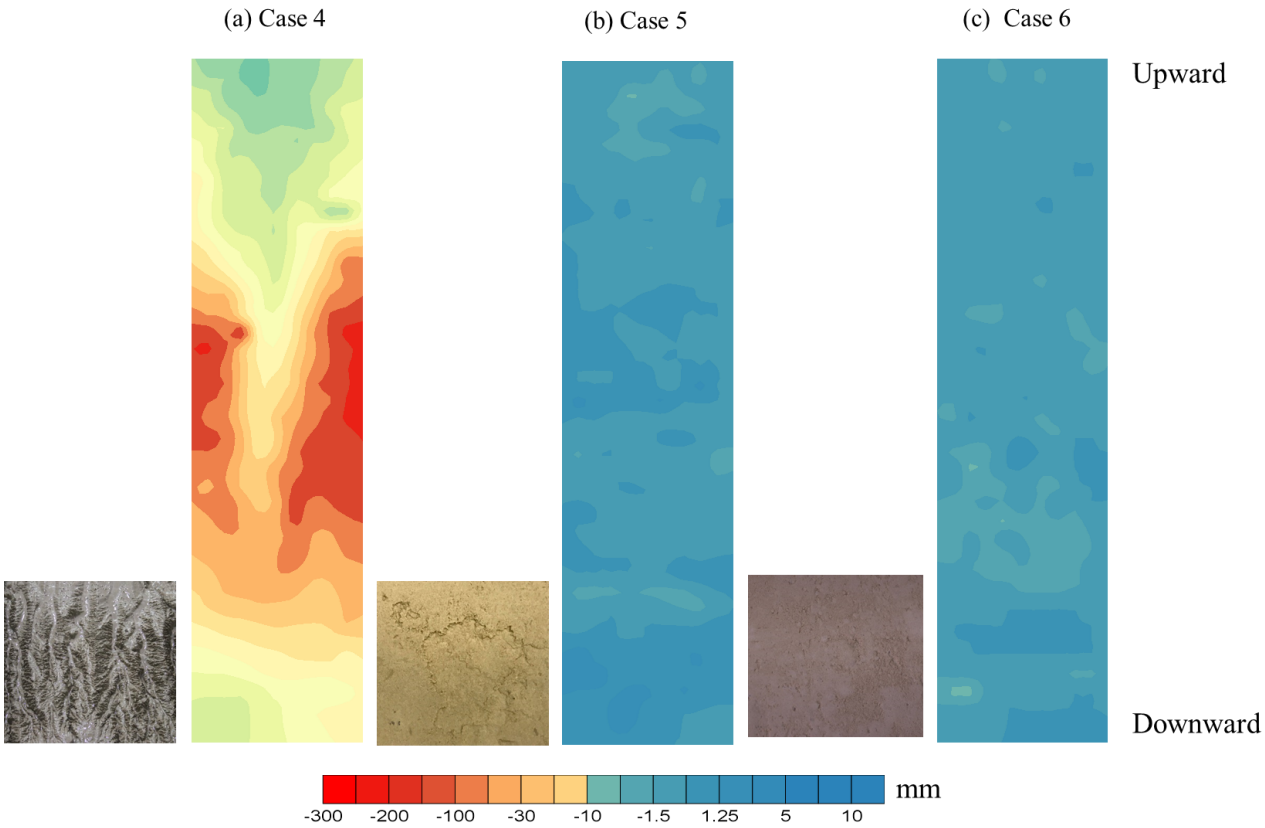

Fig 6. 14 Surface conditions of soil slope after testing 100 mm h^{-1}; pictures of surface conditions shown in each left side and each right figure shows distributions of surface displacements. (unit = mm)

6.3.2 Volume changes and soil losses_100 mm h^{-1}

The surface eroded volumes of three soil slopes and soil losses are estimated and summarized in Table 6.6. Due to the stronger rainfall intensity, a very huge eroded volume was occurred in Case 4, as well as soil losses. The estimated total soil loss for Case 4 was about 156 kg, which was a very huge amount of soil transported from the surface slope. Fig 6.15 illustrates the eroded volume of three soil slopes. The untreated soil slope was sorely eroded. The eroded volume of treated soil slope in Case 6 was much smaller than Case 4 and Case 5.

Table 6. 6 Volume changes and soil losses under rainfall intensity 100 mm h^{-1}

No	Cement Content (%)	Eroded Volume (cm^3)	Soil losses (kg)
Case 4	0	119746	155.67
Case 5	3	344.75	0.45
Case 6	5	448.4375	0.58

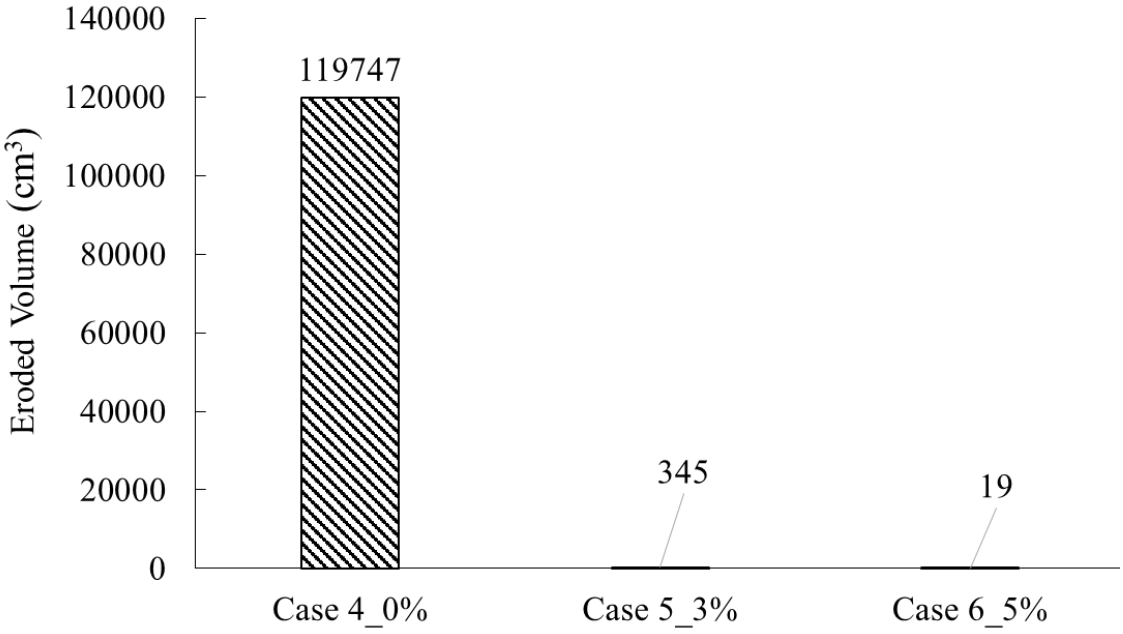

Fig 6. 15 The estimated surface eroded volume under 100 mm h^{-1}

6.3.3 Runoff and sediment collection under rainfall intensity 100 mm h^{-1}

In order to get more detail related to surface flow and sub-flow, the separation of runoff collection was applied. However, the separated collection was failed to apply for 0% because the untreated soil slope had a soft surface which caused the soil erosion quickly, in particular on the middle part down to the toe of the soil slope. So in this section, only the sub-flow of 3% and 5% are presented. The cumulative surface runoff of 0% was much greater than 3% and 5% (Fig 6.16). Similar to Case 0% of the rain erosion resistance test under 50 mm h^{-1}, the amount of rainwater

slowly infiltrated into untreated soil slope; therefore, it created more runoff. Comparing 3% and 5%, the amount of runoff in 5% was larger than 3% (Fig 6.16). In this regard, Poesen et al. (1990) reported that for soil surface covered with embedded rock fragments can create surface runoff much more compared to soil surface covered with the same rock fragments but not embedded surface. Due to higher cement content, 5%, it might create a firmly embedded surface than 3% of cement content. Thus, the surface runoff in 5% was larger than 3%.

Relating to sub-flow collection, it was successfully separated for only 2 cases, 3% and 5%. The cumulative sub-flow data is shown in Fig 6.17. The sub-flow was collected for 90 minutes after applying rainfall. The sub-flow of 3% was much greater than 5% (Fig 6.17). In this regard, it corresponded to the surface flow collection of 3%, which was less than 5% (Fig 6.16). In addition, the hydraulic conductivity data of cemented soil at 7 days of 3%, which presented in Chapter 5 showed larger hydraulic conductivity (k) values than 5% at the same curing time. Thus, it might be possible that the sub-flow collection from 3% was much greater than 5%.

With respect to the generation of surface runoff and sediment loss from soil slopes, the untreated soil slope showed a very great surface soil loss comparing to treated soil slopes, 3% and 5% of cement content as shown in Fig 6.18. Many rills were occurred on the surface soil creating a strong surface flow; this surface flow velocity was quite high to transport soil particles. As mentioned in Young and Wiersma (1973), the rills on the surface soil can cause the flow velocities several times greater than smooth surface soil causing the soil detachment by surface flow is maximized.

Typical sediment losses collect with the sub-flow are shown in Fig 6.19. For the embedded 5% of cement content, the sub-flow was relatively lower than for the 3% of cement content (Fig 6.17), but the sediment loss collected with sub-flow of 5% showed a larger amount than 3%. This phenomenon might be related to the hydration of 5% cement content created a harder soil surface and generated the flow paths between the joints of soil cement bigger than 3%. Nussabaum and Colley (1971) described that when the cement, soil, and water are proportioned and hydration to produce a hardened material, shrinkage cracks develop in soil cement which influence on seepage.

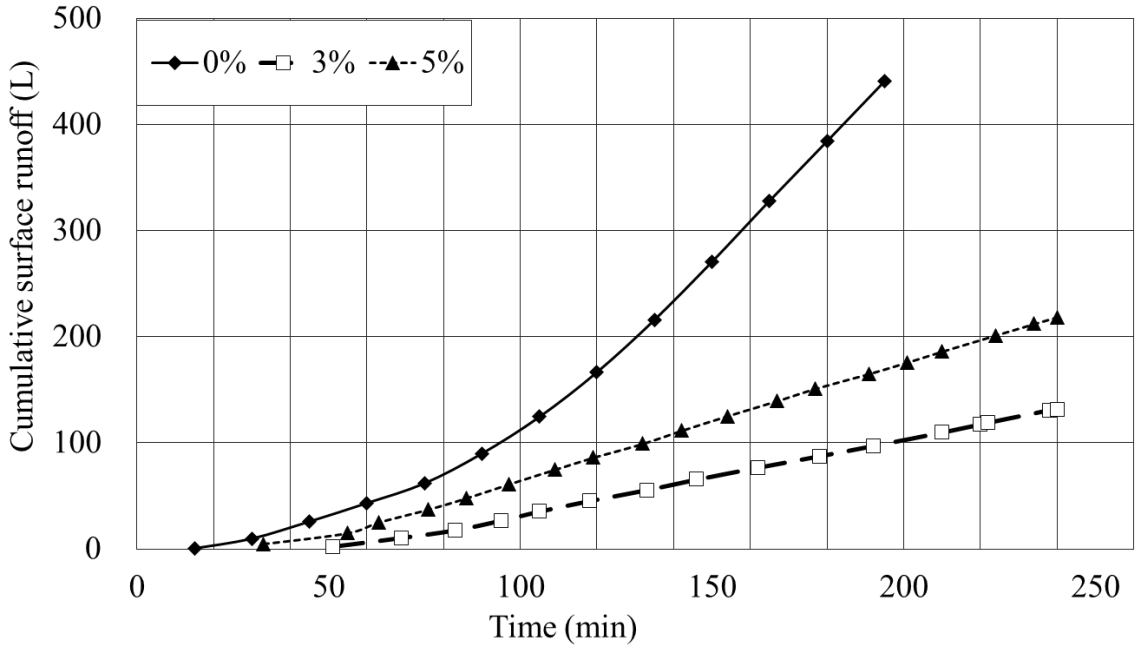

Fig 6. 16 Cumulative surface runoff under rainfall intensity 100 mm h^{-1}

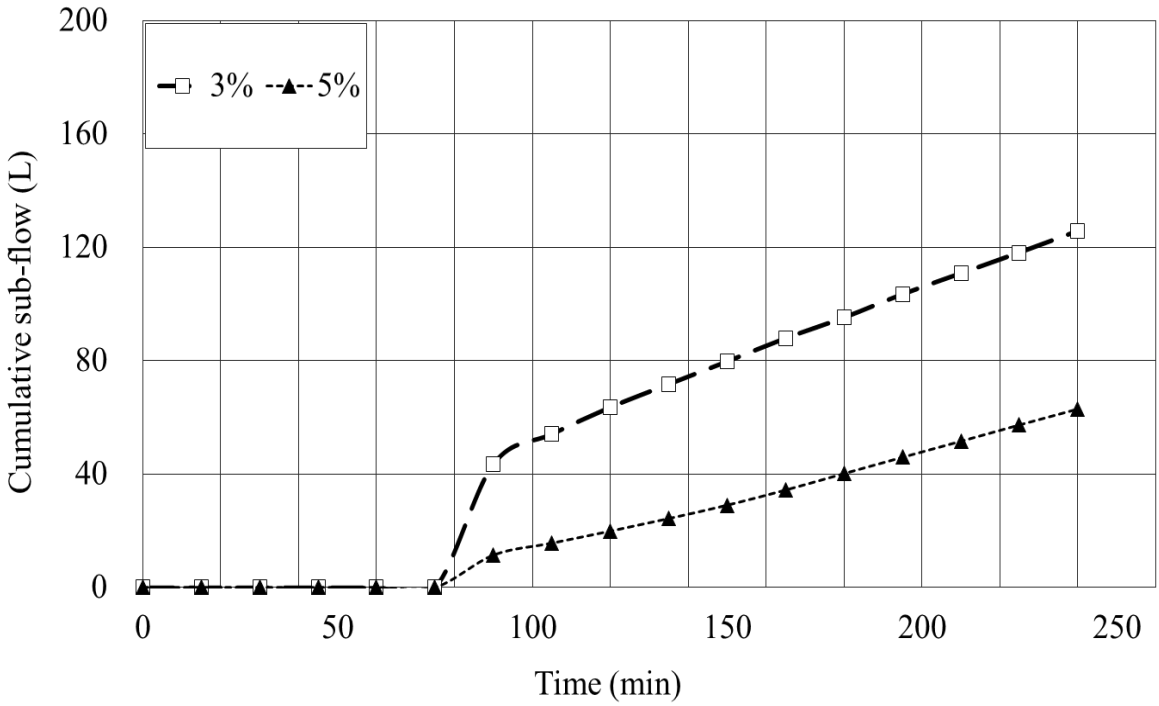

Fig 6. 17 Cumulative sub-flow under rainfall intensity 100 mm h^{-1}

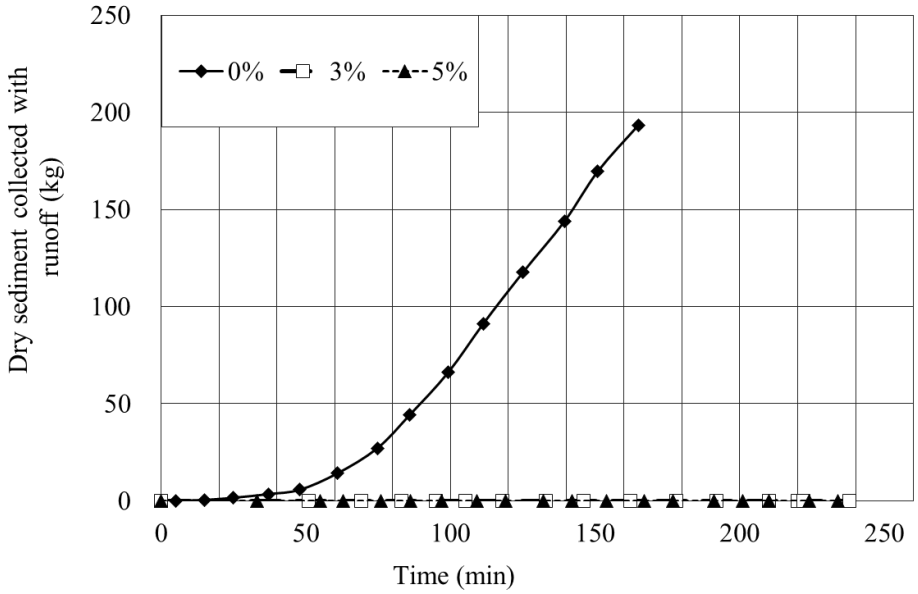

Fig 6. 18 Sediment collected with surface runoff under rain erosion resistance test_100 mm h^{-1}

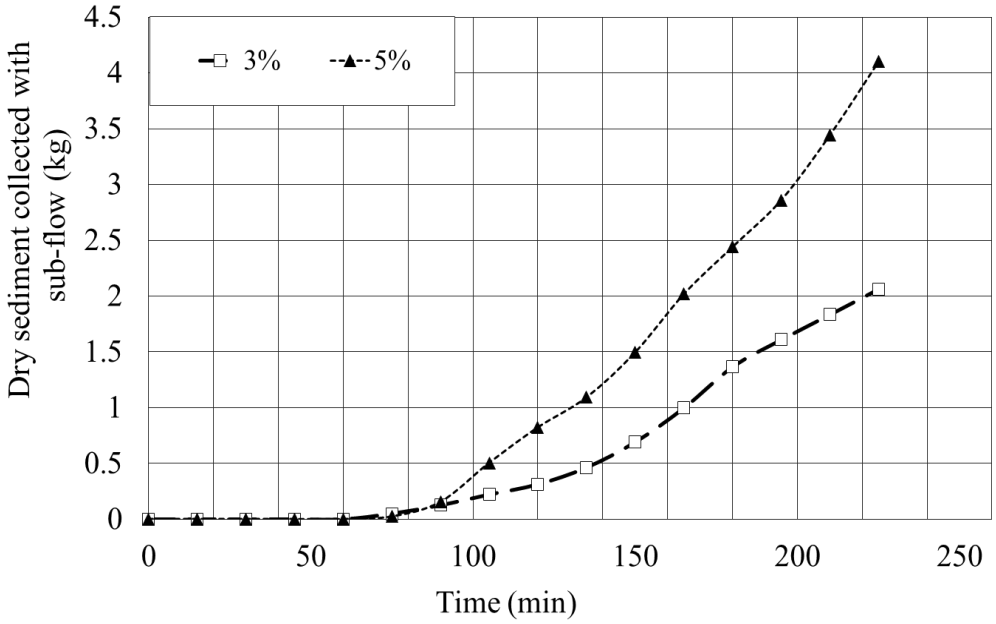

Fig 6. 19 Sediment losses collected with sub-flow under rain erosion resistance test_100 mm h^{-1}

6.3.4 Pore water pressures under rain erosion test 100 mm h^{-1}

To get more information, additional 5 pore water pressure transducers were inserted into soil slopes. In this section, seven pore water pressure data are presented. The relationship between PWPs, on the top layer of soil cement, and time shows in Fig 6.20. At the initial stage,

the values of soil cement in Case 5 and Case 6 were negative in all the cases, the minimum value was around -25. In Case 4, the negative value was less than -20. Thus, the condition of surface soil in Case 5 and Case 6 was much drier than Case 4.

The tensionmeter at position P6 showed that the PWPs in all the cases smoothly increased (Fig 6.20(a, c)). In around 10 to 15 minutes after executing rainfall, the PWPs values in all the cases simultaneously increased. For 100 minutes, the value in Case 4 started to become positive, while the values in Case 5 and Case 6 continually increased to positive in 90 minutes. Fig 6.21 shows the PWPs values of sub-layer of soil slopes, DL clay layer. All the values of PWPs commended to increase in around 35 minutes for P3 and P4, while the value of P2 started to increase at 50 minutes. The results of Case 4, 5 and 6 showed that the values of PWPs increased more rapidly than Case 1, 2 and 3. Due to the high rainfall intensity, the values of PWP was strongly affected. Note that all the soil cement slopes were found that the value of PWPs of treated soil increased more promptly than untreated soil slopes.

6.4 The surface eroded volume and soil losses under rainfall intensity 50 and 100 mm h^{-1}

In this section, the surface eroded volume and surface soil loss of two different rain erosion resistance tests are presented. As shown in Fig 6.22, the eroded volume of untreated soil slopes 0% under 100 mm h^{-1} showed a tremendous erosion compared with 0% under 50 mm h^{-1}. In case of treated soil, 3% of soil slope under 50 mm h^{-1} showed a larger eroded volume compared with 3% under 100 mm h^{-1}. However, the 5% of soil slope tested with 50 mm h^{-1} showed a smaller eroded volume than 5% under 100 mm h^{-1}. This phenomenon might relate to the swelling process. Due to the heavy rainfall 100 mm h^{-1}, much water infiltrated into the soil slope (3%). The soft base DL clay increased in volume as it gets wet. However, in case 5% under 100 mm h^{-1}, the influence of seepage caused the soil of base DL clay layer washed out, which leaded to the surface eroded volume became larger than 50 mm h^{-1}. In Fig 6.23 illustrates that the amount of surface soil loss of two rain erosion resistance tests.

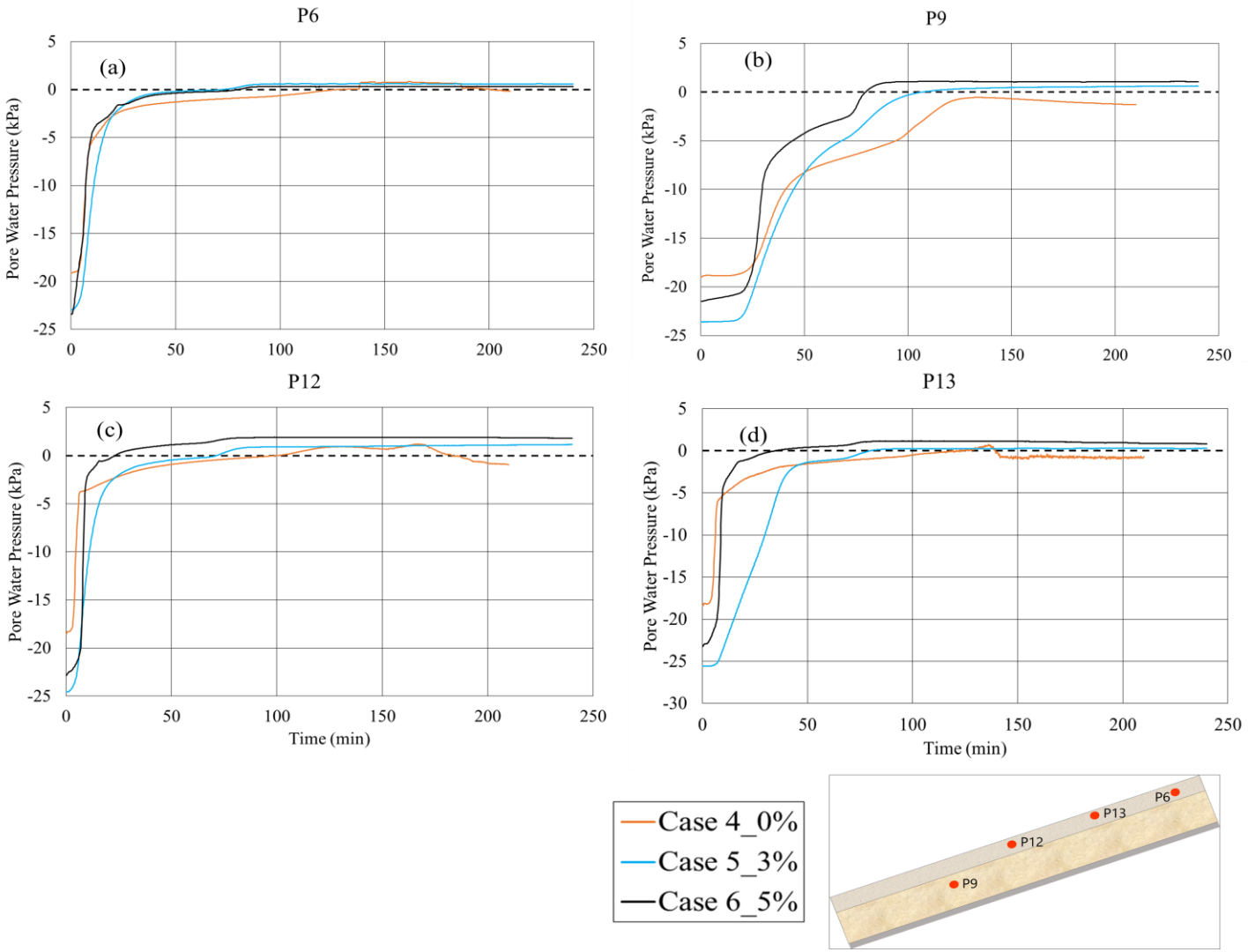

Fig 6. 20 Pore water pressure changes during rainfall applied at position P6, P9, P12, and P13 under rainfall intensity 100 mm h^{-1}

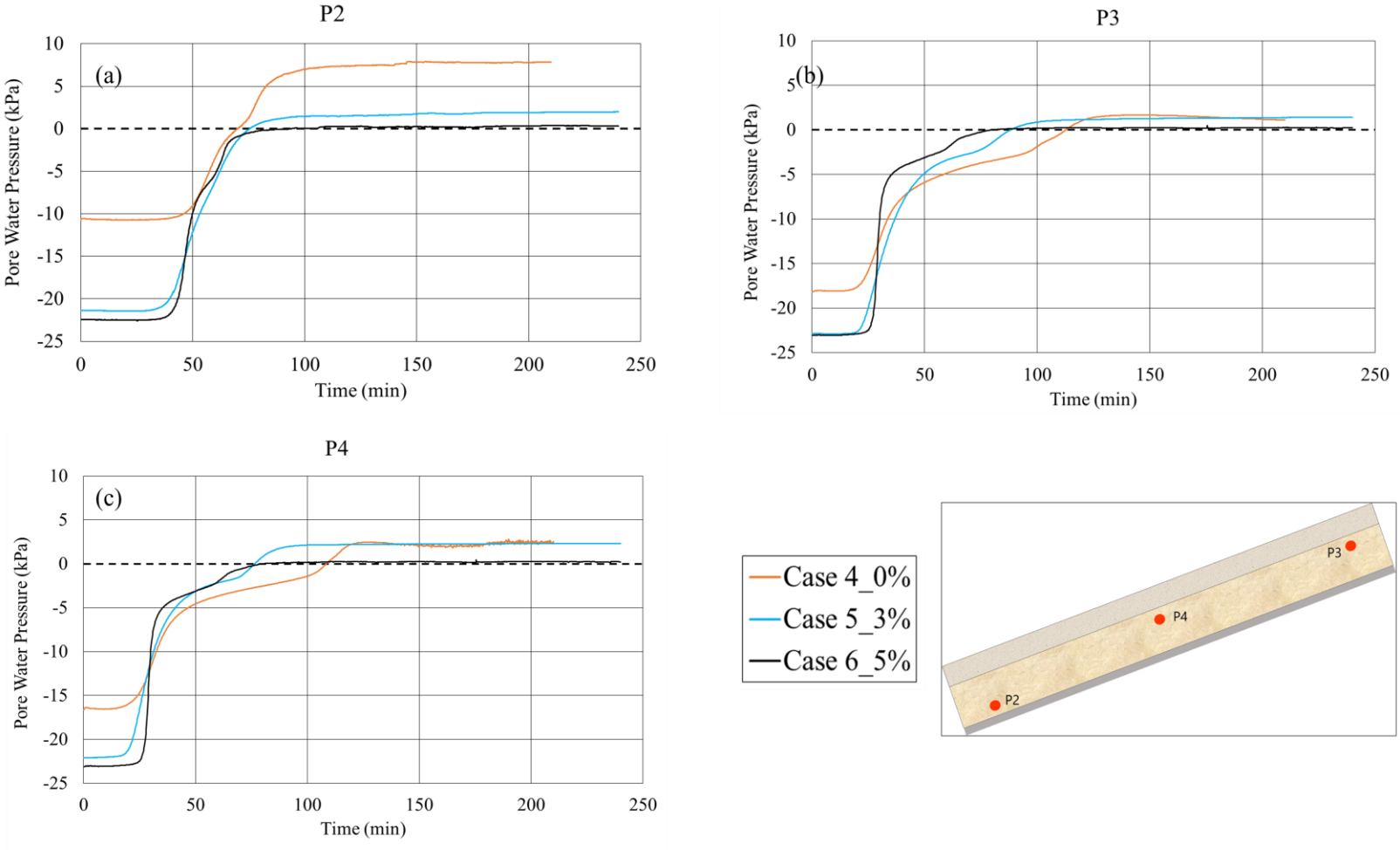

Fig 6. 21 Pore water pressure changes during rainfall applied at position P2, P3, and P4 under rainfall intensity 100 mm h^{-1}

The untreated soil slope, 0% of cement content, showed the great soil loss from the surface in both rainfall intensities comparing to treated soil slopes with cement 3% and 5%. The huge differences of surface conditions in 0% occurred due to characteristic of soil. According to the study of Wischmeier and Mannering (1969), soils that are high in silts are the most erodible soil. As the experimental soil used in this study consists of 90% silt, it easily detaches, erodes and washes away by runoff. Even soil treated with cement could prevent tremendous surface soil erosion, some crusts were observed on the surface soil slopes. The hydration process, cement reacted with water gradually bond together the soil particles causing the hardening of soil cement. As reported by Liu et al. (2006), the mechanical characteristics of the soil-cement are hard; therefore, the crusts are consequently formed when soil cement exposes to rainfall.

6.5 Pore water pressure distribution and flow direction

Fig 6.24 shows the distribution of PWPs values under rainfall intensity 50 mm h^{-1}. The initial condition of soil cement was drier than untreated soil. For 90 minutes the distribution of water near the surface of the treated soil slopes was much larger than the untreated soil slope (0%). Note that the treated surface soil slopes had sufficient infiltration capacities, but the untreated soil was not enough. Thus, rainwater infiltrated into treating soil slope faster than the untreated soil slope. Comparing the treated soil slopes, the rainwater was permeable into 3% of soil slope much more than 5% based on the distribution of the water on the surface (Fig 6.24(b, c)). The distribution of PWPs value showed that the water was accumulated at the upward and downward part of the slope for all the cases at 90 minutes. At 180 and 210 minutes, the water accumulated mainly at the toe of the slopes.

Due to the high rainfall intensity, 100 mm h^{-1}, the distribution of PWPs values of the soil slopes was rapidly changed compared to rainfall intensity 50 mm h^{-1}. At 45 minutes, the distribution of PWPs was dense at three points of the soil slopes, downward, middle and upward (Fig 6.25(a, b, c)). Not different from rainfall intensity 50 mm h^{-1}, the cumulative water was observed at the toe part of the treated soil slope at 90 minutes and 210 minutes. In case of untreated soil, the cumulative water was observed at the upward part due to the toe part of soil slope was already washed away at 50 minutes after applying rainfall (Fig 6. 25 (a)).

By using the variation of pore water pressure values, the total potential head and flow vectors were calculated. The total potential is calculated by:

$$H_t = \frac{u_w}{\rho_w g} + z \qquad (6.2)$$

Where H_t is total potential head, u_w is pore water pressure; ρ_w is water density; g is accelerate gravity; z is high of the point from datum.

The slope equipment was lifted up to θ = 20-degree, thus the slope angle was rotated resulted in change of z values. The value of z is given by:

$$z = x\sin\theta + y\cos\theta \qquad (6.3)$$

The total potential head and flow vectors at 90 and 210 minutes of six soil slopes under two rainfall intensities are shown in Fig 6.26 and Fig 6.27. Fig 6.26 shows the total potential head and flow vector under rainfall intensity 50 mm h^{-1}. At 90 minutes, the rainwater started to infiltrate straight into the soil slopes (Fig 6.26(a, b)), except Case 5% that flow vectors paralleled to the slope angle and moved upward at the toe part (Fig 6.26(c)). At 210 minutes, the flow vectors became larger for all the cases in particular Case 0%. The direction of the flow vectors moved straight forward to the toe part in Case 0% and Case 3%; while the flow vectors of Case 5% moved downward into the soil slope at 210 minutes.

Fig 6.27 depicts the total potential head and flow vectors under rainfall intensity 100 mm h^{-1}. It was observed that the direction of flow vectors started to move along the slope angles in Case 0% at 90 minutes. The flow vectors became larger and scattered at the middle part of the slope and the flow directions moved upward at 210 minutes (Fig 6.27(a)). In case of soil cement slopes, the larger and scattered flow vectors were found in Case 3% and 5%. At 90 minutes, the flow vectors moved downward; it indicated that the water still percolates into soil slopes 3% and 5% (Fig 6.17 (b, c)). However, the upward direction of flow vectors was mainly found in Case 5% in 90 minutes. The larger and scattered flow vectors were concentrated in the middle part of the soil slope (3%) at 210 minutes, and the direction of the vectors moved upward. In case of 5%, the condition of the flow vectors at 210 minutes was not different from 90 minutes. However, the scattered vectors were found at the middle part of the slope at 210 minutes. Noted that the

upward direction of the flow vectors indicated that the soils became saturated and swelling. The swelling caused by the soft base DL clay layers, mostly were found in soil cement slopes.

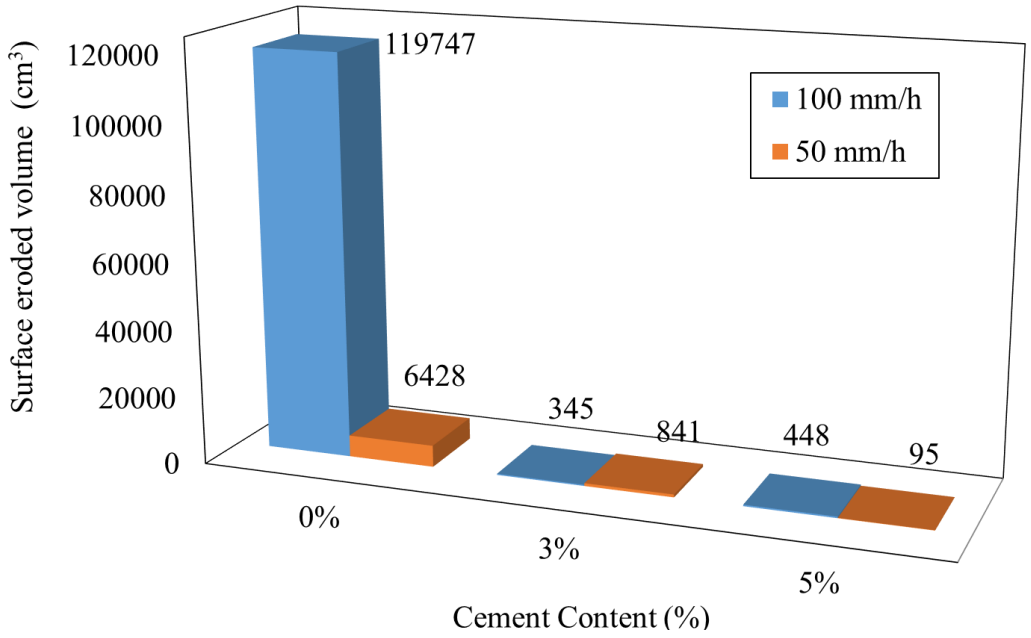

Fig 6. 22 Compare of the magnitudes of surface eroded volume under rainfall intensity 50 and 100 mm h^{-1}

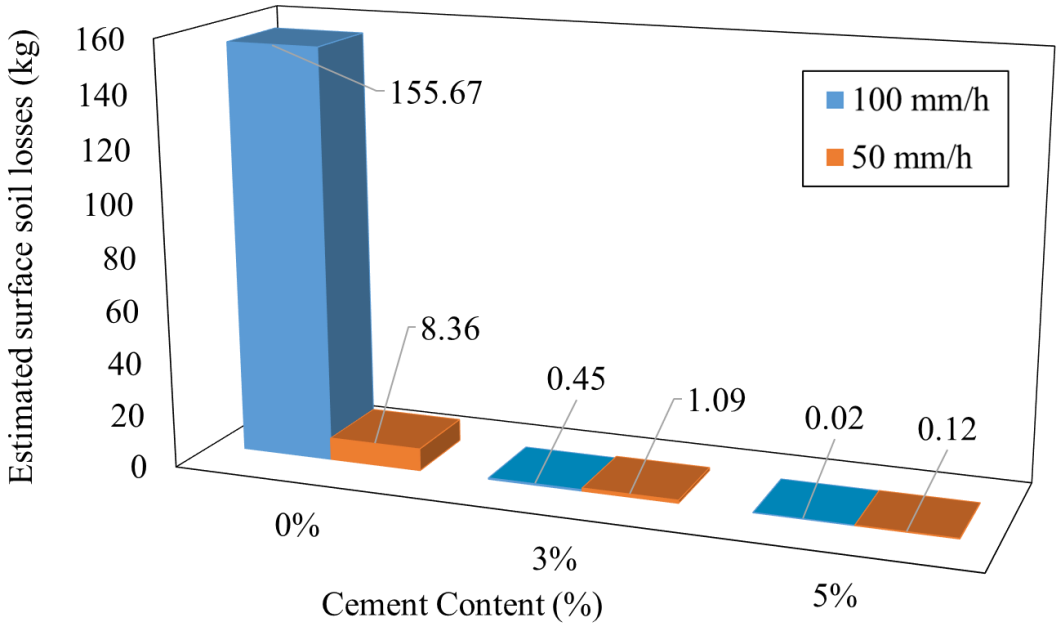

Fig 6. 23 The estimation of soil losses from surface eroded volume under rainfall intensity 50 and 100 mm h^{-1}

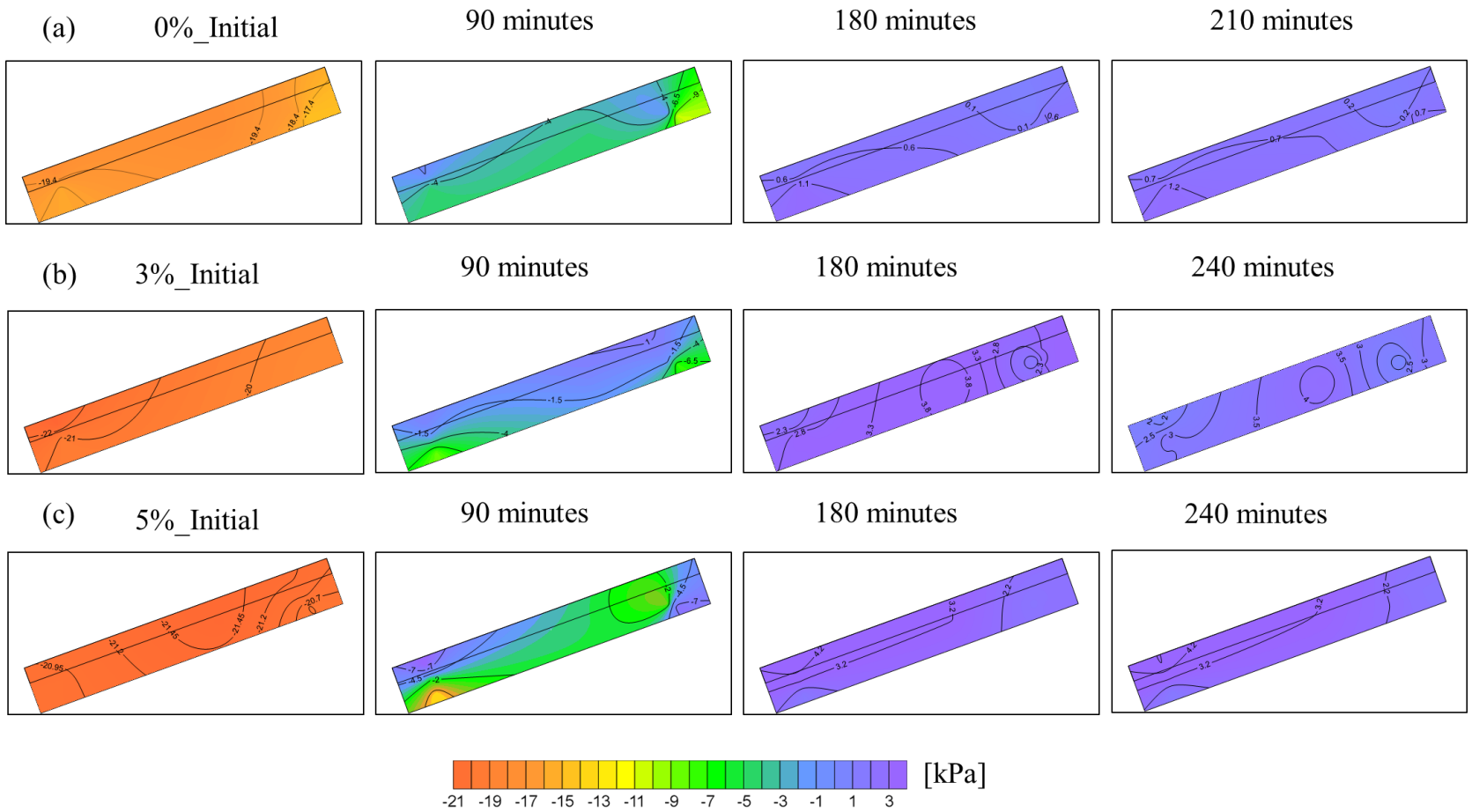

Fig 6. 24 Pore water pressure distribution within the soil slopes under rainfall intensity 50 mm h^{-1}

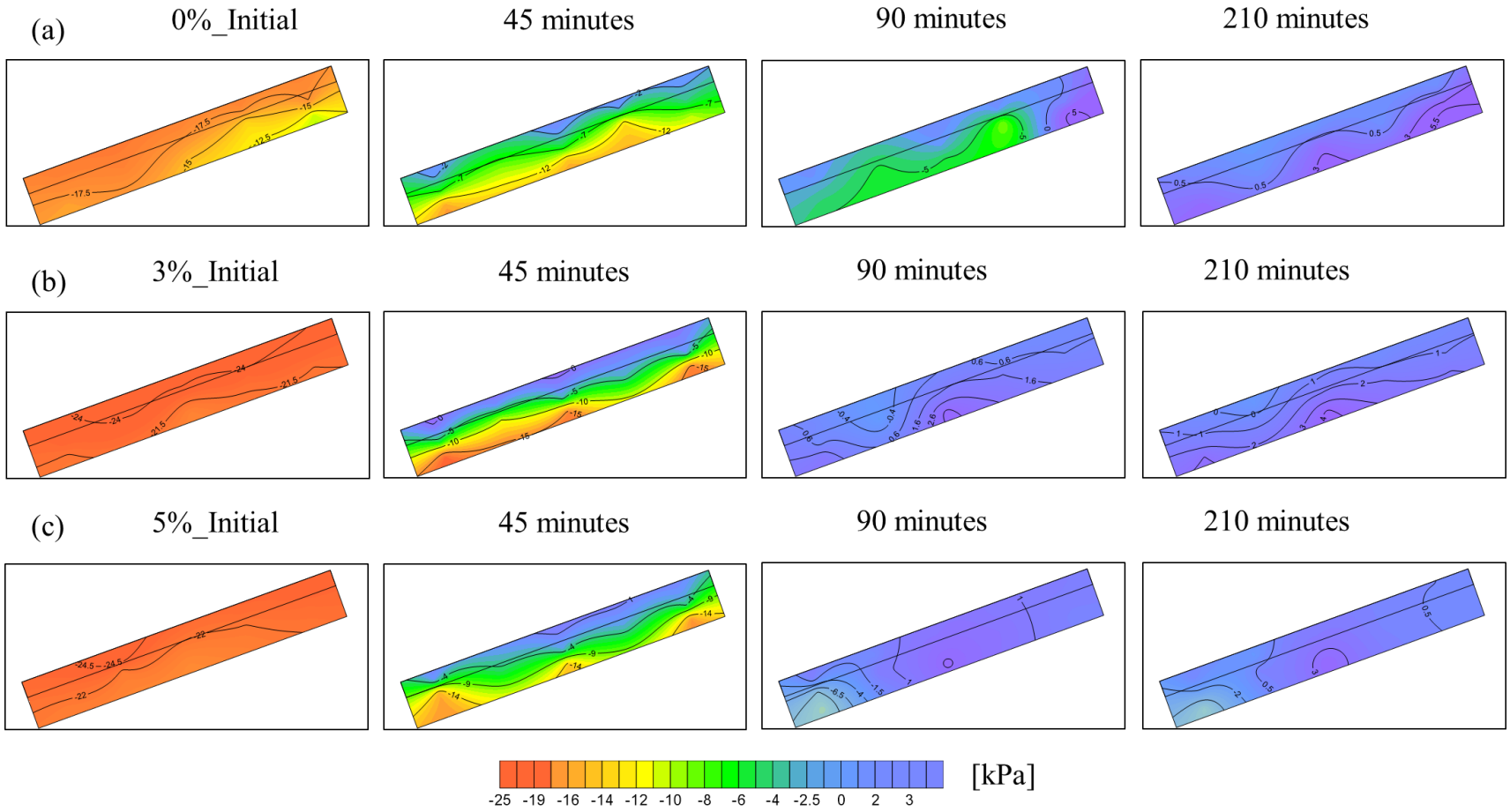

Fig 6. 25 Pore water pressure distribution within the soil slopes under rainfall intensity 100 mm h^{-1}

(a) Case 1= 0% cement content, Rainfall intensity 50 mm h^{-1}

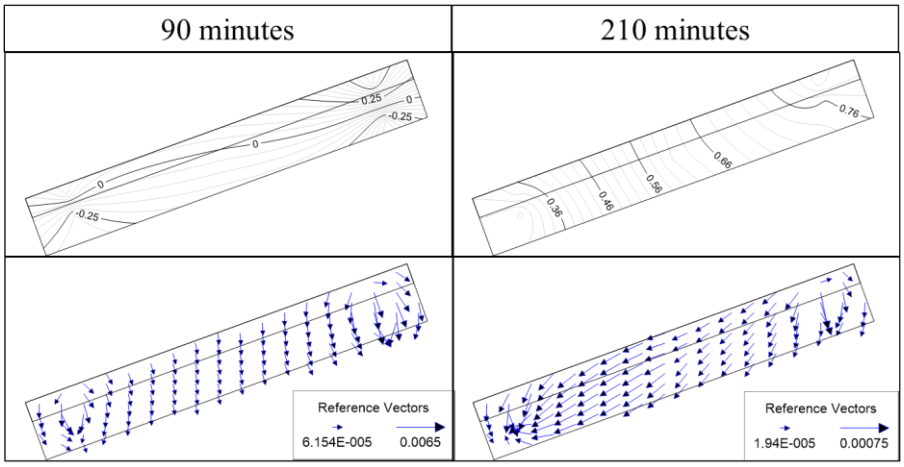

(b) Case 2= 3% cement content, Rainfall intensity 50 mm h^{-1}

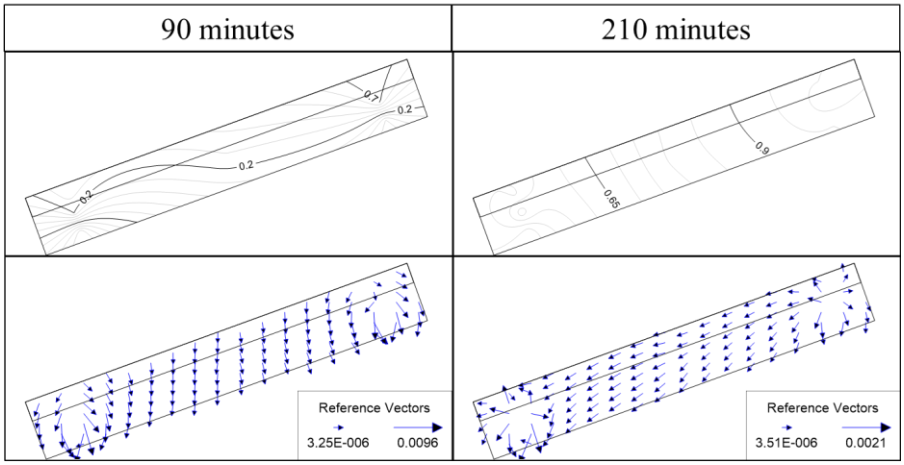

(c) Case 3= 5% cement content, Rainfall intensity 50 mm h^{-1}

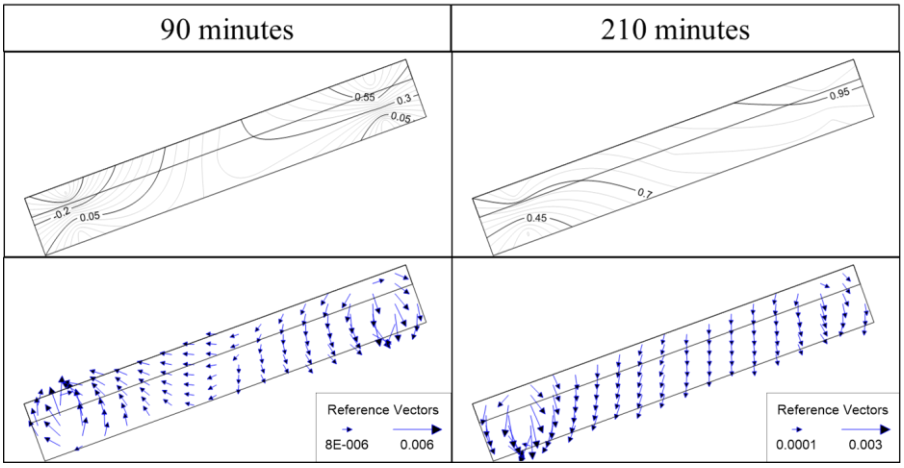

Fig 6. 26 Water velocity within the soil slopes under rainfall intensity 50 mm h^{-1} (unit=m)

(a) Case 4= 0% cement content, Rainfall intensity 100 mm h^{-1}

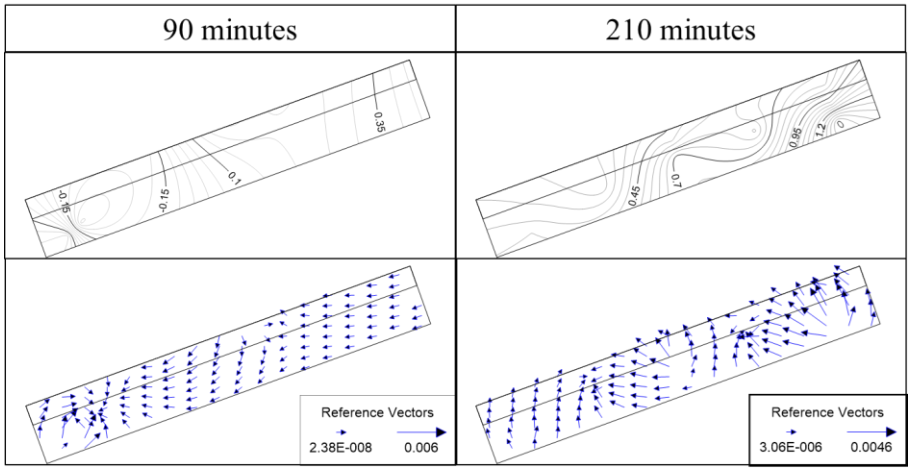

(b) Case 5= 3% cement content, Rainfall intensity 100 mm h^{-1}

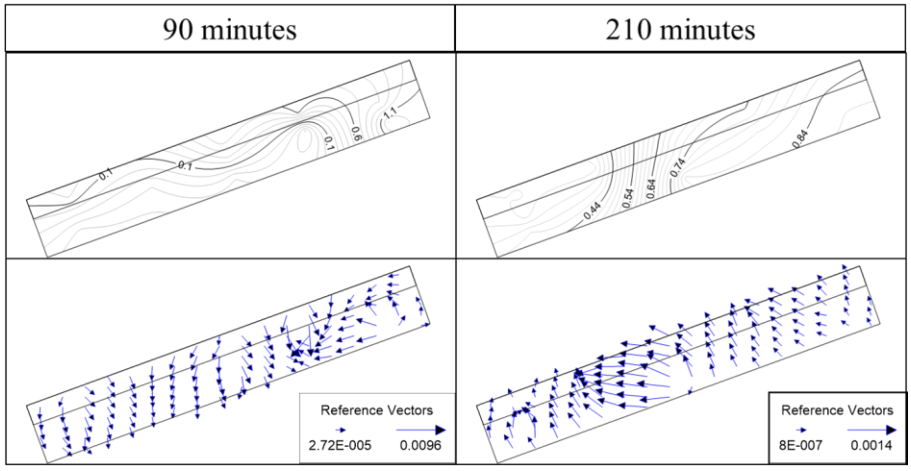

(c) Case 6= 5% cement content, Rainfall intensity 100 mm h^{-1}

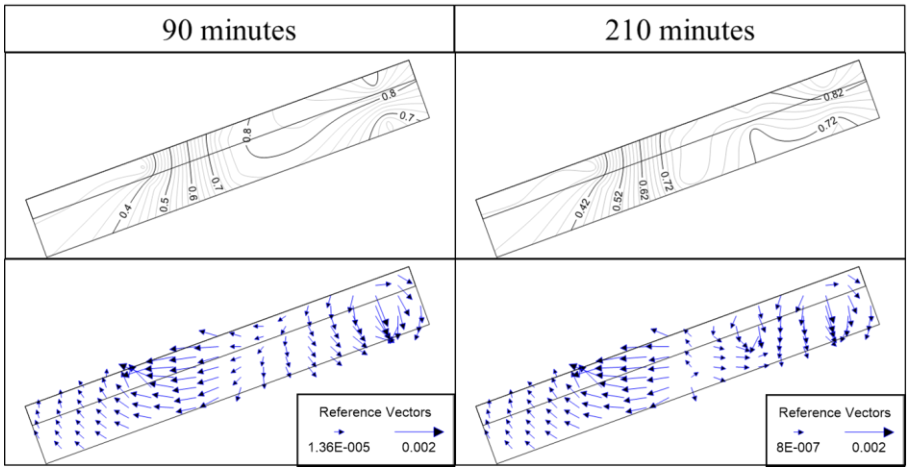

Fig 6. 27 Water velocity within the soil slopes under rainfall intensity 100 mm h^{-1}(unit=m)

6.6 Relationship of cohesion, hydraulic conductivity and soil losses

The relationship between soil strength; surface eroded volume; hydraulic conductivity and soil loss is presented in this section. The cohesion of soil cement at curing time 7 days was selected to relate the surface eroded volume of rainfall intensity 50 mm h^{-1} (Fig 6.28). From the consolidated drained triaxial test, it was observed that the soil treated with cement improved the soil shear strength. The cohesion values have profoundly influenced on the eroded volume of soil specimens. The higher the cohesion value, the smaller the eroded volume was observed (Fig 6. 28). Such a conclusion is also supported by some researchers, a small amount of soil detachment was associated with the increase in soil strength and create more resistant to erosion (Poesen, 1981; Brunori et al., 1989; Reddi et al., 2000).

Hydraulic conductivity of soil is one of the major's soil hydraulic properties. Soils have a high capacity of infiltration can reduce runoff and decrease erodibility (Morgan, 2005). The relationship between the hydraulic conductivity and the soil loss observed in this experiment is shown in Fig 6.29. The soils treated with cement showed higher hydraulic conductivity, while the untreated soil showed very low hydraulic conductivity. The cement hydration process not only creates pores; but also increase the porosity as soil cement shrinks that can create macropores (Bellezza and Fratalocchi, 2006; Nimmo, 2013). Therefore, the water might be infiltrated into the soil cement specimens faster than untreated soils. Rahardjo et al. (2018) mentioned that there is a significant increase in surface runoff when soil mixture has lower water storage. It was found that the runoff amount of the cemented layer of soil slopes became relatively small because of the performances of faster infiltration and higher water storage. As reported by Hueso et al. (2015), initial soil moisture also affects infiltration capacity. After 7 days of curing, the initial soil moisture of cemented soils was lower than the untreated soil due to the hydration process of cement. It is possible that soil cement can absorb more water when it exposes to rainfall. Poesen (1981) explained that when rain falls on a dry surface, much of the water drop is absorbed. For this reason, at the low moisture content of soil cement, more water may infiltrate into soil cement than untreated soil. In this way, the untreated soil slopes had more runoff and caused the largest soil loss compared with soil cement slopes.

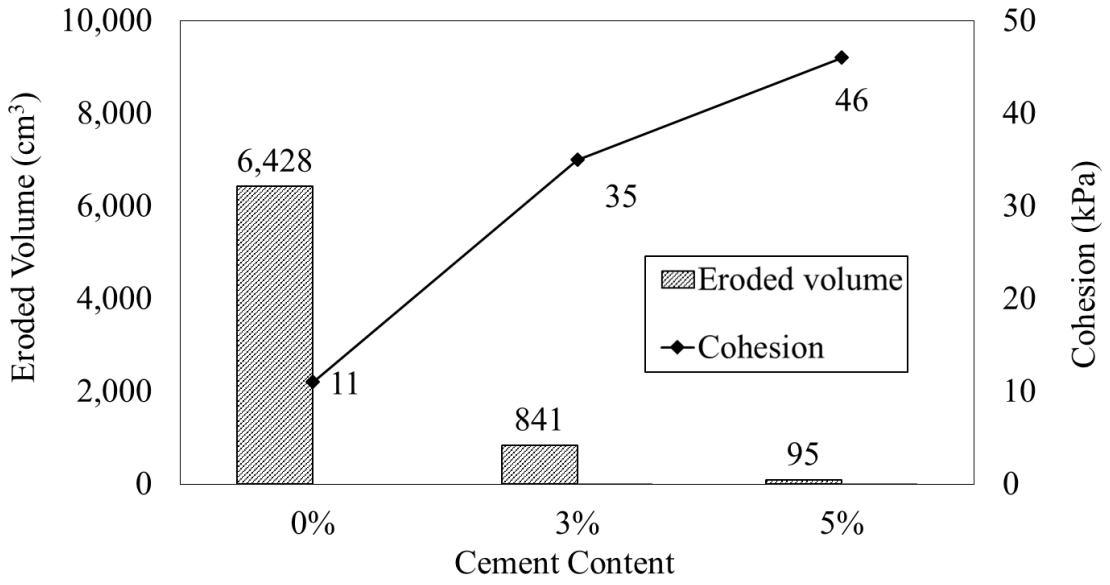

Fig 6. 28 Cohesion value of cemented DL clay at 7 days treatment and volume change of slope models under rainfall 50 mm h^{-1}

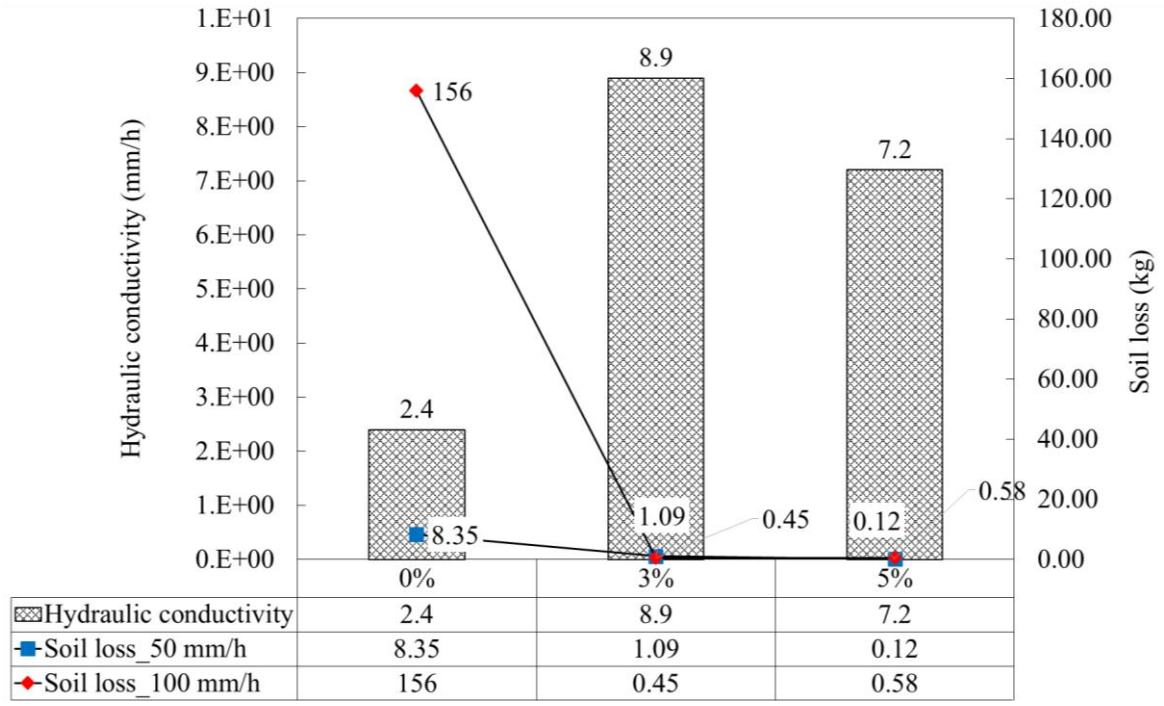

Fig 6. 29 The relationship between hydraulic conductivity, cement contents and soil losses of slope models under rainfall 50 and 100 mm h^{-1}

6.7 Concluding remarks

The results displayed small changes on the surface soil cement. Improving the soil shear strength with low cement contents, it possibly reduced the detachment on the surface soils as well as the surface runoff. Due to the hard surface of the soil treated with cement, soil detachment was prevented. The surface soil erosion of Case 0% was found 8 times and 60 times larger than Case 2 (3%) and Case 3 (5%) under rainfall intensity 50 mm h^{-1}. Under the heavy rainfall intensity, 100 mm h^{-1}, the significant erosion on the surface soil slope was observed in Case 4 (0%). The deepest erosion was 10 cm and 30 cm for untreated soil slopes Case 1 and Case 4 under rainfall intensity 50 mm h^{-1} and 100 mm h^{-1}. The surface slope of soil cement remaining in a good condition, only the shallow surface crusts were observed. The surface runoff collection of untreated soil slopes contained much sediment compared with treated soil slopes 3% and 5%. The distribution of pore water pressure showed that the surface of soil cement could absorb more water into the soil slopes. Thus, the surface runoff was reduced on the soil cement slope as well as the soil loss.

Chapter 7 Conclusions

Soil erosion is a common problem occurred on earth irrigation structures. In most developing countries, rehabilitating the eroded irrigation structure is quite challenging for a community level due to capacity and financial constraints. Thus, the community prefers to have a low cost of maintenance and rehabilitation techniques. It is necessary that the community level can afford and ensure to sustain their earth irrigation structures for a long-term use. In this context, soil cement stabilization is a merit method to prevent the earth irrigation structure from erosion at a low cost of construction. More important, it is so convenient for local community to construct; it does not require any skill for soil cement stabilization. The following conclusions can be drawn from the experimental studies related to the characterization of soil cement (1) Element testing on physical, mechanical and hydraulic properties of cemented DL clay; and (2) Rain erosion resistance test to evaluate the effectiveness of soil cement application for surface erosion protection on earth embankment.

7.1 Physical and mechanical properties of soil cement

The compaction test showed that the maximum dry density increased with the addition of cement content, while the optimum moisture content slightly decreased. From the hydraulic conductivity test, the treated soil with 3% of cement content indicated that the k value started to decrease with increasing curing times. The result of soil cement 5% indicated that the k value was fluctuated at various curing times, 7 and 14 days; but the k value increased at 28 days curing time. The k value of soil cement 7% increased with increase in curing time. The k value of cemented soil of 7% of cement content was higher than soil cement 3 and 5% at curing time 28 days. This might be related to the hydration process of cement within the soils. The hydration of cement at high cement content might create more porosities inside the soil samples, so the water can be permeable more into the soil samples. The results from suction controlled triaxial system show that the saturation volumetric water content of soil cement was greater than DL clay. The hydration of cement with soil creates the small aggregate; therefore, the soil cement had a larger volumetric water content than DL clay. In case of

cement treated soils, the volumetric water contents decreased when the percentage of cement increased for a given suction.

A series of consolidated drained triaxial compression tests were conducted for a typical silt named DL clay in which total 30 soil samples were tested under 3 confining pressures, 4 cement contents and 3 curing times. The conclusion could be obtained as follows:

(1) All the cemented specimens with σ_3 = 50 kPa expressed strain softening and dilation behaviour. The softening behaviour became weaker with an increase in confining stresses. The amounts of dilations and the peak shear strengths almost increased with an increase in cement contents, but the influence of cement contents to ultimate shear strengths was rather smaller than that to the peak shear strengths.

(2) The peak shear strength depended on curing time, namely those increased with an increase in curing times, but there were a little influences of curing times to the ultimate strengths. It was observed that the addition of cement to soil can substantially improve shear strength, but the brittle stress-strain behaviour was observed especially of the soil mixed with cement 7%. The brittle stress-strain behaviour occurred at the higher cement contents. This brittle behaviour could cause the sudden failure of soil structures.

(3) A hyperbolic equation expressed in Eq. (5. 2) could estimate the shear strength values q_{ft} for each confining pressure at curing time t. In this equation, the q_{ft} values were normalized by the associated q_{f7} at curing time = 7 days.

(4) The estimated failure lines, which had the same slope degrees, showed good estimations of peak shear strengths. The differences of cement content C_c affected only to the cohesion values c and c values increased with an increase in C_c values.

(5) It was found from the triaxial compression tests that the cemented soil with C_c = 3 – 5 % may have a sufficient shear strength and prevent cracks occurrence after peak strength. This behaviour is suitable for erosion protection.

7.2 Rain erosion resistance test

The rainfall erosion resistance tests were conducted to evaluate the effectiveness of soil cement application against surface erosion. Six soil slopes were constructed to experiment under rainfall intensity 50 and 100 mm h^{-1}. Four soil slopes were covered with soil mixed

with cement content 3 and 5% by dry weight and cured for 7 days. The slope angle 20-degree was assigned to all the soil slopes.

The results showed that the untreated soil slopes have a tremendous deformation on the surface soils. The huge amount of soil was carried away by surface runoff, in particular at rainfall intensity 100 mm h^{-1} which has the deepest erosion depth 30 cm. On the surface of the untreated soil slopes, the sheet erosion was initially observed, and it was continually developed to rill erosion. The formation of the rills on the surface soil contributed to increase the velocity of surface runoff and cause more soil losses. The serious erosion was observed at the middle part down to the downward of the untreated soil slopes.

However, the small changes were observed on the surface soil slopes covered with soil cement. Due to the hardened surface of the soil treated with cement, some soil crusts were found on the surface soil slopes when it exposed to rainfall. The hard surface soil does prevented a strong soil detachment and soil particle transportation from the surface soils. Very little soil loss was obtained from soil cement slopes. Mixing cement with soil increased the hydraulic conductivity and enhanced the infiltration of water into the soil, reducing surface runoff and soil loss. Additionally, the eroded volume of the surface soil treated with cement was much less than the untreated soil.

The cumulative surface runoff of untreated soil slopes (0%) showed a very large amount compared with treated soil slopes 3% and 5%. In case of cumulative sub-flow under 100 mm h^{-1}, the sub-flow of 3% was larger than 5%, but the amount of eroded soils was much less than 5%. It could imply that 5% did influence on seepage development.

The overall results from the element and the rain erosion resistance tests suggested clearly that soil mixed with low percentage of cement contents, 3 and 5%, effectively protected the soil surface from erosion. In rain erosion resistance tests, the 3% of cement content performed better resistance and less soil loss compared with 5%.

7.3 Recommendation for future study

The present study alone cannot prove the complete effectiveness and efficiency of soil cement for erosion protection occurred on irrigation structures, but suggests the possibility of protection associated with the soil detachment and transportation on surface soil slopes. For the future research, the research should be extended the study on:

(1) Soil mixed with cement to control earth embankment from surface erosion is practically suitable. However, implementing the cement-soil mixtures to the erosion site is another problem to overcome, in particular at the interface between soil cement and eroded soils. The interface between eroded soil surface and cemented soil will probably become the hot spot where erosion will occur. From the total potential and the flow vectors analysis in Chapter 6, the provision of soil cement could not prevent seepage development because flow paths were generated between the joints of soil cement. Thus, the deep of seepage investigation should be investigated in further study by experimenting with some filter materials at the joint to reduce the impact of infiltration on the base layers. It would be useful if there is a further study on the seepage analysis at the interface of the cemented soil by using a finer mesh in finite element analysis. However, a better define the characterization of the soil water retention curve of soil cement through a conventional experimental method, which is one of the important factors for analysis, should be carefully investigated due to the soil parameters of soil water retention curve is necessary for finite element method analysis.

(2) To improve the visualization of the surface changes, it is necessary to improve the surface detection technique by using sensor scanning on the soil slopes. The visualization of the surface change will be greatly improved. In addition, the flow visualization is necessary to verify the mechanism of flow inside the soil and on the surface soil slope. Particle image velocimetry (PIV) can help to improve the visualization of the water flow in particular from the side view of the soil slope.

References

1. Abdulla, A.A. and Kiousis, P.D., 1997. Behavior of cemented sands—I. Testing. *International Journal for Numerical and Analytical Methods in Geomechanics*, *21*(8), pp.533-547.
2. Adams, D.F. and Lewis, E.Q., 1997. Experimental assessment of four composite material shear test methods. *Journal of Testing and Evaluation*, *25*(2), pp.174-181.
3. Agrela, F., Barbudo, A., Ramírez, A., Ayuso, J., Carvajal, M.D. and Jiménez, J.R., 2012. Construction of road sections using mixed recycled aggregates treated with cement in Malaga, Spain. *Resources, Conservation and Recycling*, *58*, pp.98-106.
4. Ahnberg, H., Ljungkrantz, C. and Holmqvist, L., 1995, May. Deep stabilization of different types of soft soils. In *Proceedings 11th ECSMFE, Copenhagen* (Vol. 7, pp. 167-172).
5. Akky, M.R. and Shen, C.K., 1973. Erodibility of a cement-stabilized sandy soil. *Soil erosion: causes and mechanisms*, pp.30-41.
6. Al-Aghbari, M.Y., Mohamedzein, Y.A. and Taha, R., 2009. Stabilisation of desert sands using cement and cement dust. *Proceedings of the Institution of Civil Engineers-Ground Improvement*, *162*(3), pp.145-151.
7. Al-Durrah, M.M. and Bradford, J.M., 1982. The Mechanism of Raindrop Splash on Soil Surfaces 1. *Soil Science Society of America Journal*, *46*(5), pp.1086-1090.
8. Angers, D.A. and Caron, J., 1998. Plant-induced changes in soil structure: processes and feedbacks. *Biogeochemistry*, *42*(1-2), pp.55-72.
9. Bergado, D.T., Anderson, L.R., Miura, N. and Balasubramaniam, A.S., 1996, January. Soft ground improvement in lowland and other environments. ASCE.
10. Bellezza, I. and Fratalocchi, E., 2006. Effectiveness of cement on hydraulic conductivity of compacted soil–cement mixtures. *Proceedings of the Institution of Civil Engineers-Ground Improvement*, *10*(2), pp.77-90.
11. Brouwer, C., Goffeau, A. and Heibloem, M., 1985. Irrigation Water Management: Training Manual No. 1-Introduction to Irrigation. *Food and Agriculture Organization of the United Nations, Rome, Italy*, pp.102-103.

12. Bryan, R.B., 2000. Soil erodibility and processes of water erosion on hillslope. *Geomorphology*, *32*(3-4), pp.385-415.
13. Brunori, F., Penzo, M.C. and Torri, D., 1989. Soil shear strength: its measurement and soil detachability. *Catena*, *16*(1), pp.59-71.
14. Chueasamat, A., 2018. Study on mechanism and measures of slope failures due to rainfalls. Thesis, Tokyo University of Agriculture and Technology, Japan.
15. Clough, G.W., Sitar, N., Bachus, R.C. and Rad, N.S., 1981. Cemented sands under static loading. *Journal of Geotechnical and Geoenvironmental engineering*, *107*(ASCE 16319 Proceeding).
16. Consoli, N.C., Vendruscolo, M.A., Fonini, A. and Dalla Rosa, F., 2009. Fiber reinforcement effects on sand considering a wide cementation range. *Geotextiles and Geomembranes*, *27*(3), pp.196-203.
17. Cruse, R.M. and Larson, W.E., 1977. Effect of Soil Shear Strength on Soil Detachment due to Raindrop Impact 1. *Soil Science Society of America Journal*, *41*(4), pp.777-781.
18. Das, B.M., Yen, S.C. and Dass, R.N., 1995. Brazilian tensile strength test of lightly cemented sand. *Canadian Geotechnical Journal*, *32*(1), pp.166-171.
19. Derpsch, R., 2008. No-tillage and conservation agriculture: a progress report. *No-till farming systems. Special publication*, (3), pp.7-39.
20. De Silva, S., Johnston, R. and Sellamuttu, S., 2014. *Agriculture, irrigation and poverty reduction in Cambodia: Policy narratives and ground realities compared*. WorldFish.
21. Ellison, W.D., 1945. Some effects of raindrops and surface-flow on soil erosion and infiltration. *Eos, Transactions American Geophysical Union*, *26*(3), pp.415-429.
22. Ellison, W.D., 1948. Soil detachment by water in erosion processes. *Eos, Transactions American Geophysical Union*, *29*(4), pp.499-502.
23. Evans, R., 1980. Mechanics of water erosion and their spatial and temporal controls: an empirical viewpoint. *Soil erosion*. 109-128.
24. Fujisawa, K.K.A. and Amamoto, K., 2008. Erosion rates of compacted soils for embankments. *Doboku Gakkai Ronbunshuu C, 64*(2), 403-410.
25. Gao, Z. and Zhao, J., 2012. Constitutive modeling of artificially cemented sand by considering fabric anisotropy. *Computers and Geotechnics*, *41*, pp.57-69.

26. Ghidey, F. and Alberts, E.E., 1997. Plant root effects on soil erodibility, splash detachment, soil strength, and aggregate stability. *Transactions of the ASAE*, *40*(1), pp.129-135.
27. Gilley, J.E., Elliot, W.J., Laflen, J.M. and Simanton, J.R., 1993. Critical shear stress and critical flow rates for initiation of rilling. *Journal of Hydrology*, *142*(1-4), pp.251-271.
28. Gómez, J.A. and Nearing, M.A., 2005. Runoff and sediment losses from rough and smooth soil surfaces in a laboratory experiment. *Catena*, *59*(3), pp.253-266.
29. Gyssels, G., Poesen, J., Bochet, E. and Li, Y., 2005. Impact of plant roots on the resistance of soils to erosion by water: a review. *Progress in physical geography*, *29*(2), pp.189-217.
30. Haghighi, I., Chevalier, C. and Reiffsteck, P., 2012. An Enhanced Crumb Test for a better characterization of water effects on soils. In *6th International Conference on Scour and Erosion, Paris* (pp. 1049-1056).
31. Hayashi, H., Nishikawa, J.I., Ohishi, K. and Terashi, M., 2003. Field observation of long-term strength of cement treated soil. In *Grouting and ground treatment* (pp. 598-609).
32. Horpibulsuk, S., Rachan, R., Chinkulkijniwat, A., Raksachon, Y. and Suddeepong, A., 2010. Analysis of strength development in cement-stabilized silty clay from microstructural considerations. *Construction and building materials*, *24*(10), pp.2011-2021.
33. Hueso-González, P., Ruiz-Sinoga, J.D., Martínez-Murillo, J.F. and Lavee, H., 2015. Overland flow generation mechanisms affected by topsoil treatment: Application to soil conservation. *Geomorphology*, *228*, pp.796-804.
34. Ikegami, M., Ichiba, T., Ohishi, K. and Terashi, M., 2005. Long-term properties of cement treated soil 20 years after construction. In *Proceedings of the international conference on soil mechanics and geotechnical engineering*, 16(3), p. 1199.
35. Indraratna, B., Athukorala, R. and Vinod, J., 2012. Estimating the rate of erosion of a silty sand treated with lignosulfonate. *Journal of Geotechnical and Geoenvironmental Engineering*, *139*(5), pp.701-714.
36. JICA., 2010. Report on baseline and inventory survey of 11 model sites of the TSC3 project in 6 provinces of Cambodia.

37. Kawamura, M. and Diamond, S., 1975. Stabilization of clay soils against erosion loss. *Clays and Clay Minerals*, *23*(6), pp.444-451.
38. Kawasaki, T., Niina, A., Saitoh, S., Suzuki, Y. and Honjo, Y., 1981, June. Deep mixing method using cement hardening agent. In *Proceedings of the 10th international conference on soil mechanics and foundation engineering* (3), pp. 721-724.
39. Khaledi Darvishan, A., Sadeghi, S.H., Homaee, M. and Arabkhedri, M., 2014. Measuring sheet erosion using synthetic color-contrast aggregates. *Hydrological Processes*, *28*(15), pp.4463-4471.
40. Kitazume, M., Nakamura, T., Terashi, M. and Ohishi, K., 2003. Laboratory tests on long-term strength of cement treated soil. In *Grouting and ground treatment*, pp. 586-597.
41. Kohgo, Y., Nakano, M. and Miyazaki, T., 1993a. Theoretical aspects of constitutive modelling for unsaturated soils. *Soils and foundations*, *33*(4), pp.49-63.
42. Kohgo, Y., Nakano, M. and Miyazaki, T., 1993b. Verification of the generalized elastoplastic model for unsaturated soils. *Soils and Foundations*, *33*(4), pp.64-73.
43. Kumar, A., Walia, B.S. and Bajaj, A., 2007. Influence of fly ash, lime, and polyester fibers on compaction and strength properties of expansive soil. *Journal of materials in civil engineering*, *19*(3), pp.242-248.
44. Lade, P.V. and Overton, D.D., 1989. Cementation effects in frictional materials. *Journal of Geotechnical Engineering*, *115*(10), pp.1373-1387.
45. Léonard, J. and Richard, G., 2004. Estimation of runoff critical shear stress for soil erosion from soil shear strength. *Catena*, *57*(3), pp.233-249.
46. Liu, Y.W., Yen, T., Hsu, T.H. and Liou, J.C., 2006. Erosive resistibility of low cement high performance concrete. *Construction and Building Materials*, *20*(3), pp.128-133.
47. Little, G., Hills, D. and Hanson, B., 1993. Uniformity in pressurized irrigation systems depends on design, installation. *California Agriculture*, *47*(3), pp.18-21.
48. Lo, S.R. and Wardani, S.P., 2002. Strength and dilatancy of a silt stabilized by a cement and fly ash mixture. *Canadian Geotechnical Journal*, *39*(1), pp.77-89.
49. Maharaj, A., 2011. Use of the crumb test as a preliminary indicator of dispersive soils.

50. Mehenni, A., Cuisinier, O. and Masrouri, F., 2016. Impact of lime, cement, and clay treatments on the internal erosion of compacted soils. *Journal of Materials in Civil Engineering*, *28*(9), p.04016071.
51. Mihara, Y., 1951. Raindrop and soil erosion (in Japanese with English summary). *Bull Natl Inst Agric Sci A*, 1, pp.1-59.
52. Ministry of water resources and meteorology., 2008. *Review on nationwide irrigation development in Cambodia.*
53. Miura, N., Horpibulsuk, S. and Nagaraj, T.S., 2001. Engineering behavior of cement stabilized clay at high water content. *Soils and Foundations*, *41*(5), pp.33-45.
54. Mitchell, J.K., 1981. Soil improvement-state of the art report. In *Proc., 11th Int. Conf. on SMFE* (Vol. 4, pp. 509-565).
55. Mitchell, J. K., 1976. The properties of Cement-stabilized soils. Proceeding of Residential Workshop on Materials and Methods For Low Cost Road, Rail, and Reclamation Works, 365-404, Leura, Australia, Unisearch Ltd.
56. Morgan, R.P.C., 2005. *Soil erosion and conservation*. Blackwell publishing, Australia.
57. Mubeen, M.M., 2005. Stabilization of soft clay in irrigation projects. *Irrigation and Drainage: The journal of the International Commission on Irrigation and Drainage*, *54*(2), pp.175-187.
58. Návar, J. and Synnott, T.J., 2000. Surface runoff, soil erosion, and land use in Northeastern Mexico. *Terra Latinoamericana*, *18*(3), 247–253.
59. Nearing, M.A. and Bradford, J.M., 1985. Single Waterdrop Splash Detachment and Mechanical Properties of Soils 1. *Soil Science Society of America Journal*, *49*(3), pp.547-552.
60. Netherland Embassy., 2018. Agriculture in Cambodia. Bangkok
61. Nimmo, J.R., 2013. Porosity and Pore Size Distribution, Reference Module in Earth Systems and Environmental Sciences. Published by Elsevier Inc.
62. Nussbaum, P.J. and Colley, B.E., 1971. *Dam construction and facing with soil-cement*. Stokie: Portland Cement Association.
63. Ola, S.A. and Mbata, A., 1990. Durability of soil-cement for building purposes—rain erosion resistance test. *Construction and building materials*, *4*(4), pp.182-187.
64. Park, S.S., 2011. Unconfined compressive strength and ductility of fiber-reinforced cemented sand. *Construction and building materials*, *25*(2), pp.1134-1138.

65. Parlange, J.Y., 1976. Capillary hysteresis and the relationship between drying and wetting curves. *Water Resources Research*, *12*(2), pp.224-228.

66. Porbaha, A., Shibuya, S. and Kishida, T., 2000. State of the art in deep mixing technology. Part III: geomaterial characterization. *Proceedings of the Institution of Civil Engineers-Ground Improvement*, *4*(3), pp.91-110.

67. Poesen, J., 1981. Rainwash experiments on the erodibility of loose sediments. *Earth Surface Processes and Landforms*, *6*(3-4), pp.285-307.

68. Poesen, J., Ingelmo-Sanchez, F. and Mucher, H., 1990. The hydrological response of soil surfaces to rainfall as affected by cover and position of rock fragments in the top layer. *Earth surface processes and landforms*, *15*(7), pp.653-671.

69. Powledge, G.R., Ralston, D.C., Miller, P., Chen, Y.H., Clopper, P.E. and Temple, D.M., 1989. Mechanics of overflow erosion on embankments. II: Hydraulic and design considerations. *Journal of Hydraulic Engineering*, *115*(8), pp.1056-1075.

70. Quang, N.D. and Chai, J.C., 2015. Permeability of lime-and cement-treated clayey soils. *Canadian Geotechnical Journal*, *52*(9), pp.1221-1227.

71. Rafraf, S., Guellouz, L., Guiras, H. and Bouhlila, R., 2016. Quantification of hysteresis effects on a soil subjected to drying and wetting cycles. *International Agrophysics*, *30*(4), pp.493-499.

72. Rahardjo, H., Gofar, N. and Satyanaga, A., 2018. Effect of concrete waste particles on infiltration characteristics of soil. *Environmental earth sciences*, *77*(9), p.347.

73. Reddi, L.N., Lee, I.M. and Bonala, M.V., 2000. Comparison of internal and surface erosion using flow pump tests on a sand-kaolinite mixture. *Geotechnical testing journal*, *23*(1), pp.116-122.

74. Richter, G. and Negendank, J.F., 1977. Soil erosion processes and their measurement in the German area of the Moselle river. *Earth Surface Processes*, *2*(2-3), pp.261-278.

75. Römkens, M.J., Helming, K. and Prasad, S.N., 2002. Soil erosion under different rainfall intensities, surface roughness, and soil water regimes. *Catena*, *46*(2-3), pp.103-123.

76. Sakai, M., Van Genuchten, M.T., Alazba, A.A., Setiawan, B.I. and Minasny, B., 2015. A complete soil hydraulic model accounting for capillary and adsorptive water

retention, capillary and film conductivity, and hysteresis. *Water Resources Research*, *51*(11), pp.8757-8772.

77. Sam, S. and Shinogi, Y., 2015. Performance assessment of Farmer Water User Community: a case study in Stung Chinit irrigation system, Cambodia. *Paddy and water environment*, *13*(1), pp.19-27.
78. Sariosseiri, F. and Muhunthan, B., 2009. Effect of cement treatment on geotechnical properties of some Washington State soils. *Engineering geology*, *104*(1-2), pp.119-125.
79. Sariosseiri, F., Razavi, M., Carlson, K. and Ghazvinian, B., 2011. Stabilization of soils with portland cement and CKD and application of CKD on slope erosion control. *In Geo-Frontiers 2011 conference advances in Geotechnical Engineering*, pp. 778-787).
80. Sasanian, S. and Newson, T.A., 2014. Basic parameters governing the behaviour of cement-treated clays. *Soils and Foundations*, *54*(2), pp.209-224.
81. Schnaid, F., Prietto, P.D. and Consoli, N.C., 2001. Characterization of cemented sand in triaxial compression. *Journal of Geotechnical and Geoenvironmental Engineering*, *127*(10), pp.857-868.
82. Shein, E.V. and Mady, A.Y., 2018. Hysteresis of the water retention curve: wetting branch simulation based on the drying curve. *Moscow University soil science bulletin*, *73*(3), pp.124-128.
83. Sithirith, M., 2017. Water governance in Cambodia: From centralized water governance to farmer water user community. *Resources*, *6*(3), p.44.
84. Shooshpasha, I. and Shirvani, R.A., 2015. Effect of cement stabilization on geotechnical properties of sandy soils. *Geomechanics and Engineering*, *8*(1), pp.17-31.
85. Smets, T., Poesen, J. and Bochet, E., 2008. Impact of plot length on the effectiveness of different soil-surface covers in reducing runoff and soil loss by water. *Progress in Physical Geography*, *32*(6), pp.654-677.
86. Smith D.D., Wischmeier W.H., 1962. Rainfall erosion. *Advances in Agronomy*, 14 (C), pp. 109-148.

87. Trout, T.J. and Neibling, W.H., 1993. Erosion and sedimentation processes on irrigated fields. *Journal of irrigation and drainage engineering*, *119*(6), pp.947-963.

88. Tuller, M. and Or, D., 2004. Retention of water in soil and the soil water characteristic curve. *Encyclopedia of Soils in the Environment*, *4*, pp.278-289.

89. Uddin, K., Balasubramaniam, A.S. and Bergado, D.T., 1997. Engineering behavior of cement-treated Bangkok soft clay. *Geotechnical Engineering*, *28*, pp.89-119.

90. Van Dijk, A.I.J.M., Bruijnzeel, L.A. and Rosewell, C.J., 2002. Rainfall intensity–kinetic energy relationships: a critical literature appraisal. *Journal of Hydrology*, *261*(1-4), pp.1-23.

91. Vereecken, H., Kasteel, R., Vanderborght, J. and Harter, T., 2007. Upscaling hydraulic properties and soil water flow processes in heterogeneous soils. *Vadose Zone Journal*, *6*(1), pp.1-28.

92. Wang, Y.H. and Leung, S.C., 2008. Characterization of cemented sand by experimental and numerical investigations. *Journal of geotechnical and geoenvironmental engineering*, *134*(7), pp.992-1004.

93. White, G.W. and Gnanendran, C.T., 2005. The influence of compaction method and density on the strength and modulus of cementitiously stabilised pavement materials. *International Journal of Pavement Engineering*, *6*(2), pp.97-110.

94. Wilcox, B.P., Wood, M.K. and Tromble, J.M., 1988. Factors influencing infiltrability of semiarid mountain slopes. Journal of Range Management, pp.197-206.

95. Wischmeier, W.H. and Mannering, J.V., 1969. Relation of soil properties to its erodibility 1. *Soil Science Society of America Journal*, *33*(1), pp.131-137.

96. Yin, J.H. and Lai, C.K., 1998. Strength and stiffness of Hong Kong marine deposits mixed with cement. *Geotechnical Engineering*, *29*(1).

97. Yoon, S. and Abu-Farsakh, M., 2009. Laboratory investigation on the strength characteristics of cement-sand as base material. *KSCE Journal of Civil Engineering*, *13*(1), p.15.

98. Young, R.A., 1980. Characteristics of eroded sediment. *Transactions of the ASAE*, *23*(5), pp.1139-1146.

99. Young, R.A. and Wiersma, J.L., 1973. The role of rainfall impact in soil detachment and transport. *Water Resources Research*, *9*(6), pp.1629-1636.

100. Zanetti, C., Vennetier, M., Mériaux, P., Royet, P. and Provansal, M., 2011. Managing woody vegetation on earth dikes: risks assessment and maintenance solutions. *Procedia environmental sciences*, *9*, pp.196-200.

101. Zhao, L., Hou, R., Wu, F. and Keesstra, S., 2018. Effect of soil surface roughness on infiltration water, ponding and runoff on tilled soils under rainfall simulation experiments. *Soil and Tillage Research*, *179*, pp.47-53.